Nuclear Structure and Reactions in Fermionic Molecular Dynamics

Thomas Neff

28th Indian-Summer School of Physics
Ab Initio Methods in Nuclear Physics

Czech Academy of Sciences
Charles University in Prague

Prague, Czech Republic

August 29 - September 2, 2016

HELMHOLTZ ASSOCIATION

GSI

Overview: UCOM

Nuclear degrees of freedom and nuclear interactions

Short-range correlations

Unitary Correlation Operator Method (UCOM)

Similarity Renormalization Goup (SRG)

No-Core Shell Model (NCSM)

Nuclear Degrees of Freedom

RIA Physics White Paper

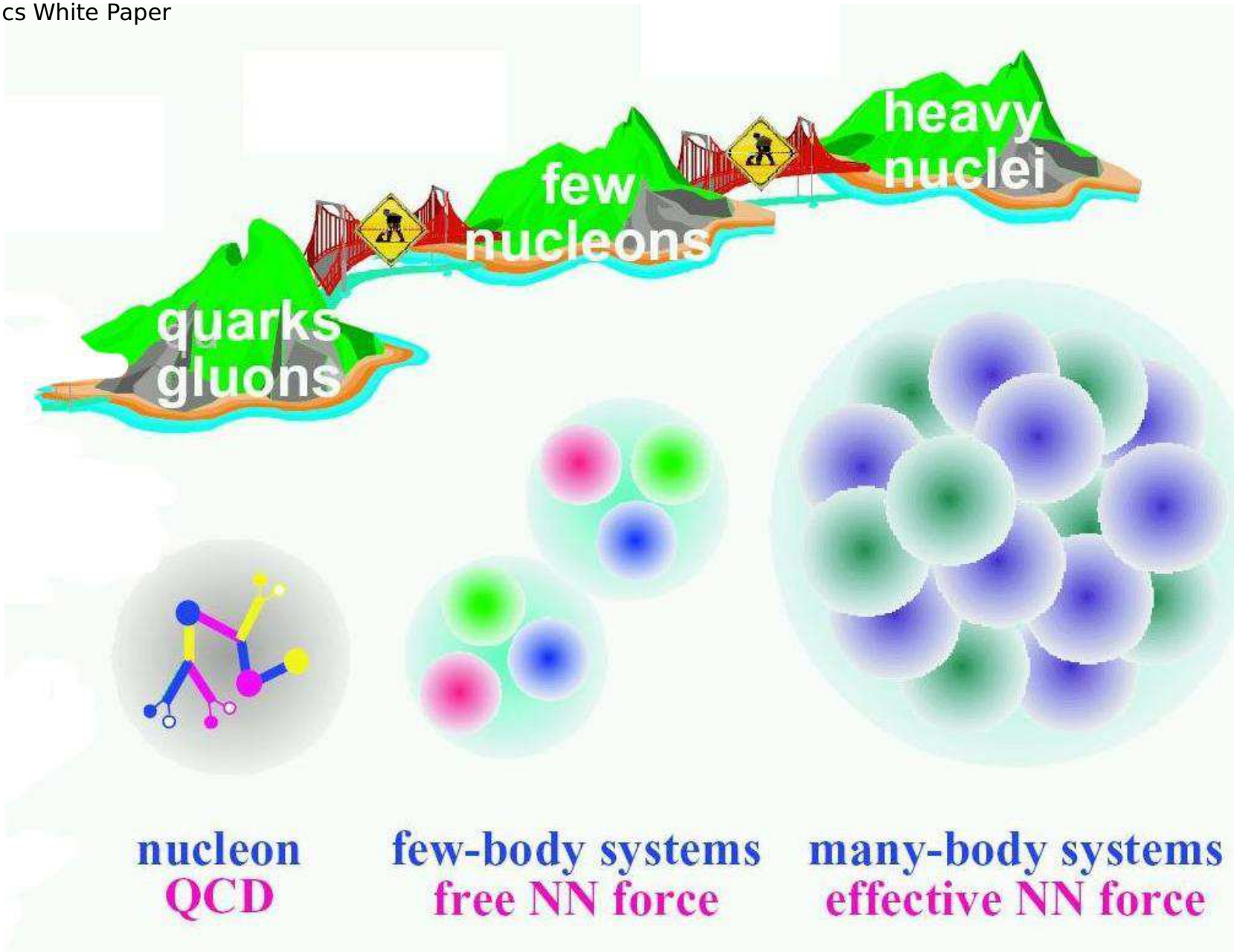

Nucleons as effective Degrees of Freedom

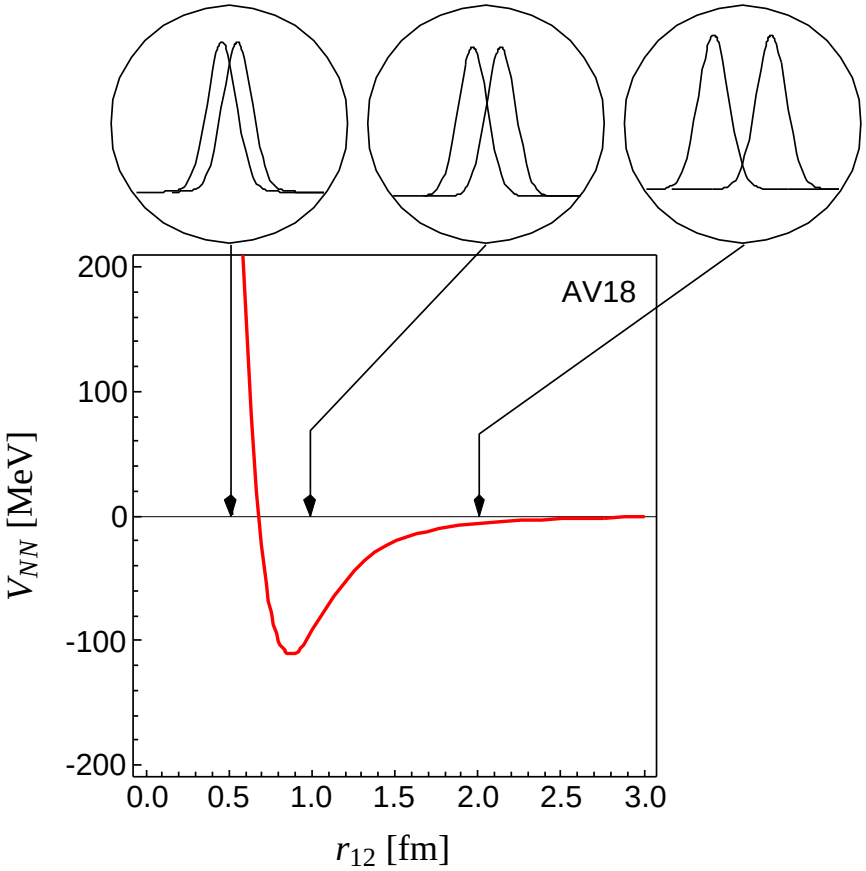

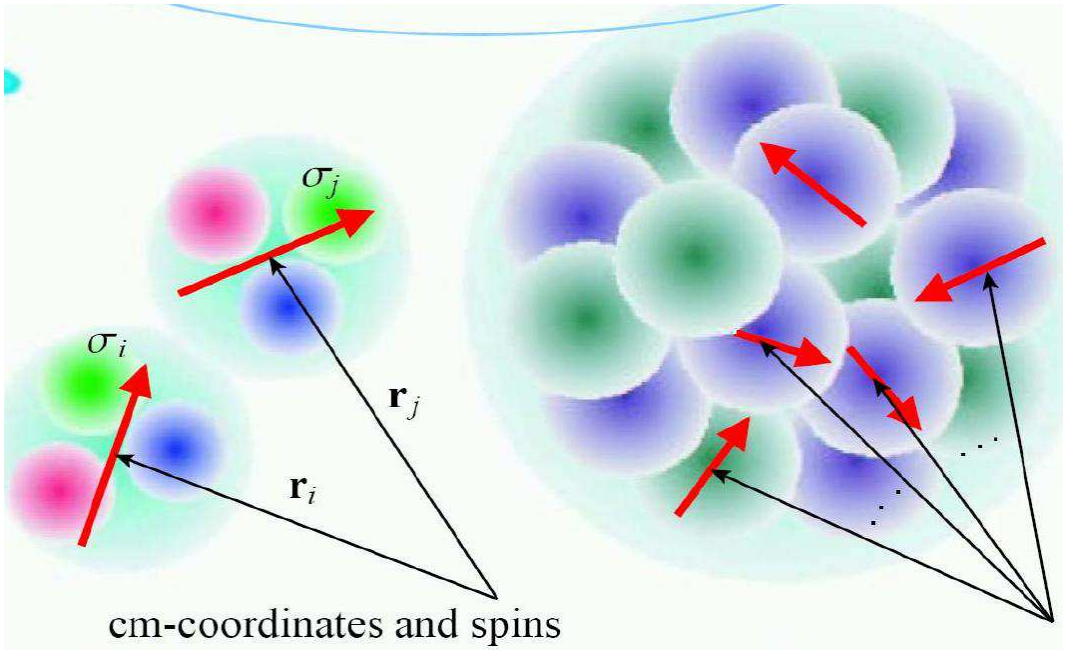

- at low energies nuclei can be described as a system of nucleons – we neglect pions, deltas, . . .
- nucleons are not point-like particles, proton charge radius $r_p \approx 0.88\,\text{fm}$

➳ nucleon-nucleon force is something like the van-der-Waals force between atoms

Two-Nucleon System (Relative Motion)

- Couple Spin and Isospin

$$\left| S, M_S \right\rangle = \sum_{m_{s1}, m_{s2}} \mathrm{C} \left(\begin{matrix} \frac{1}{2} & \frac{1}{2} \\ m_{s1} & m_{s2} \end{matrix} \middle| \begin{matrix} S \\ M_S \end{matrix} \right) \left| \tfrac{1}{2}, m_{s1} \right\rangle \otimes \left| \tfrac{1}{2}, m_{s2} \right\rangle, \qquad S = 0, 1$$

$$\left| T, M_T \right\rangle = \sum_{m_{t1}, m_{t2}} \mathrm{C} \left(\begin{matrix} \frac{1}{2} & \frac{1}{2} \\ m_{t1} & m_{t2} \end{matrix} \middle| \begin{matrix} T \\ M_T \end{matrix} \right) \left| \tfrac{1}{2}, m_{t1} \right\rangle \otimes \left| \tfrac{1}{2}, m_{t2} \right\rangle, \qquad T = 0, 1$$

Spin/Isospin
Singlet, Triplet

- Couple Orbital Angular Momentum with Spin

$$\left\langle \mathbf{r} \middle| \alpha, (LS)JM; TM_T \right\rangle = \sum_{M_L, M_S} \mathrm{C} \left(\begin{matrix} L & S \\ M_L & M_S \end{matrix} \middle| \begin{matrix} J \\ M \end{matrix} \right) \phi_\alpha(r) Y_{LM_L}(\hat{\mathbf{r}}) \left| S, M_S \right\rangle \otimes \left| T, M_T \right\rangle$$

- Antisymmetry

$$(S, T) = (0, 1) \text{ or } (1, 0) \quad \longrightarrow \quad L = 0, 2, 4, \ldots$$

$$(S, T) = (0, 0) \text{ or } (1, 1) \quad \longrightarrow \quad L = 1, 3, 5, \ldots$$

Even channels

Odd channels

Nucleon-Nucleon Force

NN scattering data

$^{2S+1}L_J$

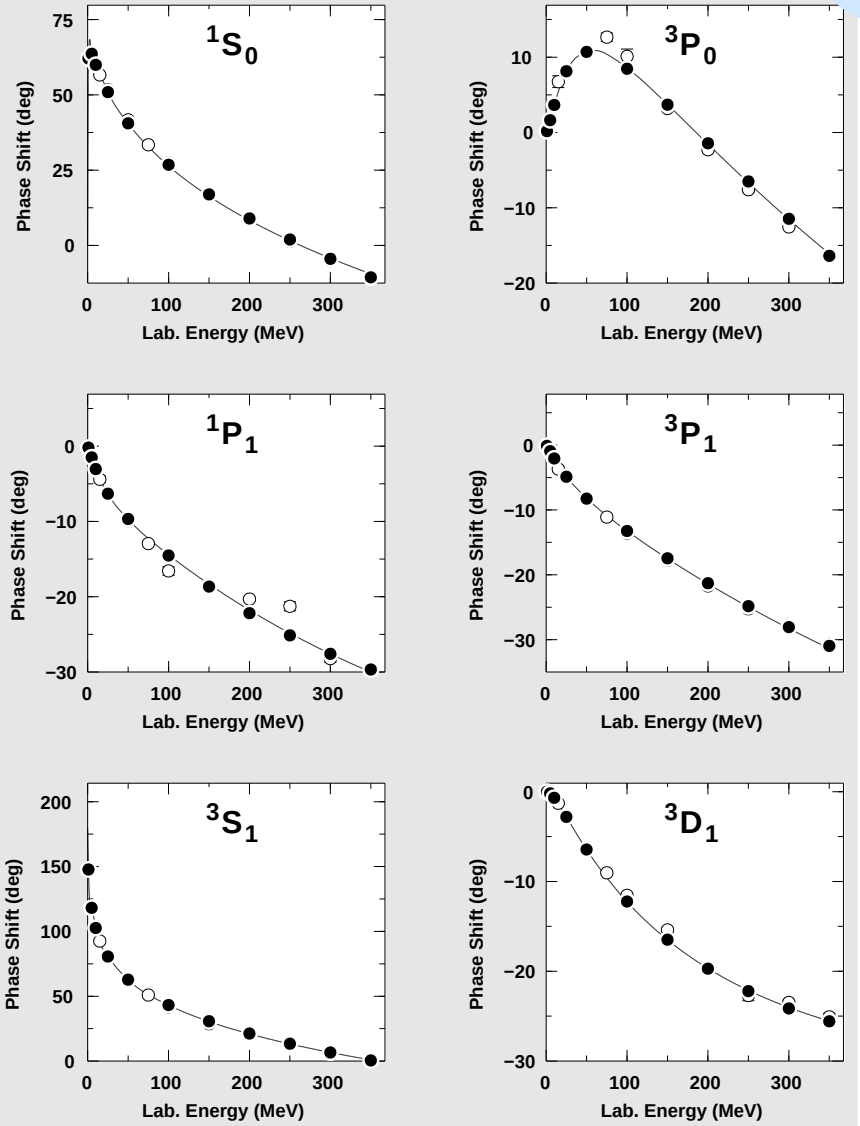

Machleidt, Phys. Rev. C **63**, 024001 (2001)

Realistic Interactions

- describe NN phaseshifts (χ^2/datum ≈ 1)
- describe deuteron properties

- short-range (high-momentum) and off-shell behavior not constrained by data

➳ **nucleon-nucleon force not completely constrained**

Some Realistic Interactions

- **Bonn**-Potentials (based on meson-exchange)
- **Argonne V18** (pion-exchange, phenomenological short-range)
- interactions based on **Chiral Perturbation Theory**

Interaction from Chiral Perturbation Theory

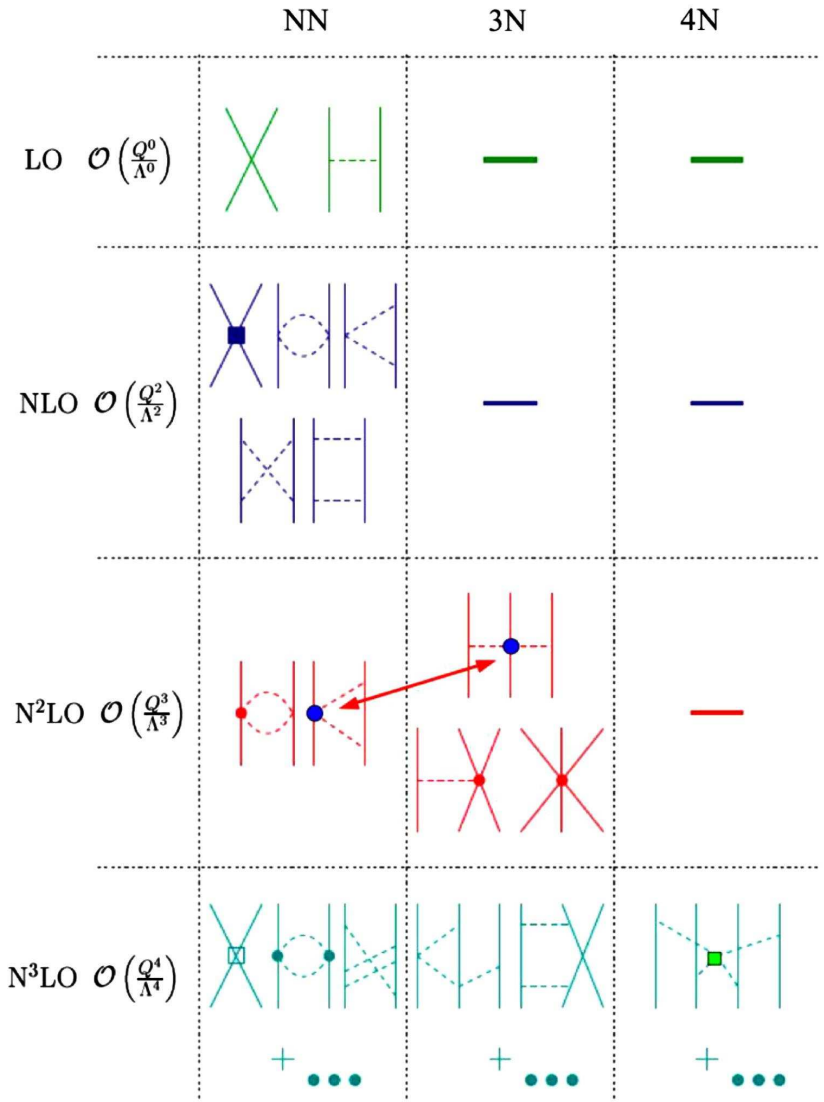

Entem, Machleidt, PRC 68, 041001 (2003)

- derived using chiral EFT
- includes full pion dynamics
- short-range behavior given by contact-terms
- power counting
- regulated by cut-off (500 MeV)

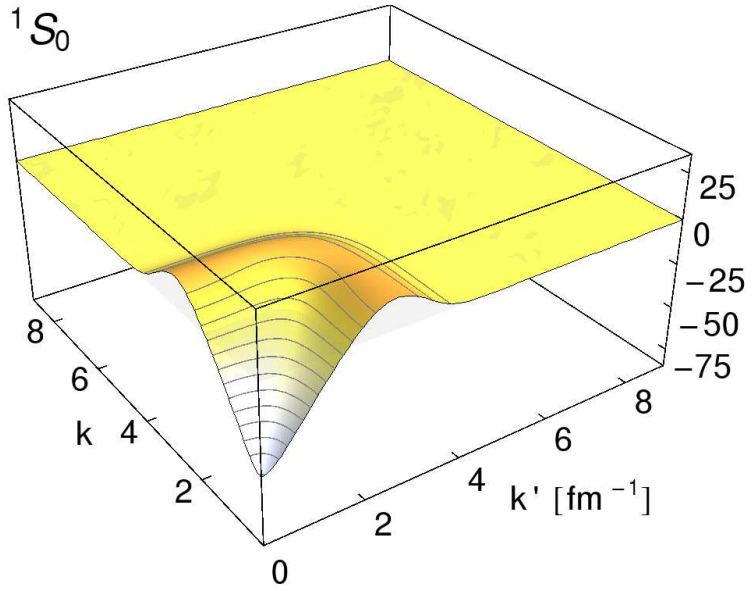

$$\langle k(LS)J \left| \underset{\sim}{V} \right| k'(L'S)J \rangle$$

Argonne V18 Interaction

- (almost) local interaction in coordinate space

Central

$$V(\mathbf{r_1}, \mathbf{r_2}, \mathbf{p_1}, \mathbf{p_2}, \boldsymbol{\sigma}_1, \boldsymbol{\sigma}_2, \boldsymbol{\tau}_1, \boldsymbol{\tau}_2) = V(r) + V^{\sigma}(r)\boldsymbol{\sigma}_1 \cdot \boldsymbol{\sigma}_2 + V^{\tau}(r)\boldsymbol{\tau}_1 \cdot \boldsymbol{\tau}_2 + V^{\sigma\tau}(r)\boldsymbol{\sigma}_1 \cdot \boldsymbol{\sigma}_2 \boldsymbol{\tau}_1 \cdot \boldsymbol{\tau}_2 +$$

$$V_{l^2}(r)\mathbf{L}^2 + V^{\sigma}_{l^2}(r)\boldsymbol{\sigma}_1 \cdot \boldsymbol{\sigma}_2 \mathbf{L}^2 + V^{\tau}_{l^2}(r)\boldsymbol{\tau}_1 \cdot \boldsymbol{\tau}_2 \mathbf{L}^2 + V^{\sigma\tau}_{l^2}(r)\boldsymbol{\sigma}_1 \cdot \boldsymbol{\sigma}_2 \boldsymbol{\tau}_1 \cdot \boldsymbol{\tau}_2 \mathbf{L}^2 +$$

Spin-Orbit

$$V_{ls}(r)\mathbf{L} \cdot \mathbf{S} + V^{\tau}_{ls}(r)\boldsymbol{\tau}_1 \cdot \boldsymbol{\tau}_2 \mathbf{L} \cdot \mathbf{S} +$$

$$V_{ls^2}(r)(\mathbf{L} \cdot \mathbf{S})^2 + V^{\tau}_{ls^2}(r)\boldsymbol{\tau}_1 \cdot \boldsymbol{\tau}_2 (\mathbf{L} \cdot \mathbf{S})^2 +$$

Tensor

$$V_t(r)S_{12} + V^{\tau}_t(r)\boldsymbol{\tau}_1 \cdot \boldsymbol{\tau}_2 S_{12} +$$

four charge dependent and charge asymmetric terms

$$\mathbf{r} = \mathbf{r}_1 - \mathbf{r}_2, \qquad \mathbf{p} = \tfrac{1}{2}(\mathbf{p}_1 - \mathbf{p}_2)$$

$$\mathbf{L} = \mathbf{r} \times \mathbf{p}, \qquad \mathbf{S} = \tfrac{1}{2}(\boldsymbol{\sigma}_1 + \boldsymbol{\sigma}_2)$$

$$S_{12} = 3(\boldsymbol{\sigma}_1 \cdot \hat{\mathbf{r}})(\boldsymbol{\sigma}_2 \cdot \hat{\mathbf{r}}) - \boldsymbol{\sigma}_1 \cdot \boldsymbol{\sigma}_2$$

Unitary Correlation Operator Method

Short-range Correlations

Unitary Correlation Operator Method

- Unitary Transformation
- Central Correlations
- Tensor Correlations
- Interaction in Momentum Space

Nuclear Force

Argonne V18 (T=0)

spins aligned parallel or perpendicular to the relative distance vector

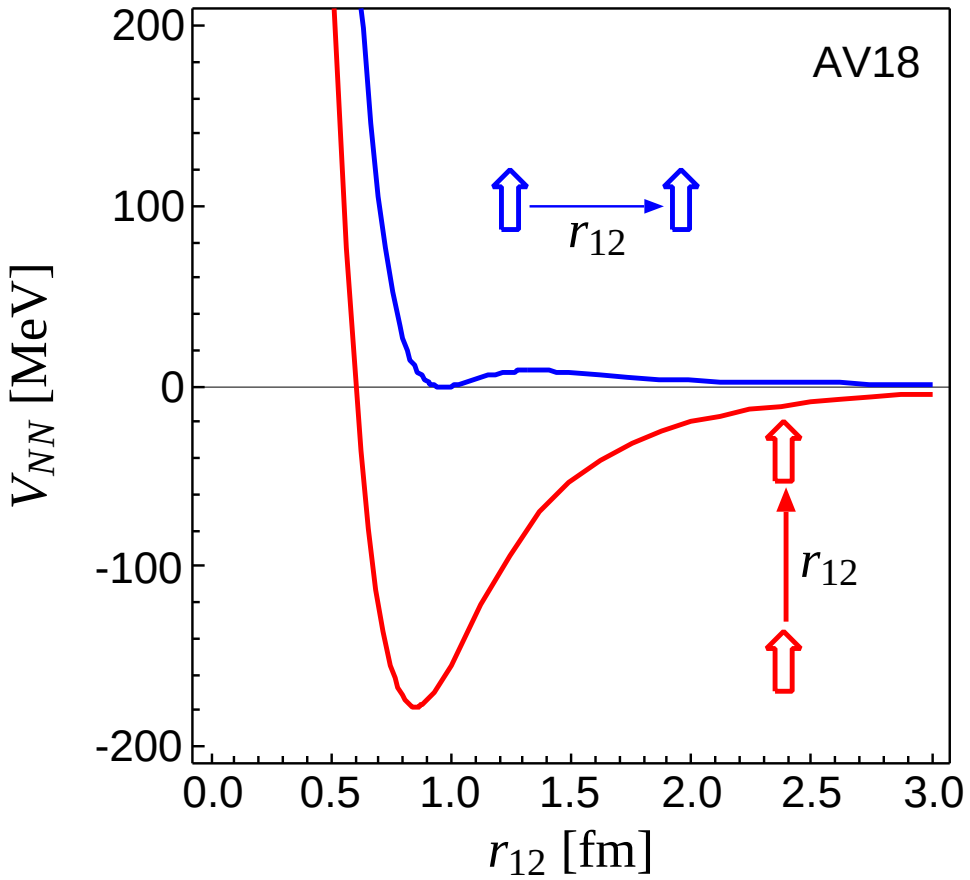

- strong repulsive core: nucleons can not get closer than ≈ 0.5 fm

➳ **central correlations**

- strong dependence on the orientation of the spins due to the tensor force

➳ **tensor correlations**

Nuclear Force

Argonne V18 (T=0)

spins aligned parallel or perpendicular to the relative distance vector

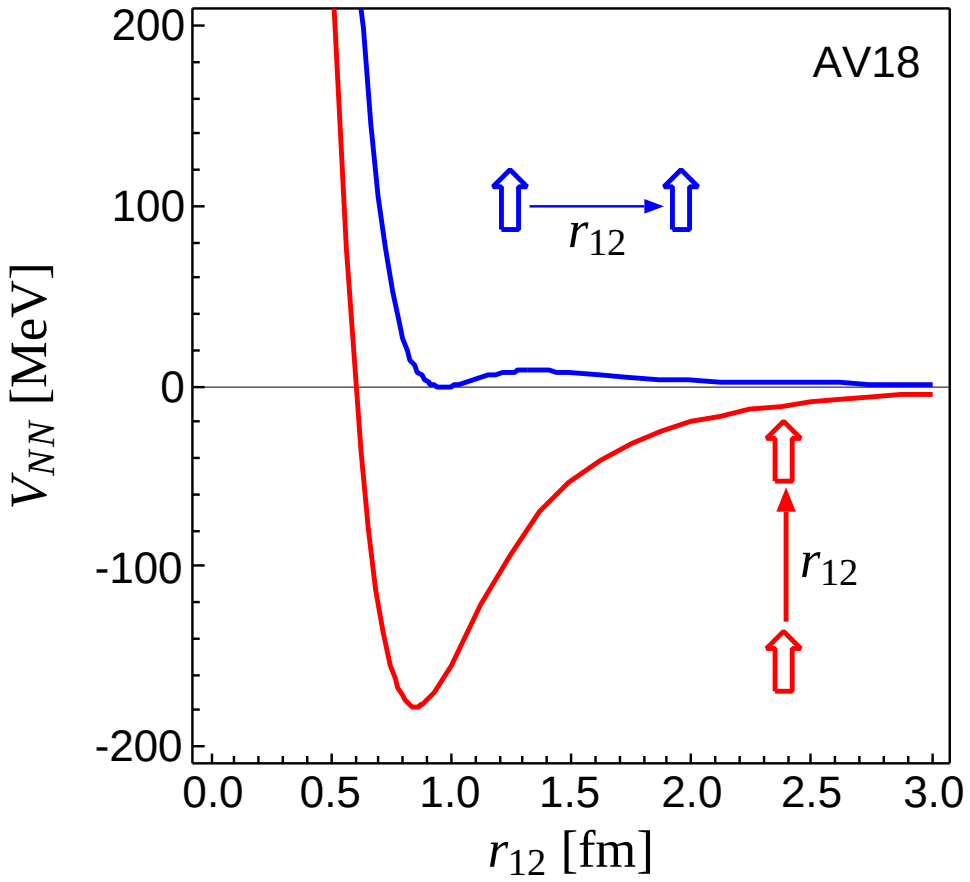

- strong repulsive core: nucleons can not get closer than ≈ 0.5 fm

➳ **central correlations**

- strong dependence on the orientation of the spins due to the tensor force

➳ **tensor correlations**

the nuclear force will induce **strong short-range correlations** in the nuclear wave function

One- and Two-Body Densities

(Diagonal) One-body density

$$\rho^{(1)}(\mathbf{r}) = \sum_{m_t, m_s} \left\langle \Psi \left| \underset{\sim}{a}^{\dagger}_{m_s, m_t}(\mathbf{r})\, \underset{\sim}{a}_{m_s, m_t}(\mathbf{r}) \right| \Psi \right\rangle$$

Probability to find **one nucleon** at position **r**

(Diagonal) Two-body density

$$\rho^{(2)}_{S,M_S;T,M_T}(\mathbf{r}, \mathbf{r}') = \sum_{m_s, m_s'} \mathrm{C}\left(\begin{matrix} \frac{1}{2} & \frac{1}{2} \\ m_s & m_s' \end{matrix} \middle| \begin{matrix} S \\ M_S \end{matrix} \right) \sum_{m_t, m_t'} \mathrm{C}\left(\begin{matrix} \frac{1}{2} & \frac{1}{2} \\ m_t & m_t' \end{matrix} \middle| \begin{matrix} T \\ M_T \end{matrix} \right) \times$$
$$\left\langle \Psi \left| \underset{\sim}{a}^{\dagger}_{m_s, m_t}(\mathbf{r})\, \underset{\sim}{a}^{\dagger}_{m_s', m_t'}(\mathbf{r}')\, \underset{\sim}{a}_{m_s', m_t'}(\mathbf{r}')\, \underset{\sim}{a}_{m_s, m_t}(\mathbf{r}) \right| \Psi \right\rangle$$

$$\rho^{(2)}_{S,M_S;T,M_T}(\mathbf{r}) = \int \mathrm{d}^3R\, \rho^{(2)}_{S,M_S;T,M_T}(\tfrac{1}{2}\mathbf{R} + \mathbf{r}, \tfrac{1}{2}\mathbf{R} - \mathbf{r})$$

Probability to find **a pair of nucleons** at a relative distance **r**

One-body densities

coordinate space

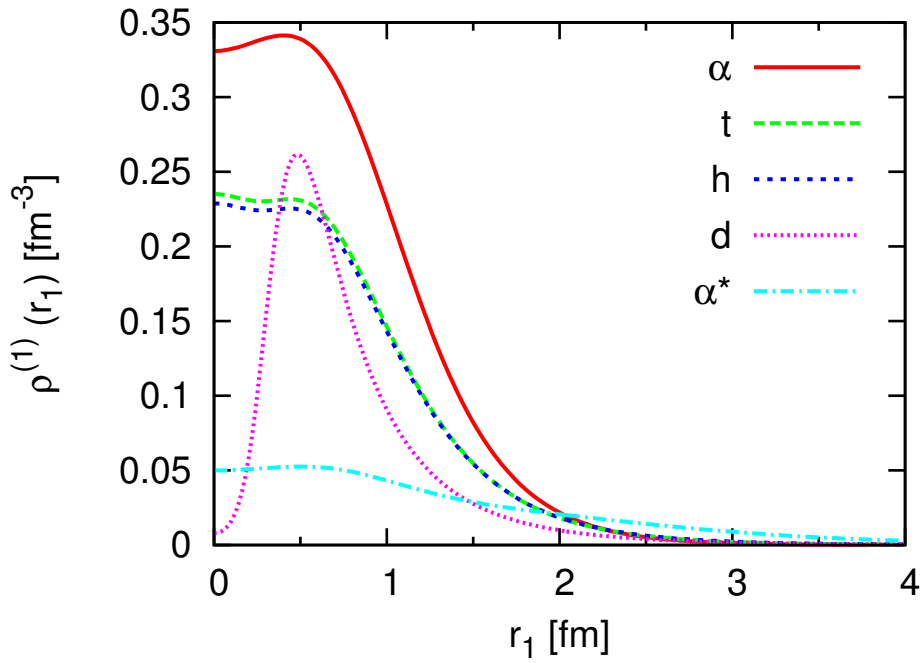

momentum space

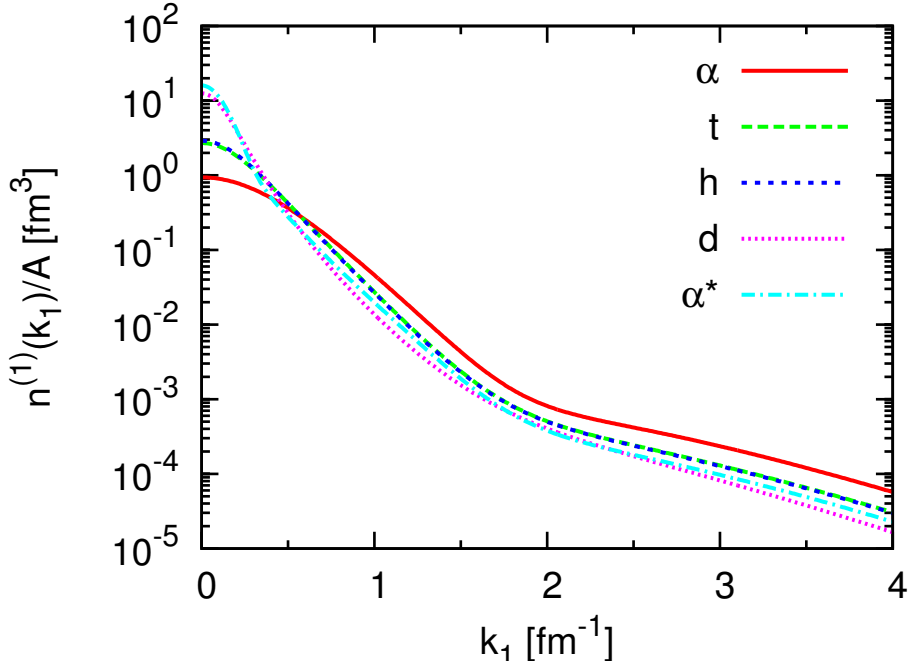

- one-body densities calculated from exact wave functions for AV8' interaction
- coordinate space densities reflect different sizes and densities of ^{2}H, ^{3}H, ^{3}He, ^{4}He and the 0_2^+ state in ^{4}He
- similar high-momentum tails in the momentum densities

Feldmeier, Horiuchi, Neff, Suzuki, Phys. Rev. C **84**, 054003 (2011)

Two-body densities in $A = 2, 3, 4$ Nuclei — AV8'

coordinate space

$S = 1, M_S = 1, T = 0$

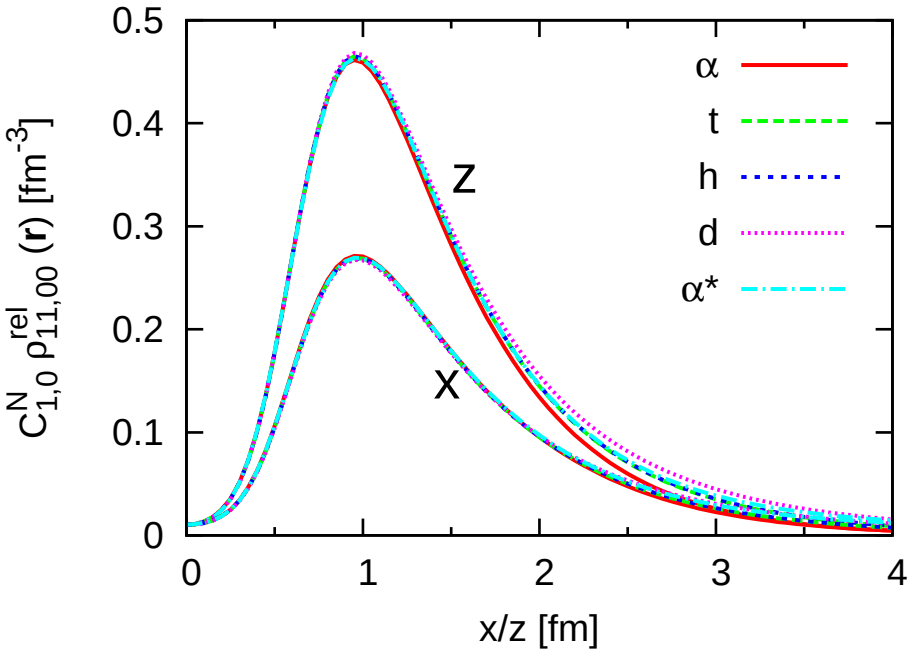

momentum space

$S = 1, T = 0$

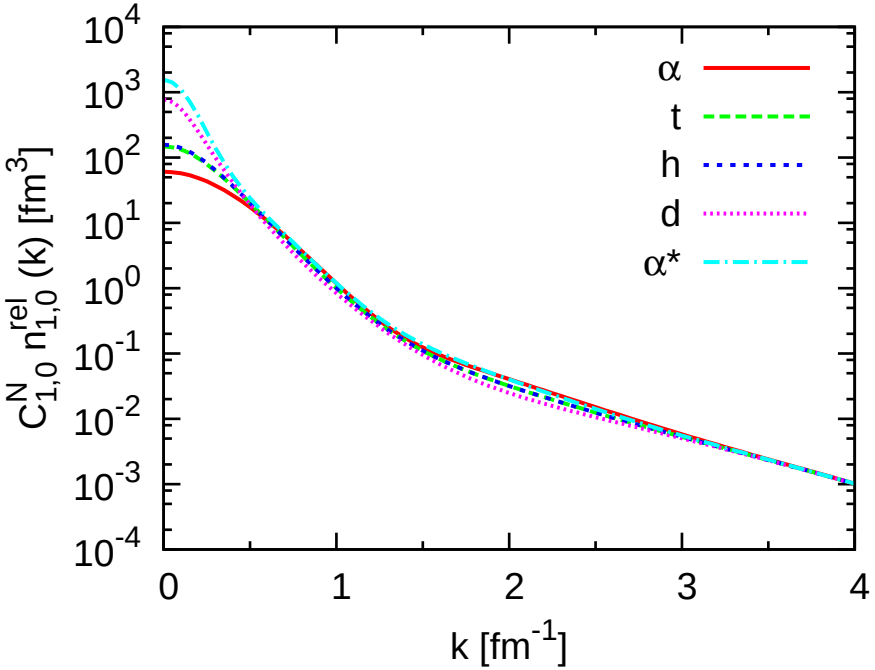

- normalize two-body density in coordinate space at r=1.0 fm
- normalized two-body densities in coordinate space are identical at short distances for all nuclei
- use the **same** normalization factor in momentum space – high momentum tails agree for all nuclei

Feldmeier, Horiuchi, Neff, Suzuki, Phys. Rev. C **84**, 054003 (2011)

Realistic and Effective Nucleon-Nucleon Interactions

Realistic Interactions

- reproduce scattering data and deutron properties
- meson-exchange (Bonn), phenomenological (AV18), χ-PT (Idaho)
- **repulsive core** and **tensor force** induce **strong short-range correlations**

Realistic and Effective Nucleon-Nucleon Interactions

Realistic Interactions

- reproduce scattering data and deutron properties
- meson-exchange (Bonn), phenomenological (AV18), χ-PT (Idaho)
- **repulsive core** and **tensor force** induce **strong short-range correlations**

Effective Interactions

- phenomenological effective interactions describe many properties of nuclear systems like energies, radii, spectra successfully using simple many-body wave functions (HF, shell model, microscopic cluster models)
- No-Core Shell Model uses Lee-Suzuki transformation in oscillator basis
- G-matrix and V_{lowk} derive effective interaction in momentum space

UCOM
Realistic and Effective Nucleon-Nucleon Interactions

Realistic Interactions

- reproduce scattering data and deutron properties
- meson-exchange (Bonn), phenomenological (AV18), χ-PT (Idaho)
- **repulsive core** and **tensor force** induce **strong short-range correlations**

Effective Interactions

- phenomenological effective interactions describe many properties of nuclear systems like energies, radii, spectra successfully using simple many-body wave functions (HF, shell model, microscopic cluster models)
- No-Core Shell Model uses Lee-Suzuki transformation in oscillator basis
- G-matrix and V_{lowk} derive effective interaction in momentum space

Our approach

- derive **effective interaction** from **realistic interaction** by explicitly including correlations with **unitary correlation operator** $\underset{\sim}{C}$ formulated in **coordinate space**
- correlated (effective) interaction

$$\underset{\sim}{\hat{H}} = \underset{\sim}{C}^{\dagger} \underset{\sim}{H} \underset{\sim}{C}$$

UCOM

Unitary Transformation

Transform the eigenvalue problem

$$\underset{\sim}{H}\left|\,\hat{\Psi}_n\,\right\rangle = E_n\left|\,\hat{\Psi}_n\,\right\rangle$$

with the unitary operator $\underset{\sim}{C}$

$$\left|\,\hat{\Psi}_n\,\right\rangle = \underset{\sim}{C}\left|\,\Psi_n\,\right\rangle, \quad \underset{\sim}{C}^{-1} = \underset{\sim}{C}^{\dagger}$$

into the equivalent eigenvalue problem

$$\underset{\sim}{\hat{H}}\left|\,\Psi_n\,\right\rangle = (\underset{\sim}{C}^{\dagger}\underset{\sim}{H}\underset{\sim}{C})\left|\,\Psi_n\,\right\rangle = E_n\left|\,\Psi_n\,\right\rangle$$

Finally solve eigenvalue problem in a (relatively small) model space
$\left\{\left|\,\Psi_n\,\right\rangle, n = 1, \ldots, N\right\}$

“pre-diagonalization”

correlator $\underset{\sim}{C}$ describes short-range correlations that are very similar (for the states in the model space)

correlator $\underset{\sim}{C}$ admixes components from outside the model space

it does not project on the model space

Unitary Correlation Operator Method

Correlation Operator

- induce short-range (two-body) central and tensor correlations into the many-body state

$$\underset{\sim}{C} = \underset{\sim}{C}_\Omega \underset{\sim}{C}_r = \exp\Big[-i \sum_{i<j} \underset{\sim}{g}_{\Omega,ij}\Big] \exp\Big[-i \sum_{i<j} \underset{\sim}{g}_{r,ij}\Big] \quad , \quad \underset{\sim}{C}^\dagger \underset{\sim}{C} = \underset{\sim}{1}$$

- correlation operator should conserve the symmetries of the Hamiltonian and should be of finite-range, correlated interaction **phase shift equivalent** to bare interaction by construction

Correlated Operators

- correlated operators will have contributions in higher cluster orders

$$\underset{\sim}{C}^\dagger \underset{\sim}{O} \underset{\sim}{C} = \underset{\sim}{\hat{O}}^{[1]} + \underset{\sim}{\hat{O}}^{[2]} + \underset{\sim}{\hat{O}}^{[3]} + \ldots$$

- two-body approximation: correlation range should be small compared to mean particle distance

Correlated Interaction

$$\underset{\sim}{C}^\dagger (\underset{\sim}{T} + \underset{\sim}{V}) \underset{\sim}{C} = \underset{\sim}{T} + \underset{\sim}{V}_{\mathrm{UCOM}} + \underset{\sim}{V}^{[3]}_{\mathrm{UCOM}} + \ldots$$

UCOM
Central Correlations

- radial distance-dependent **shift in the relative coordinate** of each nucleon pair

$$g_r = \tfrac{1}{2}\left[p_r\, s(r) + s(r)\, p_r\right] \quad , \quad p_r = \tfrac{1}{2}\left[\mathbf{p}\cdot\mathbf{r} + \mathbf{r}\cdot\mathbf{p}\right]$$

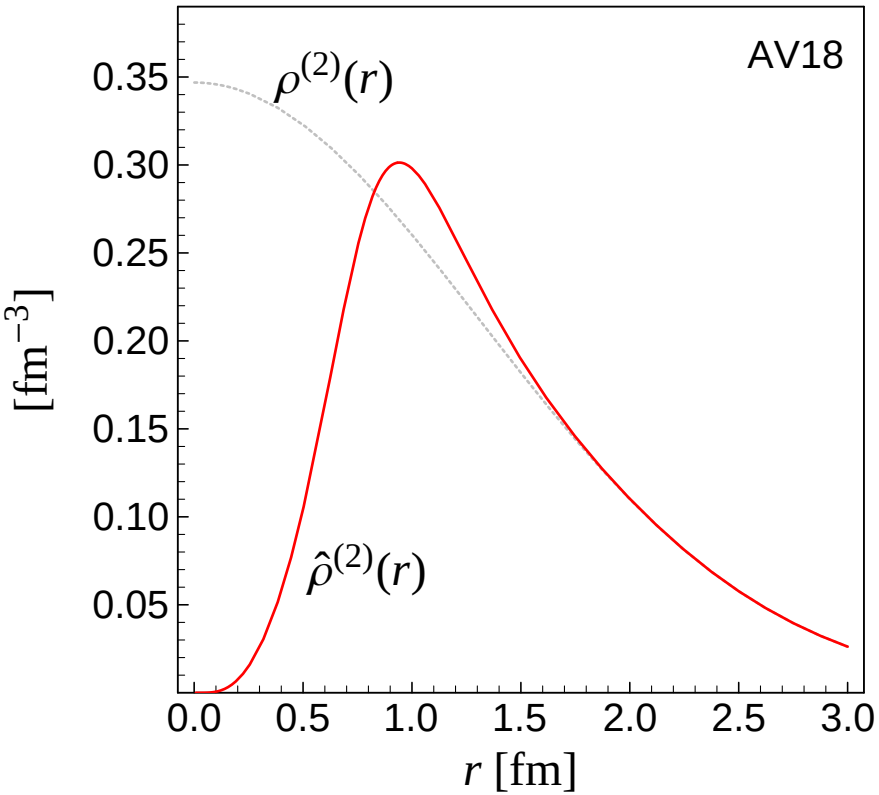

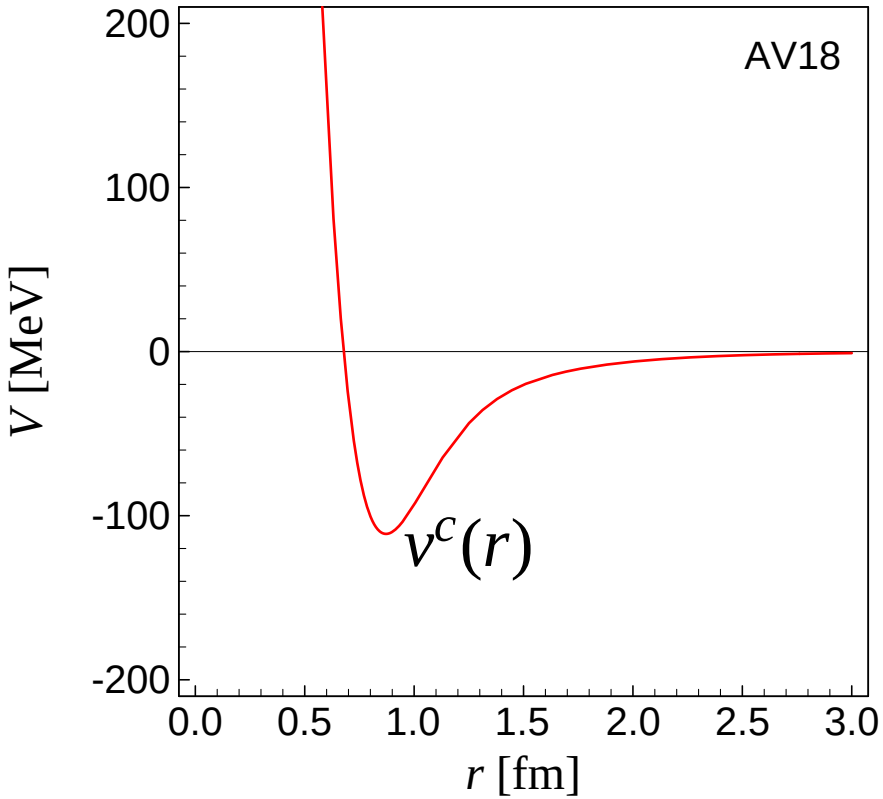

$S = 0, T = 1$

nucleons shifted out of repulsive core

Tensor Correlations

- **angular shift in the relative coordinate** of each nucleon pair depending on the orientation of the spins

$$g_\Omega = \vartheta(r)\left[\tfrac{3}{2}(\boldsymbol{\sigma}_1\cdot\mathbf{p}_\Omega)(\boldsymbol{\sigma}_2\cdot\mathbf{r}) + \tfrac{3}{2}(\boldsymbol{\sigma}_1\cdot\mathbf{r})(\boldsymbol{\sigma}_2\cdot\mathbf{p}_\Omega)\right] \quad , \quad \mathbf{p}_\Omega = \mathbf{p} - \mathbf{r}\,p_r$$

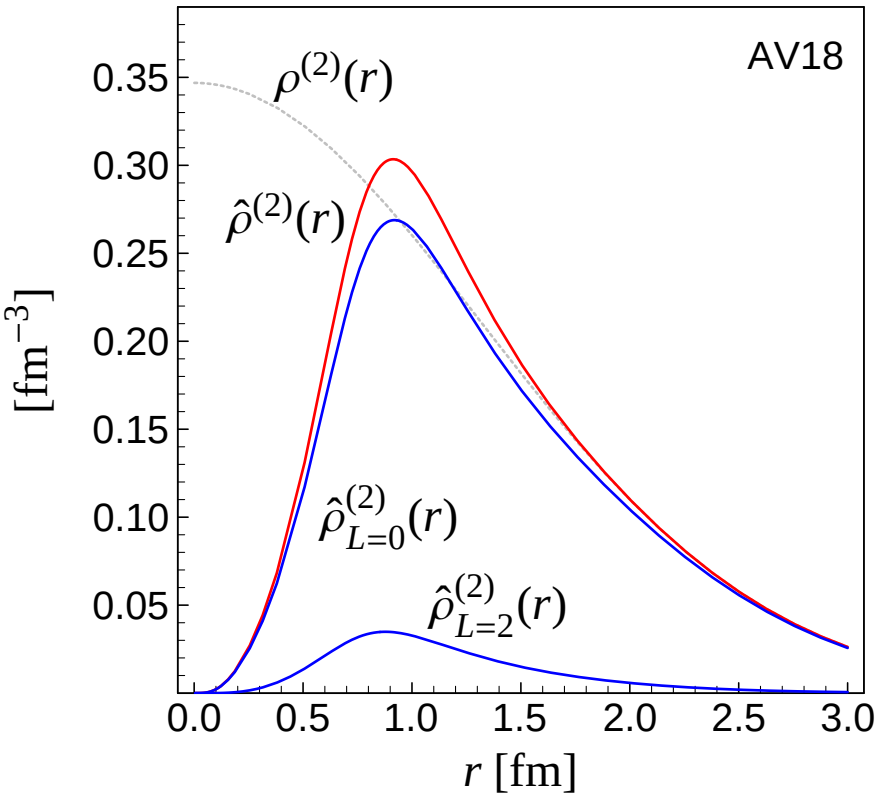

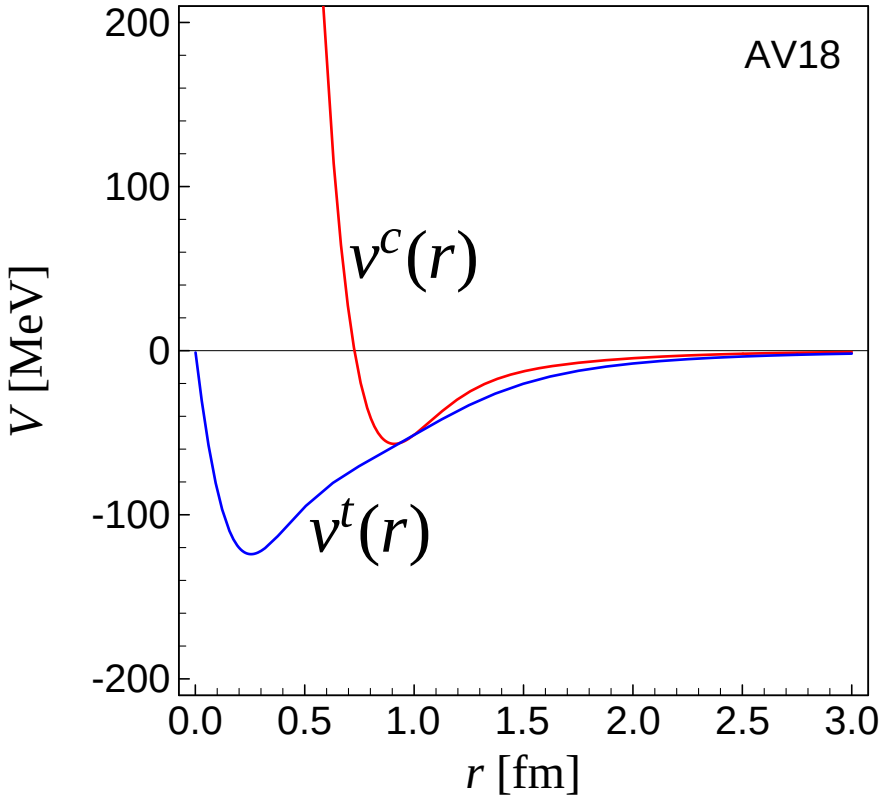

$S = 1, T = 0$

nucleons aligned with total spin of nucleon pair

UCOM

Central and Tensor Correlations

$$\underset{\sim}{C} = \underset{\sim}{C}_\Omega \underset{\sim}{C}_r$$

$$\mathbf{p} = \mathbf{p}_r + \mathbf{p}_\Omega$$

$$\mathbf{p}_r = \frac{1}{2}\left\{\frac{\mathbf{r}}{r}\left(\frac{\mathbf{r}}{r}\mathbf{p}\right) + \left(\mathbf{p}\frac{\mathbf{r}}{r}\right)\frac{\mathbf{r}}{r}\right\}, \qquad \mathbf{p}_\Omega = \frac{1}{2r}\left\{\mathbf{l}\times\frac{\mathbf{r}}{r} - \frac{\mathbf{r}}{r}\times\mathbf{l}\right\}$$

UCOM

Central and Tensor Correlations

$$\underset{\sim}{C} = \underset{\sim}{C}_\Omega \underset{\sim}{C}_r$$

$$\mathbf{p} = \mathbf{p}_r + \mathbf{p}_\Omega$$

$$\mathbf{p}_r = \frac{1}{2}\left\{\frac{\mathbf{r}}{r}\left(\frac{\mathbf{r}}{r}\mathbf{p}\right) + \left(\mathbf{p}\frac{\mathbf{r}}{r}\right)\frac{\mathbf{r}}{r}\right\}, \qquad \mathbf{p}_\Omega = \frac{1}{2r}\left\{\mathbf{l}\times\frac{\mathbf{r}}{r} - \frac{\mathbf{r}}{r}\times\mathbf{l}\right\}$$

Central Correlations

$$\underset{\sim}{c}_r = \exp\left\{-\frac{i}{2}\{p_r s(r) + s(r) p_r\}\right\}$$

- probability density shifted out of the repulsive core

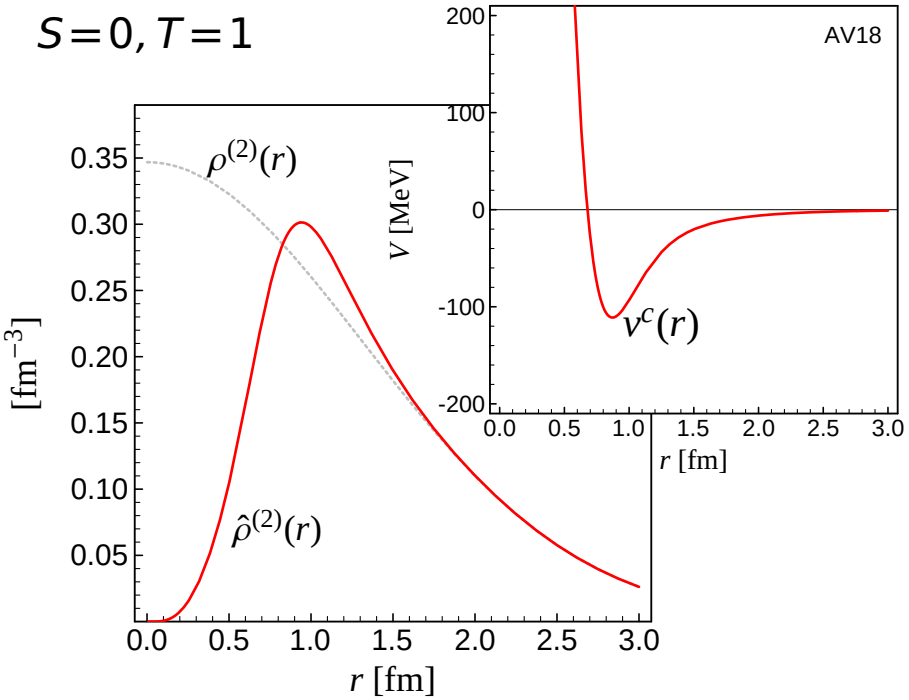

UCOM

Central and Tensor Correlations

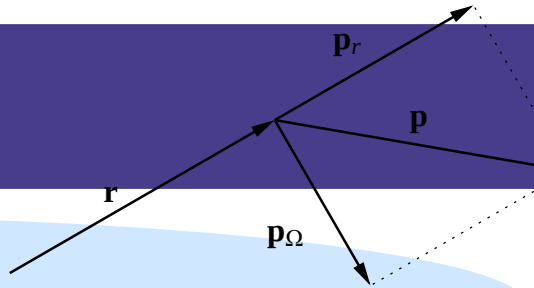

$$\underset{\sim}{C} = \underset{\sim}{C}_\Omega \underset{\sim}{C}_r$$

$$\mathbf{p} = \mathbf{p}_r + \mathbf{p}_\Omega$$

$$\mathbf{p}_r = \frac{1}{2}\left\{\frac{\mathbf{r}}{r}\left(\frac{\mathbf{r}}{r}\mathbf{p}\right) + \left(\mathbf{p}\frac{\mathbf{r}}{r}\right)\frac{\mathbf{r}}{r}\right\}, \qquad \mathbf{p}_\Omega = \frac{1}{2r}\left\{\mathbf{l}\times\frac{\mathbf{r}}{r} - \frac{\mathbf{r}}{r}\times\mathbf{l}\right\}$$

Central Correlations

$$\underset{\sim}{C}_r = \exp\left\{-\frac{i}{2}\{p_r s(r) + s(r) p_r\}\right\}$$

- probability density shifted out of the repulsive core

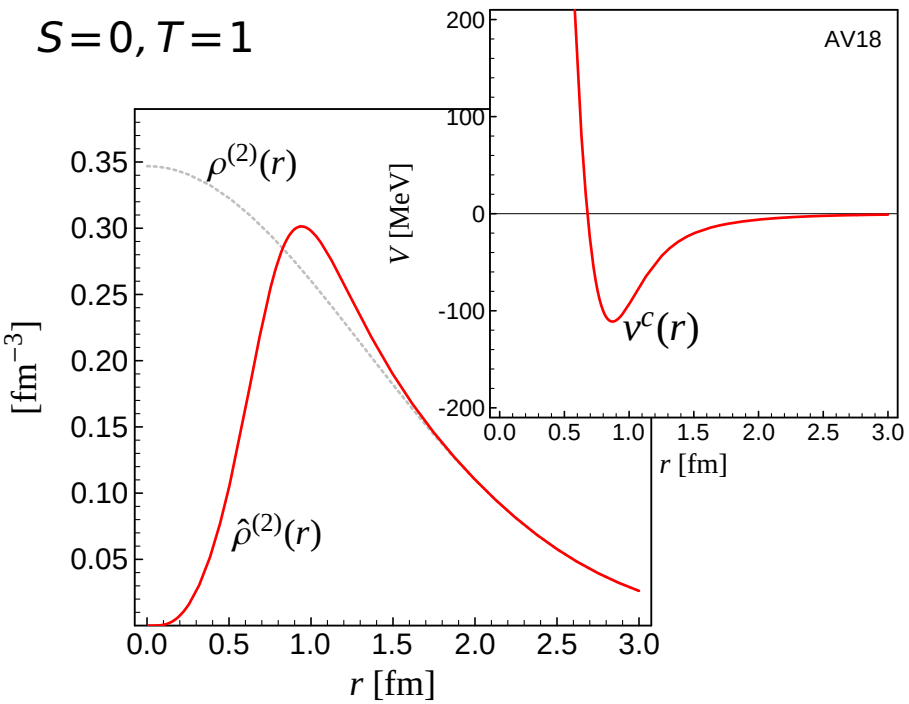

Tensor Correlations

$$\underset{\sim}{C}_\Omega = \exp\left\{-i\vartheta(r)\left\{\frac{3}{2}(\boldsymbol{\sigma}_1\cdot\mathbf{p}_\Omega)(\boldsymbol{\sigma}_2\cdot\mathbf{r}) + \frac{3}{2}(\boldsymbol{\sigma}_1\cdot\mathbf{r})(\boldsymbol{\sigma}_2\cdot\mathbf{p}_\Omega)\right.\right.$$

- tensor force admixes other angular momenta

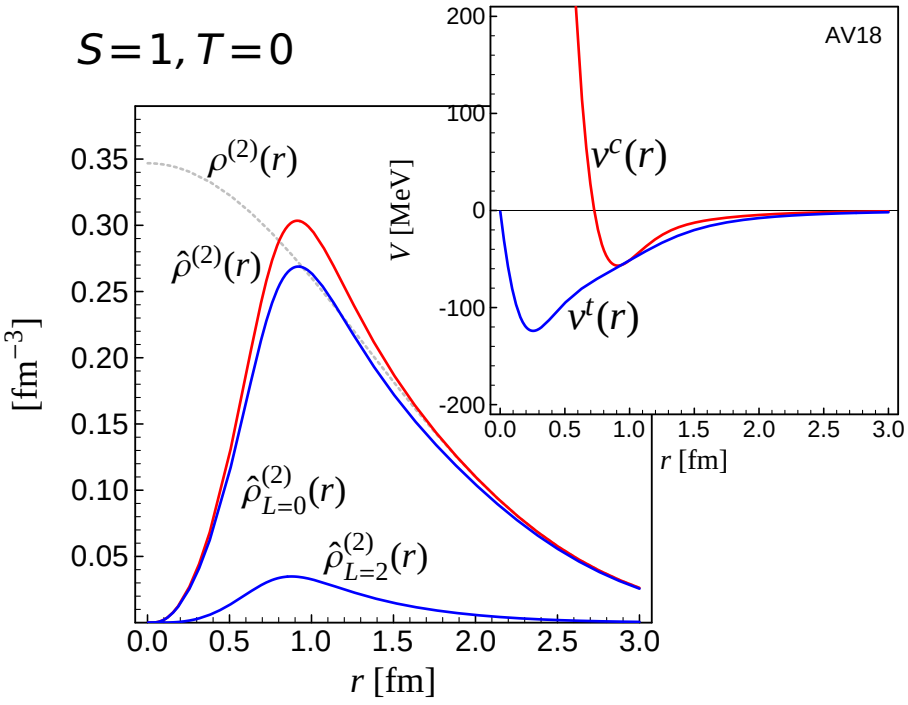

UCOM
Central and Tensor Correlations

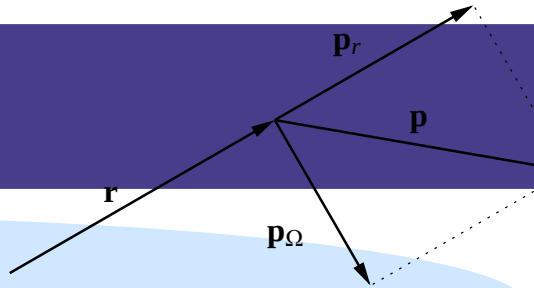

$$\underset{\sim}{C} = \underset{\sim}{C}_\Omega \underset{\sim}{C}_r$$

$$\mathbf{p} = \mathbf{p}_r + \mathbf{p}_\Omega$$

$$\mathbf{p}_r = \frac{1}{2}\left\{\frac{\mathbf{r}}{r}\left(\frac{\mathbf{r}}{r}\mathbf{p}\right) + \left(\mathbf{p}\frac{\mathbf{r}}{r}\right)\frac{\mathbf{r}}{r}\right\}, \qquad \mathbf{p}_\Omega = \frac{1}{2r}\left\{\mathbf{l}\times\frac{\mathbf{r}}{r} - \frac{\mathbf{r}}{r}\times\mathbf{l}\right\}$$

Central Correlations

$$\underset{\sim}{c}_r = \exp\left\{-\frac{i}{2}\{p_r s(r) + s(r) p_r\}\right\}$$

- probability density shifted out of the repulsive core

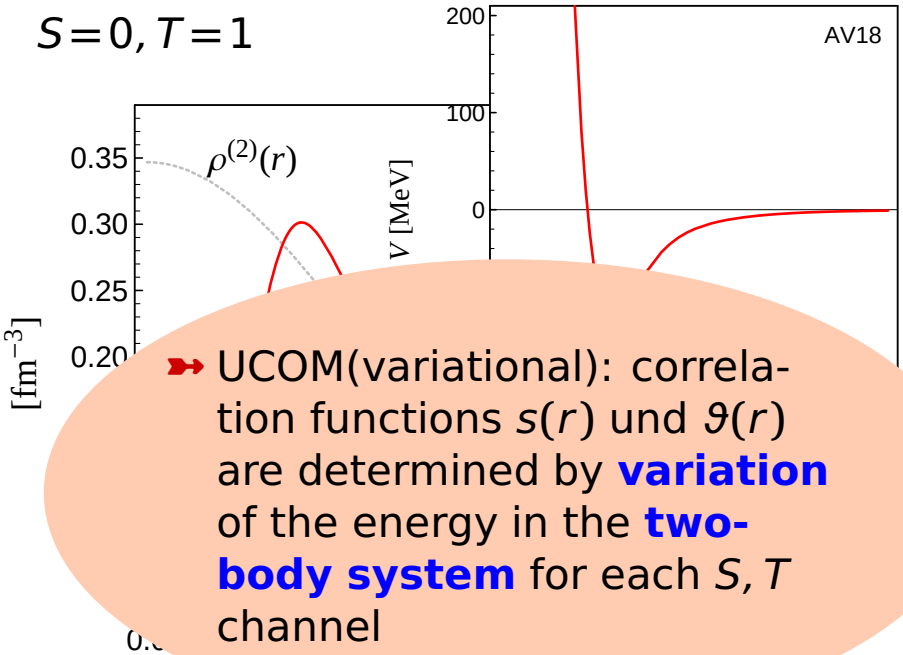

- UCOM(variational): correlation functions $s(r)$ und $\vartheta(r)$ are determined by **variation** of the energy in the **two-body system** for each S, T channel

Tensor Correlations

$$\underset{\sim}{c}_\Omega = \exp\left\{-i\vartheta(r)\left\{\frac{3}{2}(\boldsymbol{\sigma}_1\cdot\mathbf{p}_\Omega)(\boldsymbol{\sigma}_2\cdot\mathbf{r}) + \frac{3}{2}(\boldsymbol{\sigma}_1\cdot\mathbf{r})(\boldsymbol{\sigma}_2\cdot\mathbf{p}_\Omega)\right.\right.$$

- tensor force admixes other angular momenta

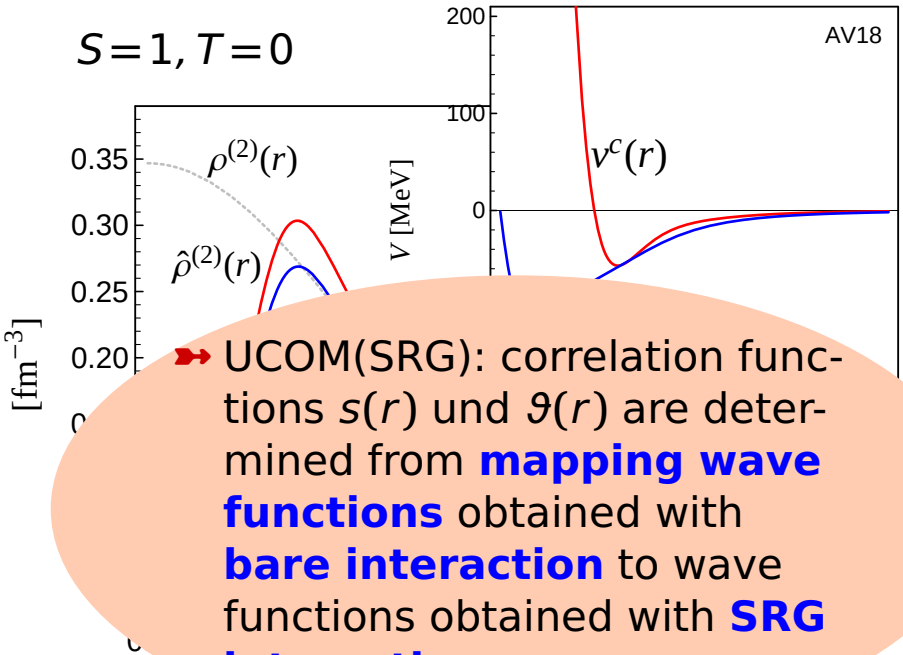

- UCOM(SRG): correlation functions $s(r)$ und $\vartheta(r)$ are determined from **mapping wave functions** obtained with **bare interaction** to wave functions obtained with **SRG interaction**

Correlations and Energies

two-body densities

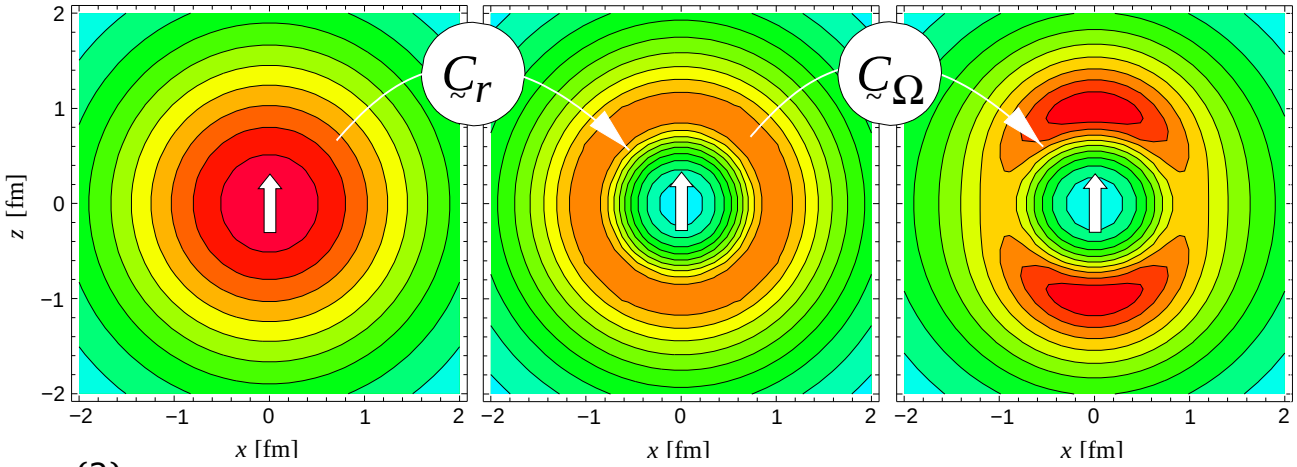

$\rho^{(2)}_{S,T}(\mathbf{r}_1 - \mathbf{r}_2) \quad S = 1, M_S = 1, T = 0$

central correlator C_r shifts density out of the repulsive core

tensor correlator C_Ω aligns density with spin orientation

Neff and Feldmeier, Nucl. Phys. **A713** (2003) 311

Correlations and Energies

two-body densities

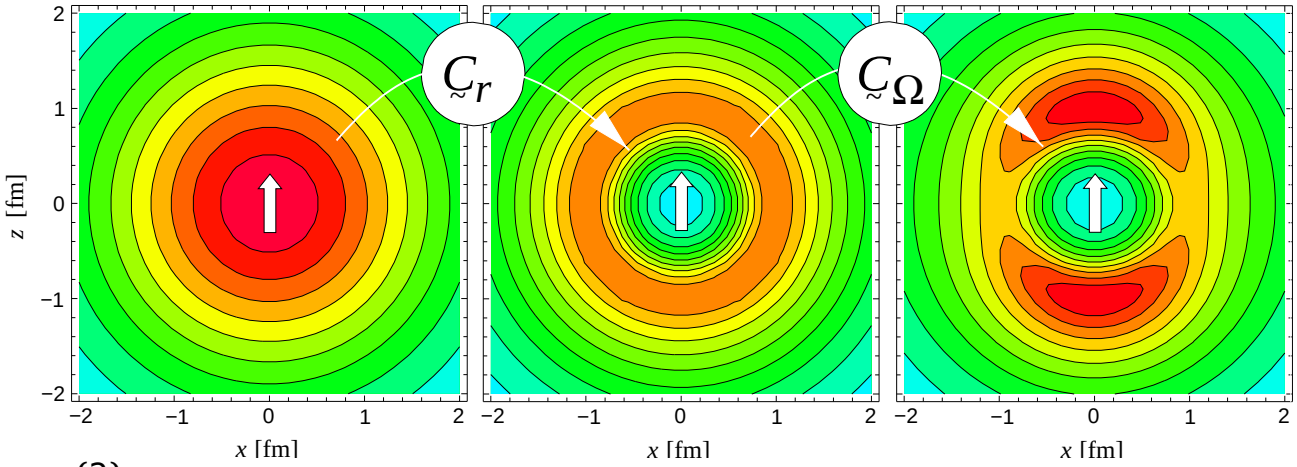

$\rho^{(2)}_{S,T}(\mathbf{r}_1 - \mathbf{r}_2) \quad S = 1, M_S = 1, T = 0$

central correlator C_r shifts density out of the repulsive core

tensor correlator C_Ω aligns density with spin orientation

both central and tensor correlations are essential for binding

energies

$0\hbar\omega$ Harmonic Oscillator

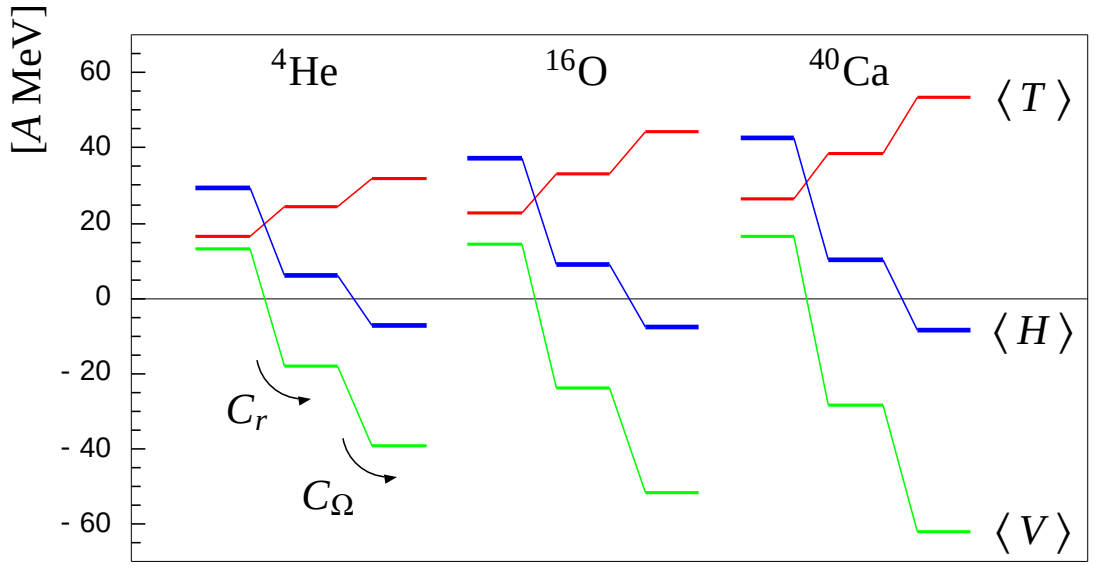

Neff and Feldmeier, Nucl. Phys. **A713** (2003) 311

Two-body Densities

coordinate space

$S = 1, M_S = 1, T = 0$

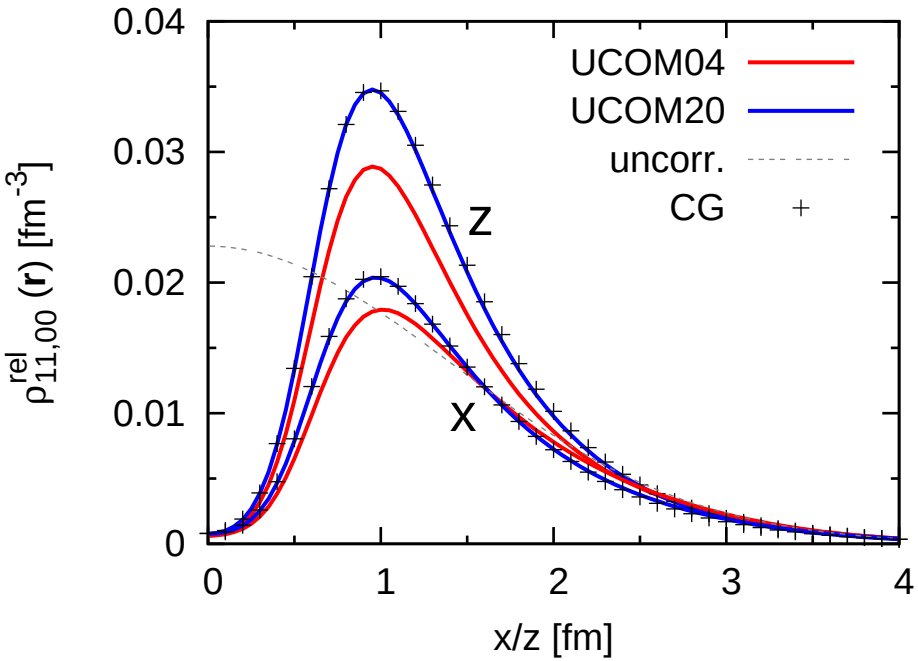

momentum space

$S = 1, T = 0$

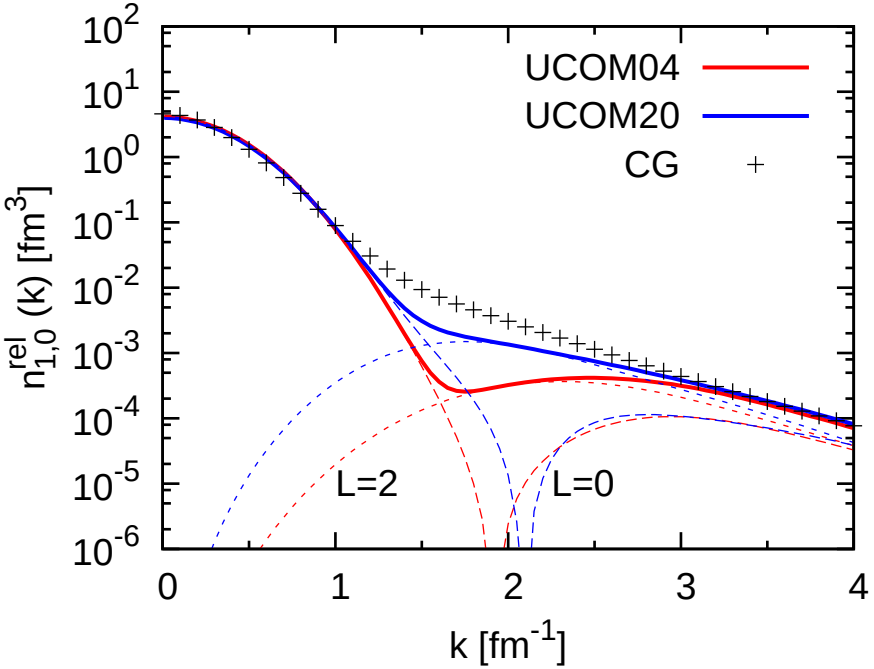

- two-body densities calculated from $0\hbar\Omega$ ^{4}He and correlated density operators
- high-momentum components dominated by tensor correlations
- long-range correlations should fill up momentum space two-body density above the Fermi momentum

Feldmeier, Horiuchi, Neff, Suzuki, Phys. Rev. C **84**, 054003 (2011)

Correlated Interaction in Momentum Space

$^3S_1$ bare

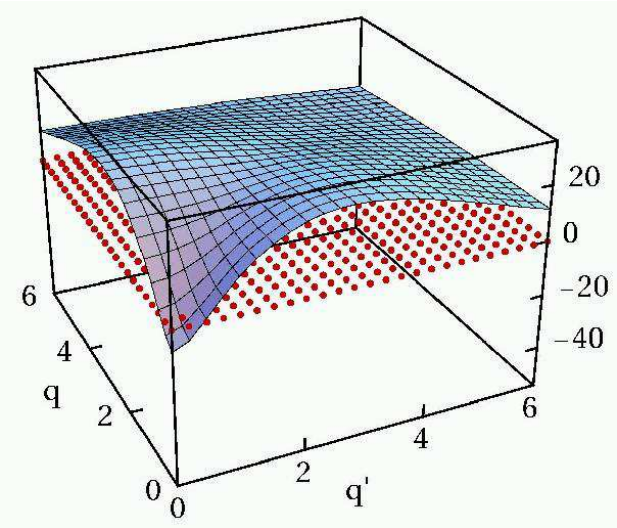

bare interaction has **strong** **off-diagonal** matrix elements connecting to high momenta

$^3S_1$ - $^3D_1$ bare

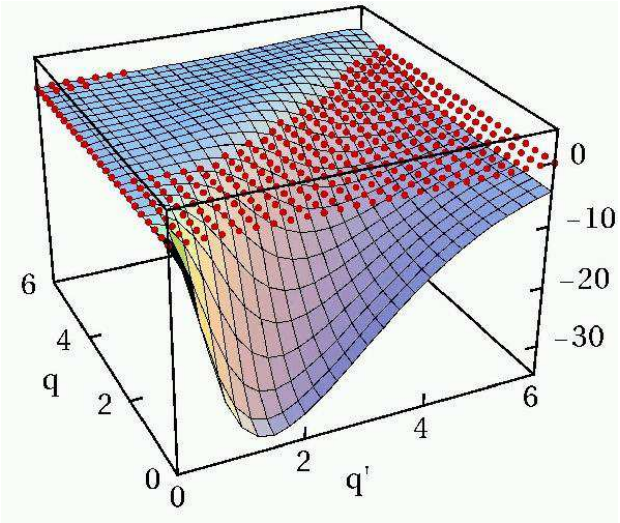

Roth, Hergert, Papakonstaninou, Neff, Feldmeier, Phys. Rev. C **72**, 034002 (2005)

Correlated Interaction in Momentum Space

$^3S_1$ bare

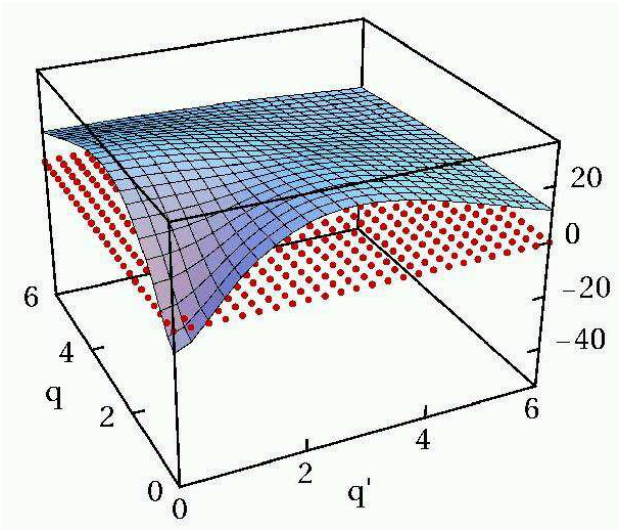

bare interaction has **strong off-diagonal** matrix elements connecting to high momenta

$^3S_1$ - $^3D_1$ bare

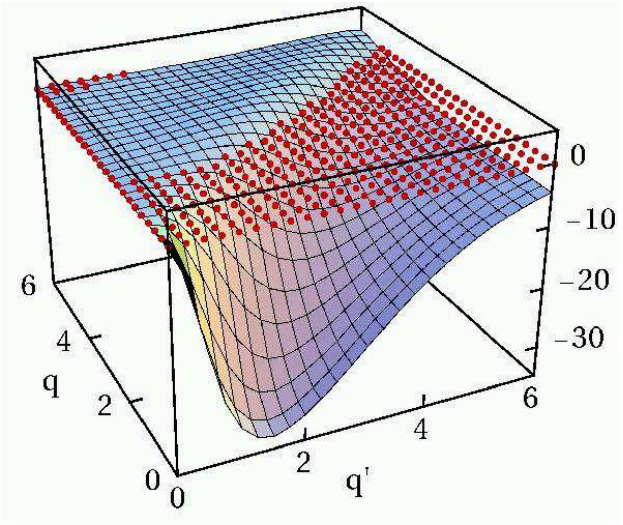

$^3S_1$ correlated

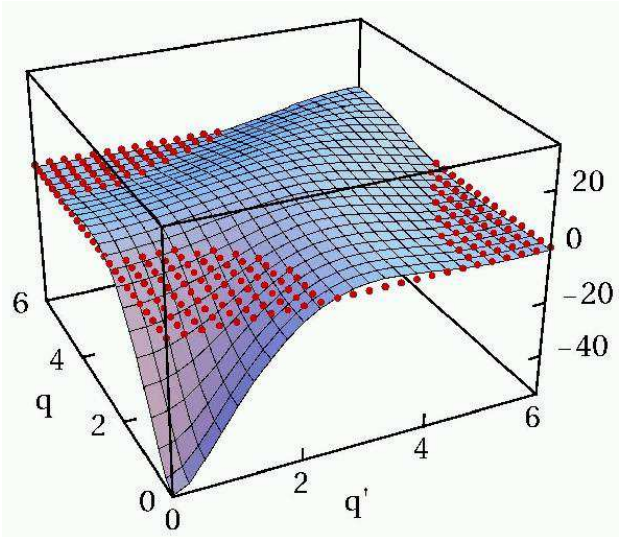

correlated interaction is **more attractive** at low momenta

off-diagonal matrix elements connecting low- and high- momentum states are **strongly reduced**

$^3S_1$ - $^3D_1$ correlated

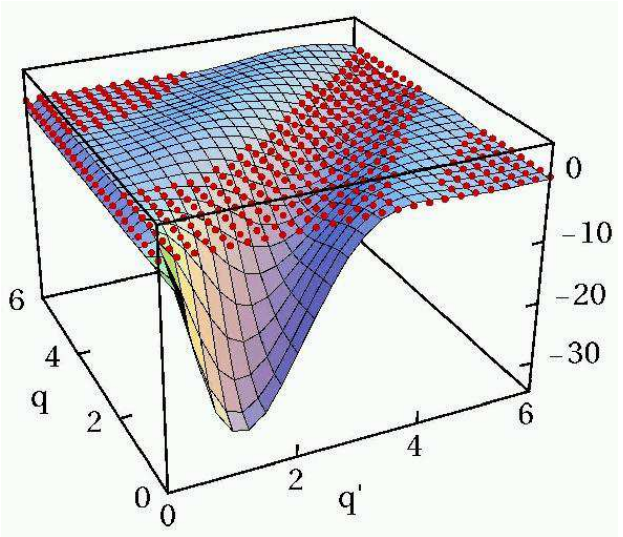

Roth, Hergert, Papakonstaninou, Neff, Feldmeier, Phys. Rev. C **72**, 034002 (2005)

Correlated Interaction in Momentum Space

$^3S_1$ bare

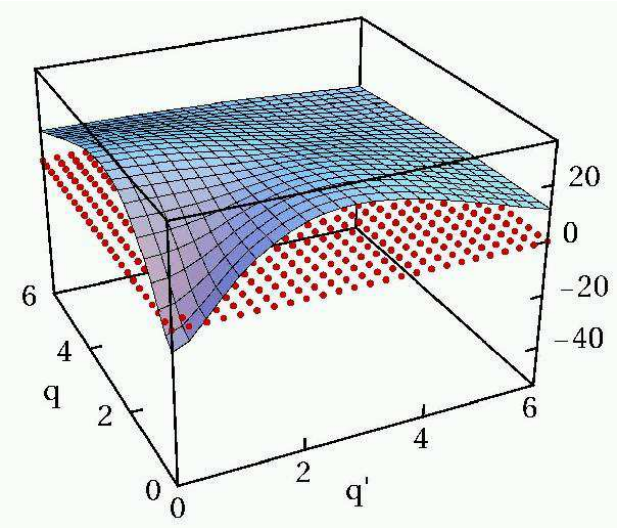

bare interaction has **strong off-diagonal** matrix elements connecting to high momenta

$^3S_1$ - $^3D_1$ bare

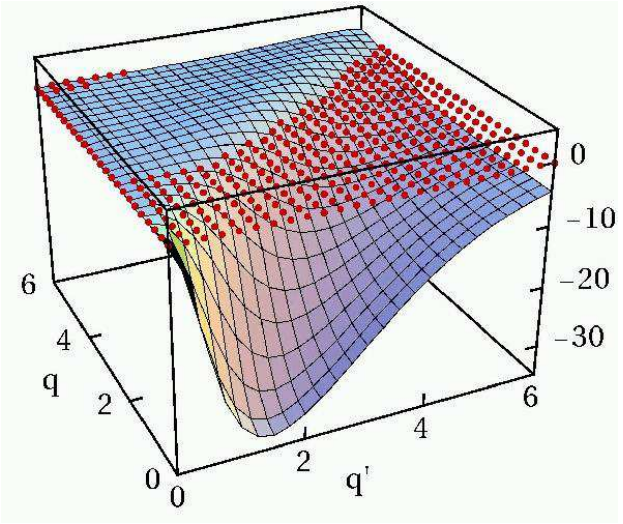

$^3S_1$ correlated

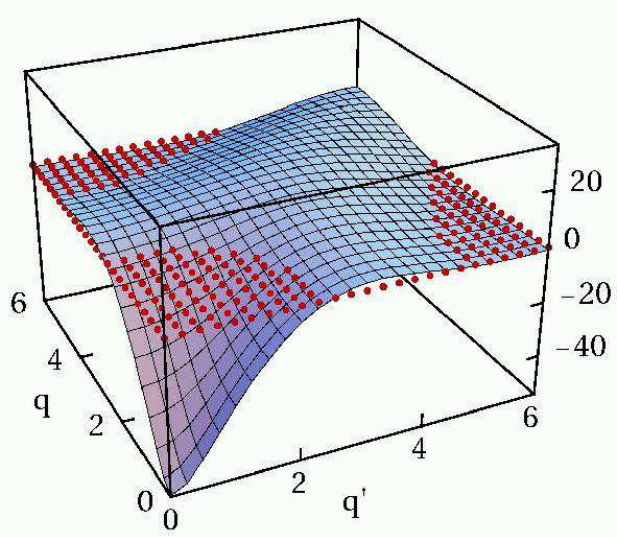

correlated interaction is **more attractive** at low momenta

off-diagonal matrix elements connecting low- and high- momentum states are **strongly reduced**

$^3S_1$ - $^3D_1$ correlated

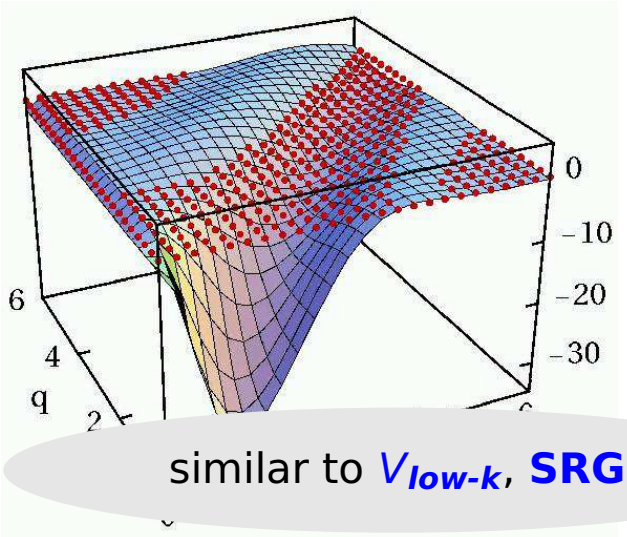

similar to $V_{low\text{-}k}$, **SRG**

Roth, Hergert, Papakonstaninou, Neff, Feldmeier, Phys. Rev. C **72**, 034002 (2005)

Similarity Renormalization Group

SRG Interaction

Connection between UCOM and SRG

SRG in Momentum Space

Many-Body Calculations

Similarity Renormalization Group

SRG approach

- Unitary transformation of the Hamiltonian

$$\tilde{\underset{\sim}{H}}(\alpha) = \underset{\sim}{C}^{\dagger}(\alpha)\underset{\sim}{H}\underset{\sim}{C}(\alpha)$$

- Transformation given by Flow Equation

$$\tilde{\underset{\sim}{H}}(0) = \underset{\sim}{H}, \quad \frac{d}{d\alpha}\tilde{\underset{\sim}{H}}(\alpha) = [\underset{\sim}{\eta}(\alpha), \tilde{\underset{\sim}{H}}(\alpha)]_-$$

- Generator $\eta(\alpha)$ chosen to evolve Hamiltonian into band-diagonal structure in momentum-space

$$\underset{\sim}{\eta}(\alpha) = [\underset{\sim}{T}, \tilde{\underset{\sim}{H}}(\alpha)]_-$$

- Technically flow-equation is easily solved in given (momentum) basis

Hergert, Roth, Phys. Rev. C **75**, 051001(R) (2007)
Bogner *et. al.*, Phys. Rev. C **75**, 061001(R) (2007)

SRG and UCOM

- UCOM generators for central and tensor correlations are generated by flow equation

$$[\underset{\sim}{p_r}^2, V(r)]_- = -i\left(\underset{\sim}{p_r}V'(r) + V'(r)\underset{\sim}{p_r}\right)$$

$$[\frac{\underset{\sim}{\mathbf{L}}^2}{r^2}, V_T(r)\underset{\sim}{S}_{12}(\hat{r},\hat{r})]_- = -4i\frac{V_T(r)}{r^2}\underset{\sim}{S}_{12}(\mathbf{r},\mathbf{p}_\Omega)$$

- Generator for $\alpha = 0$ has the form of the UCOM generator

$$\underset{\sim}{\eta}(0) = \frac{i}{2}\left(\underset{\sim}{p_r}S(r) + S(r)\underset{\sim}{p_r}\right) + i\Theta(r)\underset{\sim}{S}_{12}(\mathbf{r},\mathbf{p}_\Omega)$$

UCOM(SRG)

- Define UCOM correlation functions by mapping of S- and P-wave zero-energy scattering solutions:

$$\left|\tilde{\psi}(0)\right\rangle = \underset{\sim}{C}_\Omega\underset{\sim}{C}_r\left|\tilde{\psi}(\alpha)\right\rangle$$

SRG Evolution

AV18

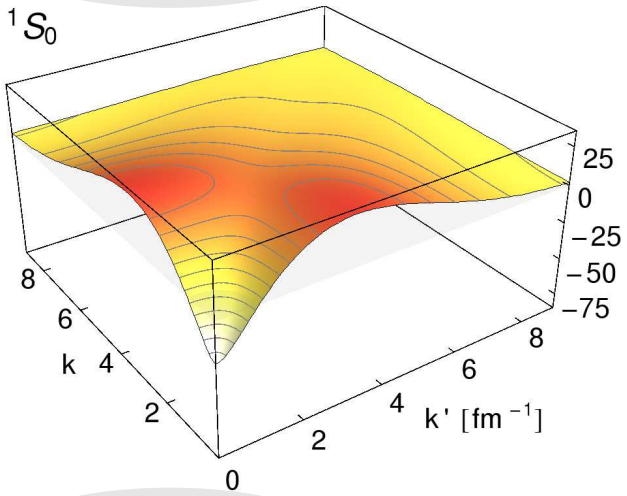

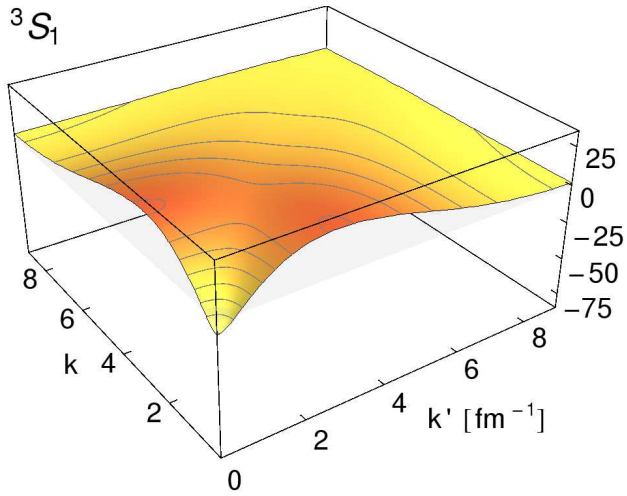

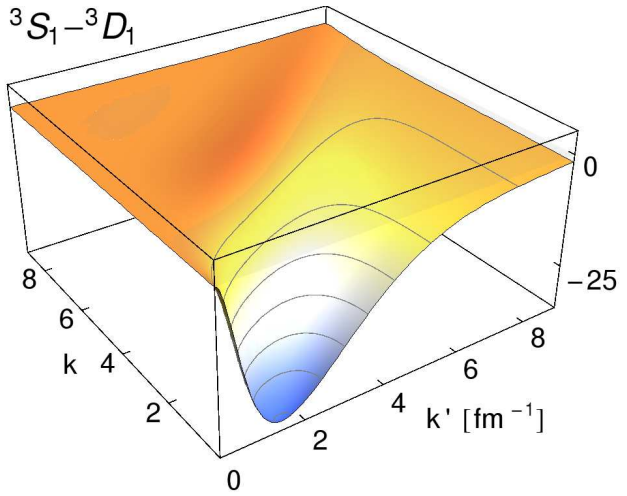

N3LO

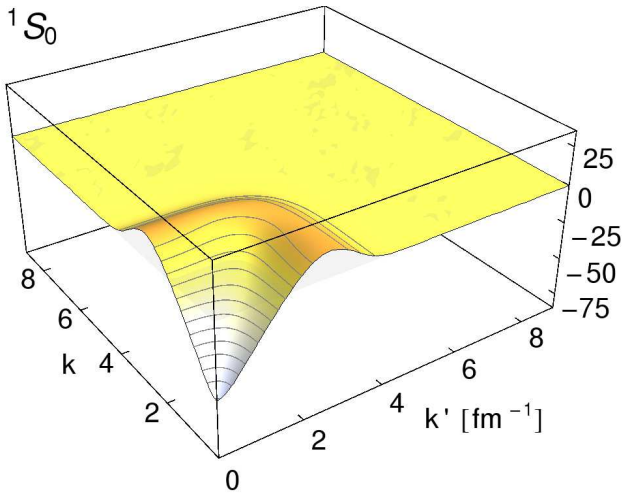

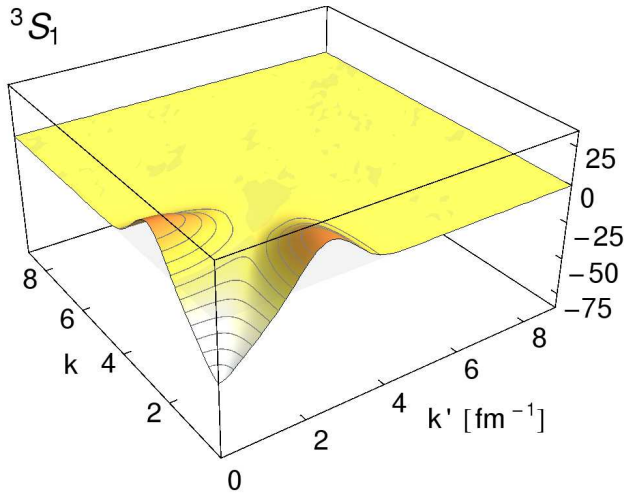

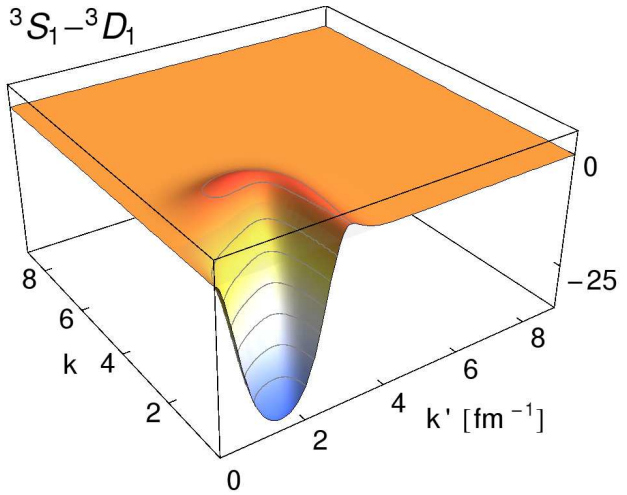

$\alpha = 0.00\text{fm}^4$

SRG Evolution

AV18

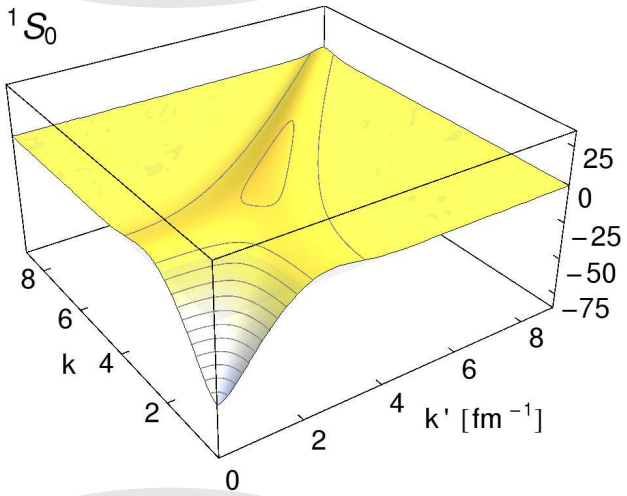

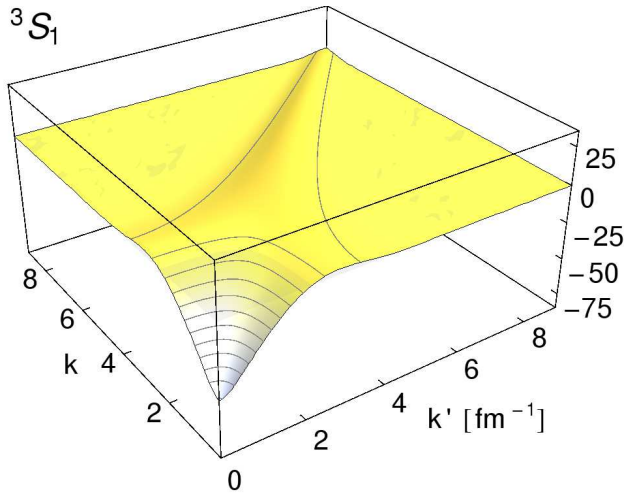

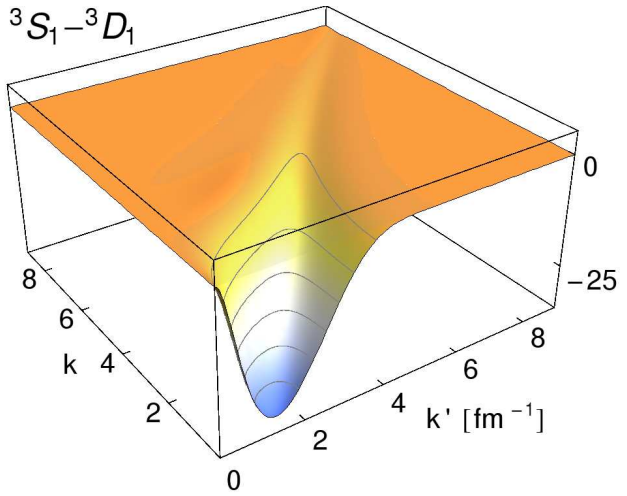

N3LO

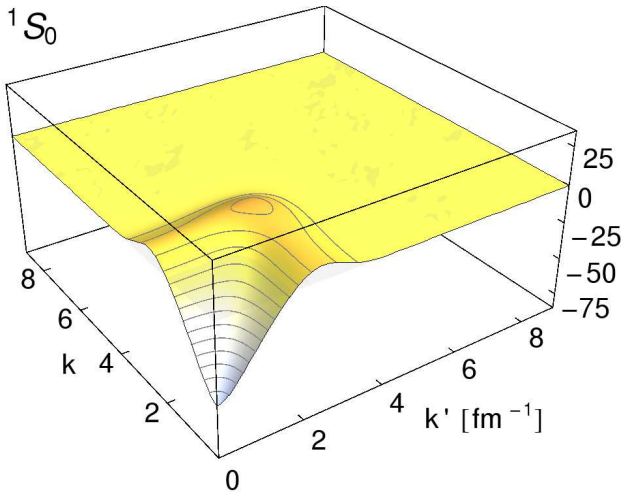

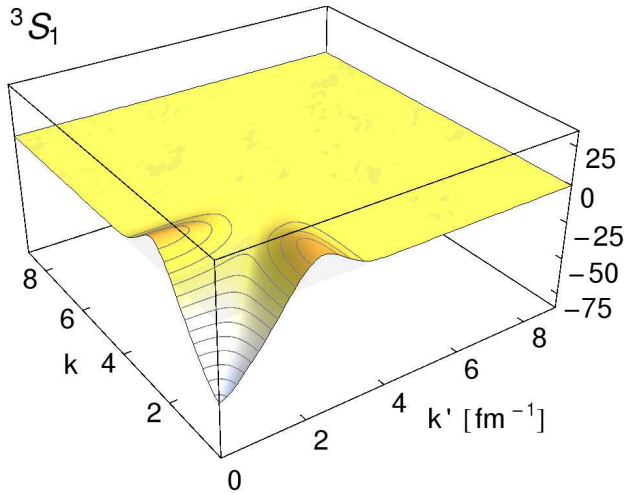

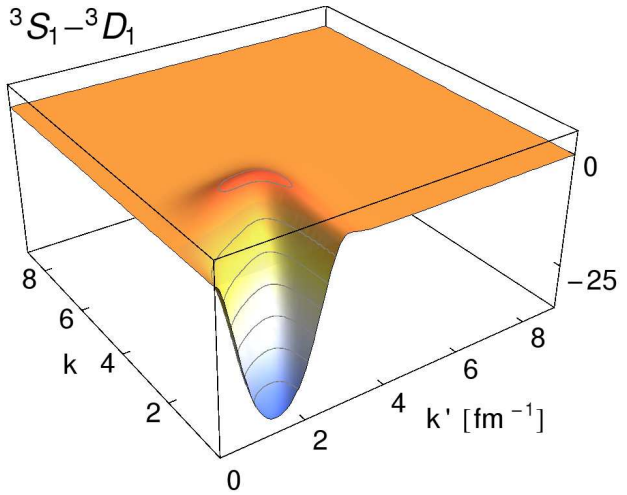

$\alpha = 0.01\text{fm}^4$

SRG Evolution

AV18

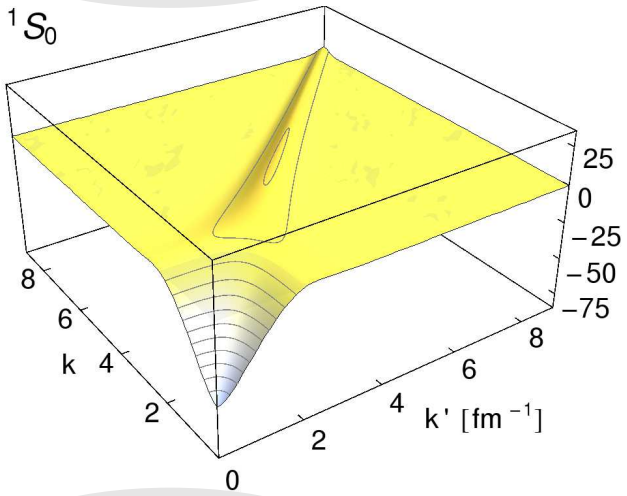

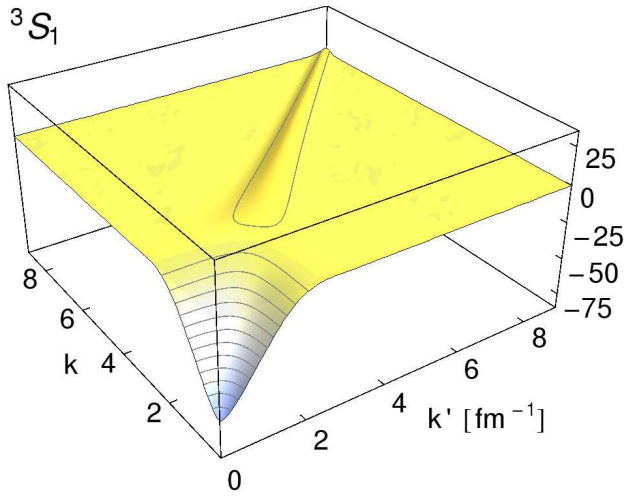

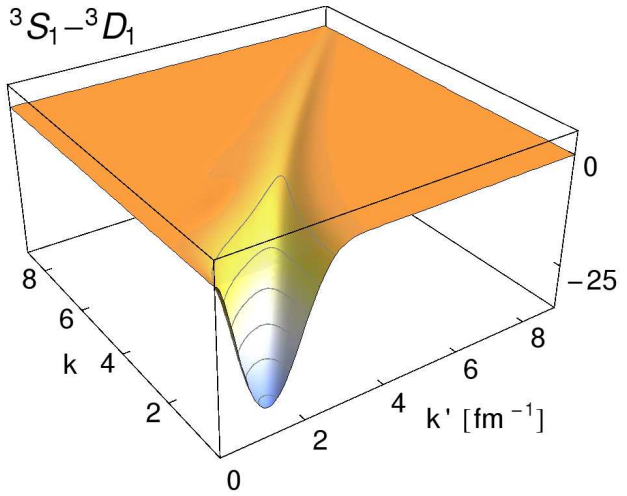

N3LO

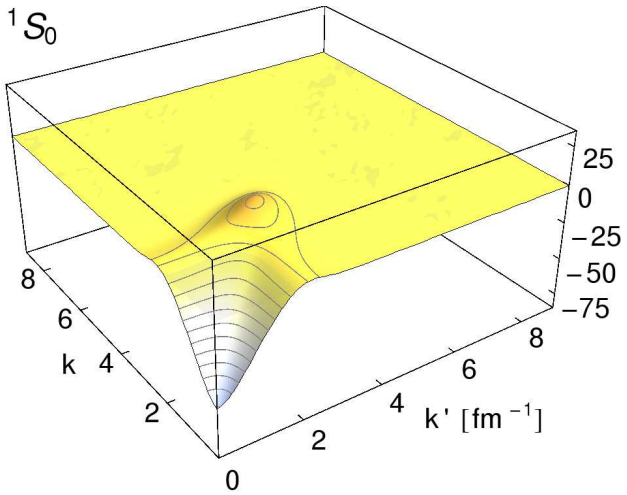

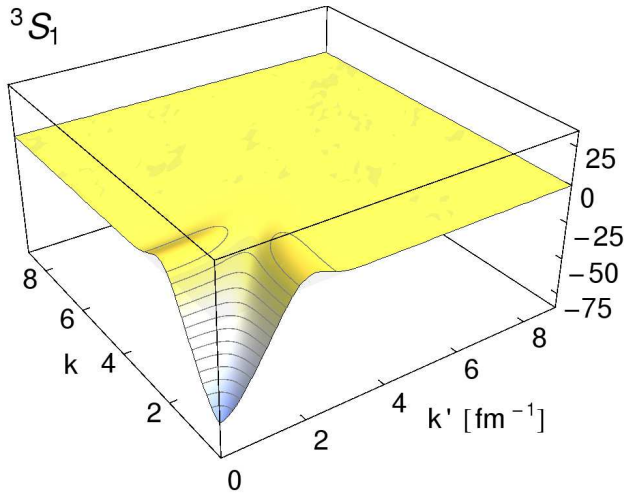

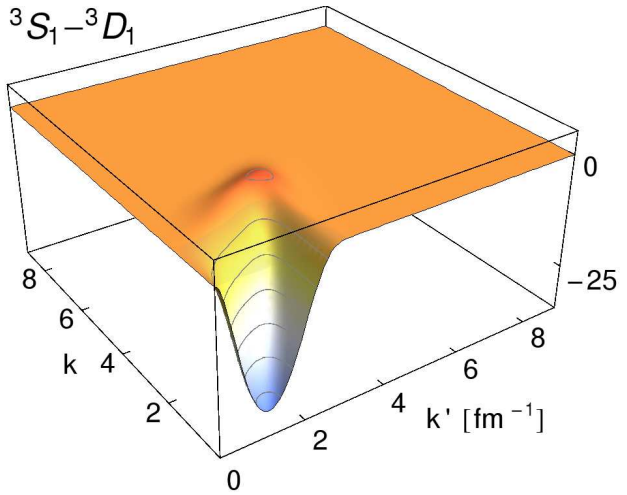

$\alpha = 0.04\text{fm}^4$

SRG Evolution

AV18

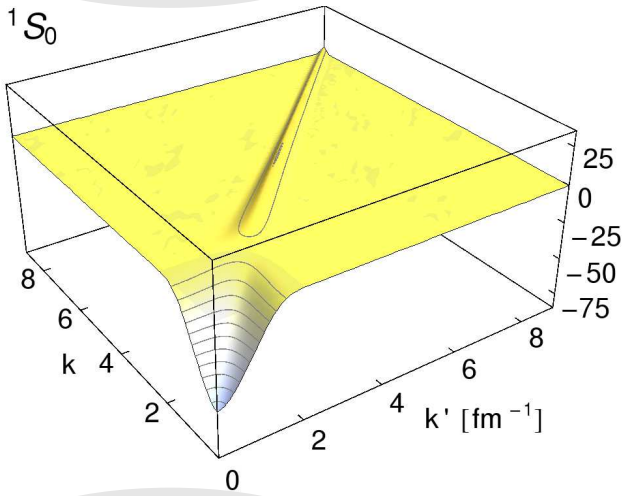

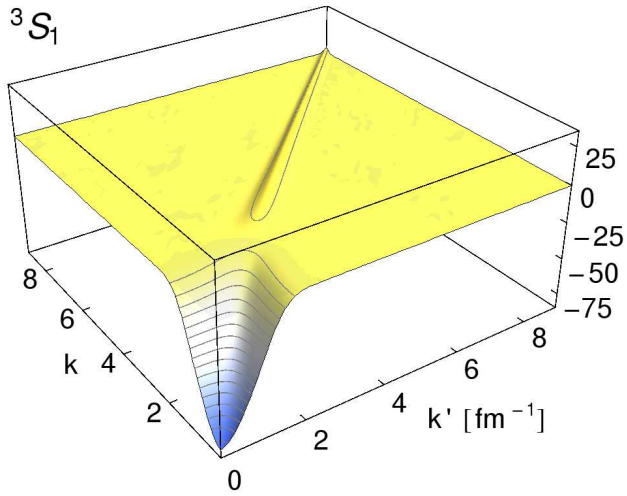

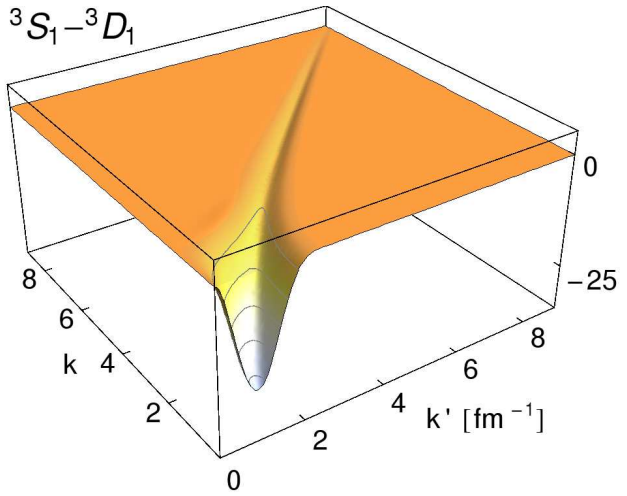

N3LO

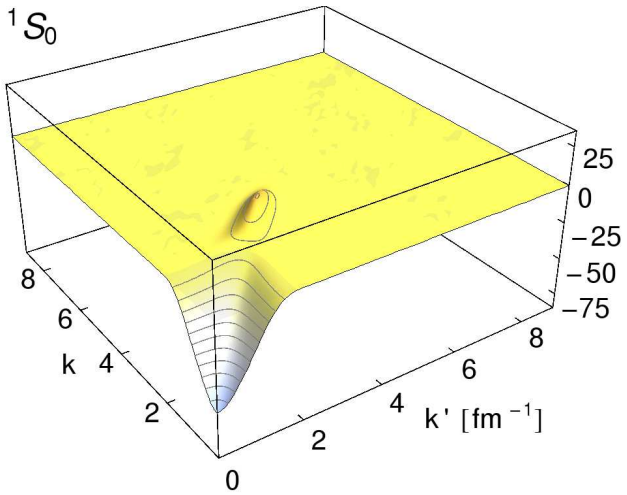

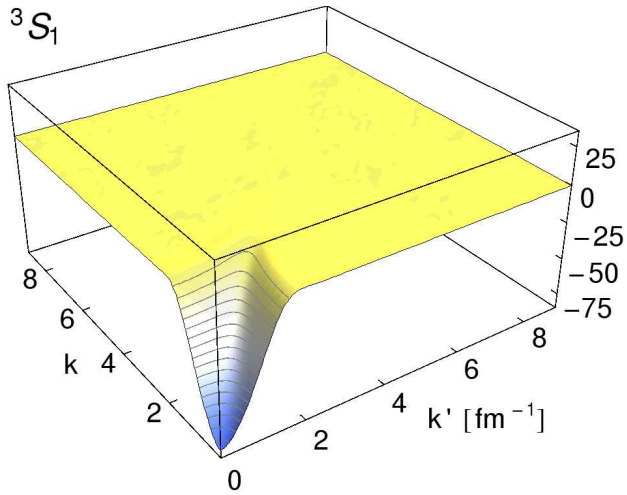

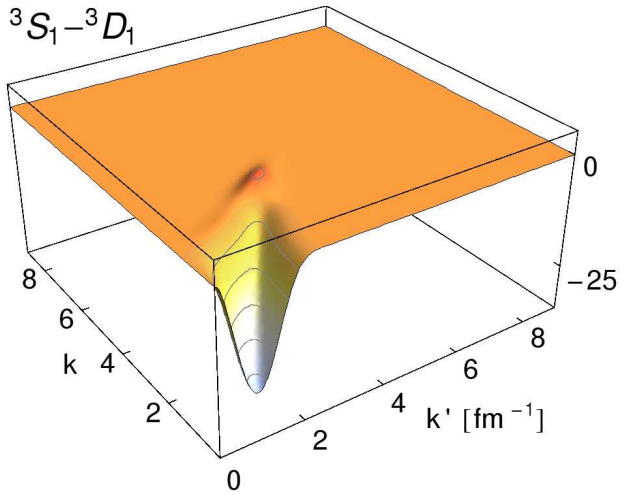

$\alpha = 0.20\text{fm}^4$

No-Core Shell Model

- Diagonalize Hamiltonian
- Slater determinants built from harmonic oscillator single-particle states

- $0\hbar\Omega$ configurations: occupy lowest single particle orbits
- $N\hbar\Omega$ configurations: N oscillator quanta above $0\hbar\Omega$ configuration
- use all configurations with $N \leq N_{\max}$

- Check for convergence with respect to $N_{\max}$
- Check for independence with respect to oscillator parameter

- Model space sizes grow rapidly with N and A

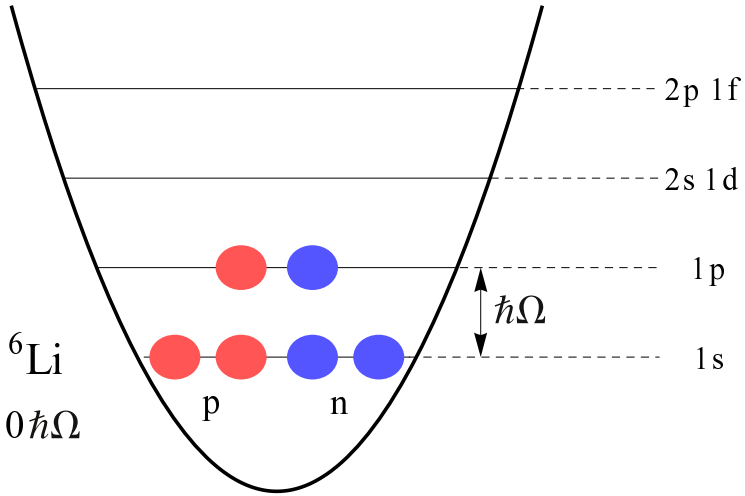

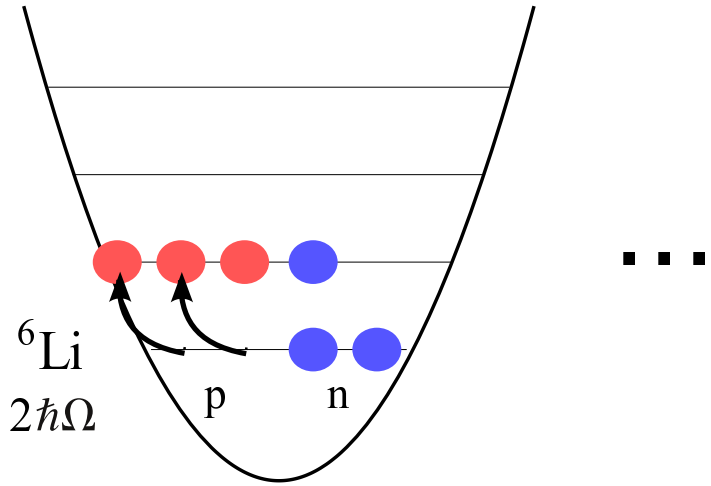

Navratil, Kamuntavicius, Barrett, PRC 61, 044001 (2000)

No-Core Shell Model Calculations

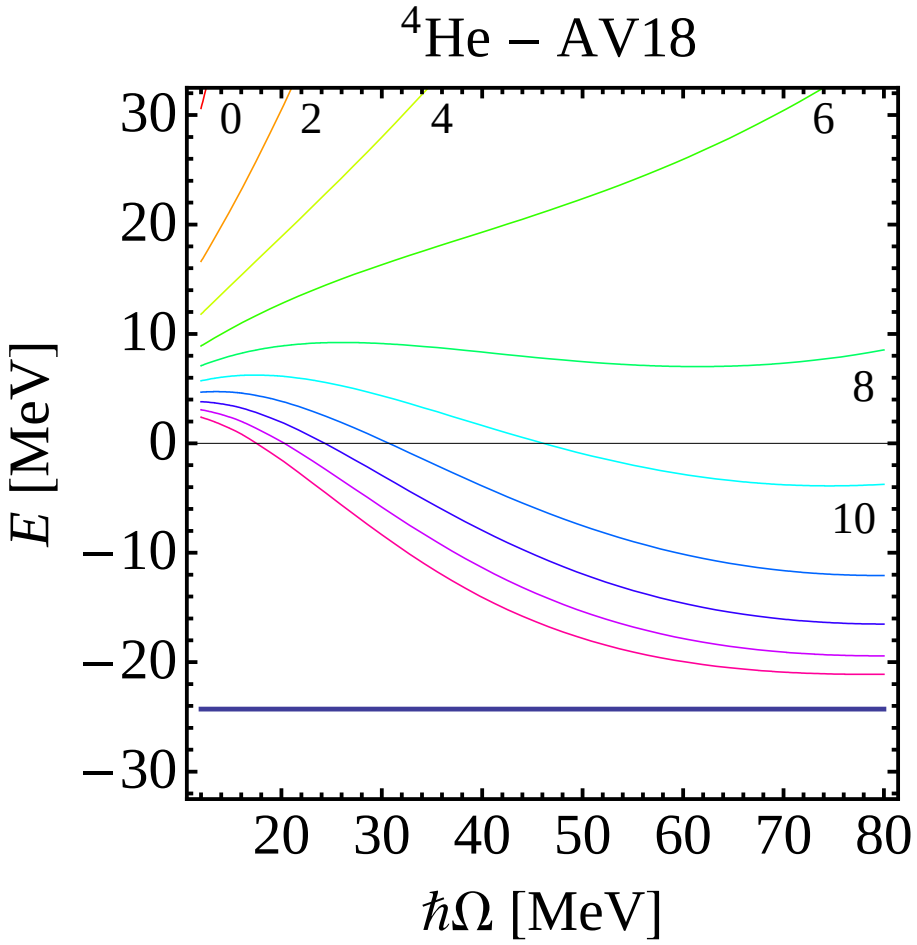

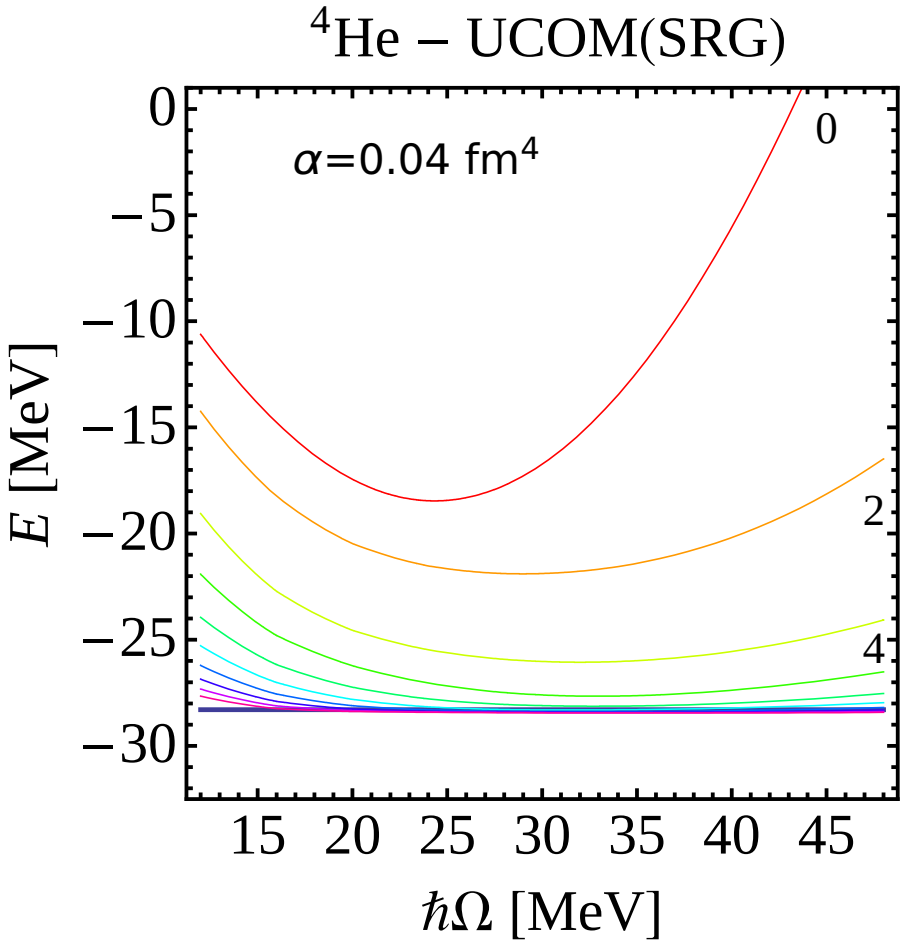

- convergence much improved compared to bare interaction
- effective interaction – in two-body approximation – converges to different energy then bare interaction

Roth, Neff, Feldmeier, Prog. Part. Nucl. Phys. **65**, 50 (2010)

Tjon-line

- transformations are not unitary on the many-body level!
- many-body results depend on the flow parameter α
- unitarily transformed two-body Hamiltonian gives results closer to experimental results for light nuclei
- partial cancellation of induced and genuine three-body forces

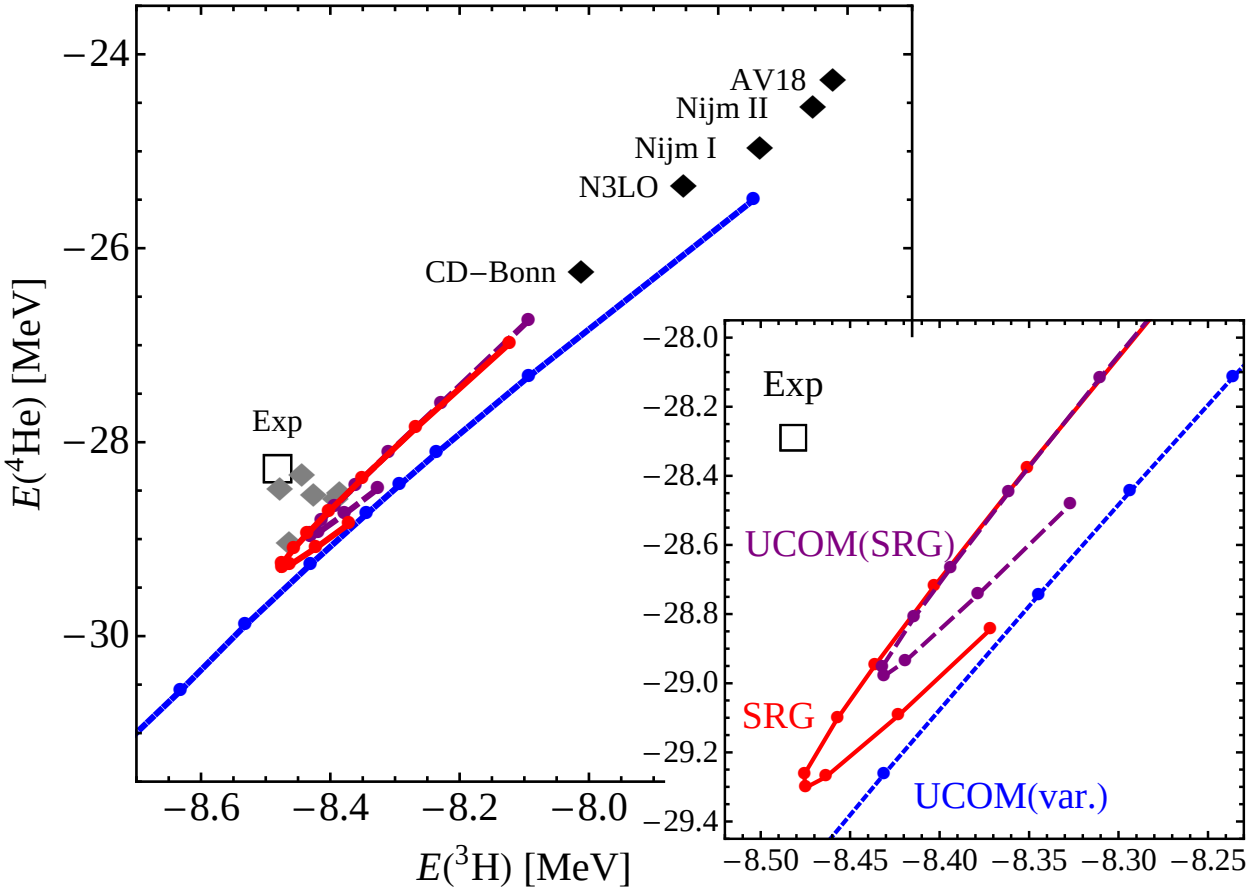

UCOM(SRG)

NCSM ^{6}Li/^{7}Li ground state energy

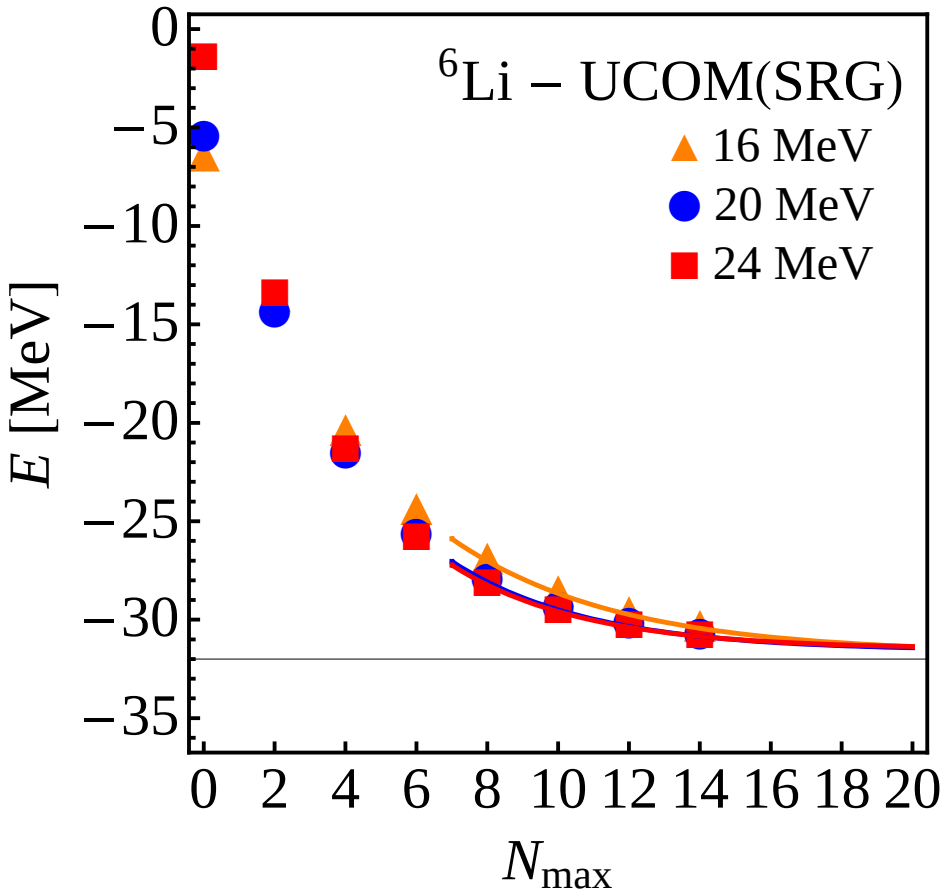

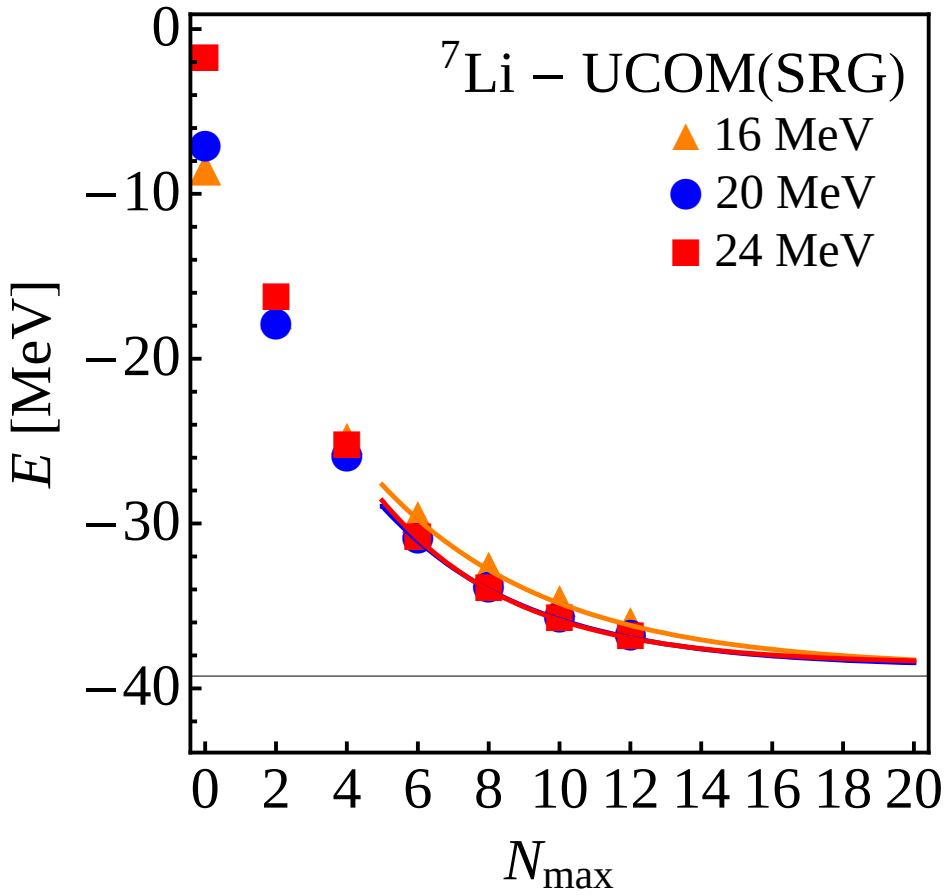

- effective two-body interaction also works well for (slightly) heavier nuclei

NCSM Li6 spectrum

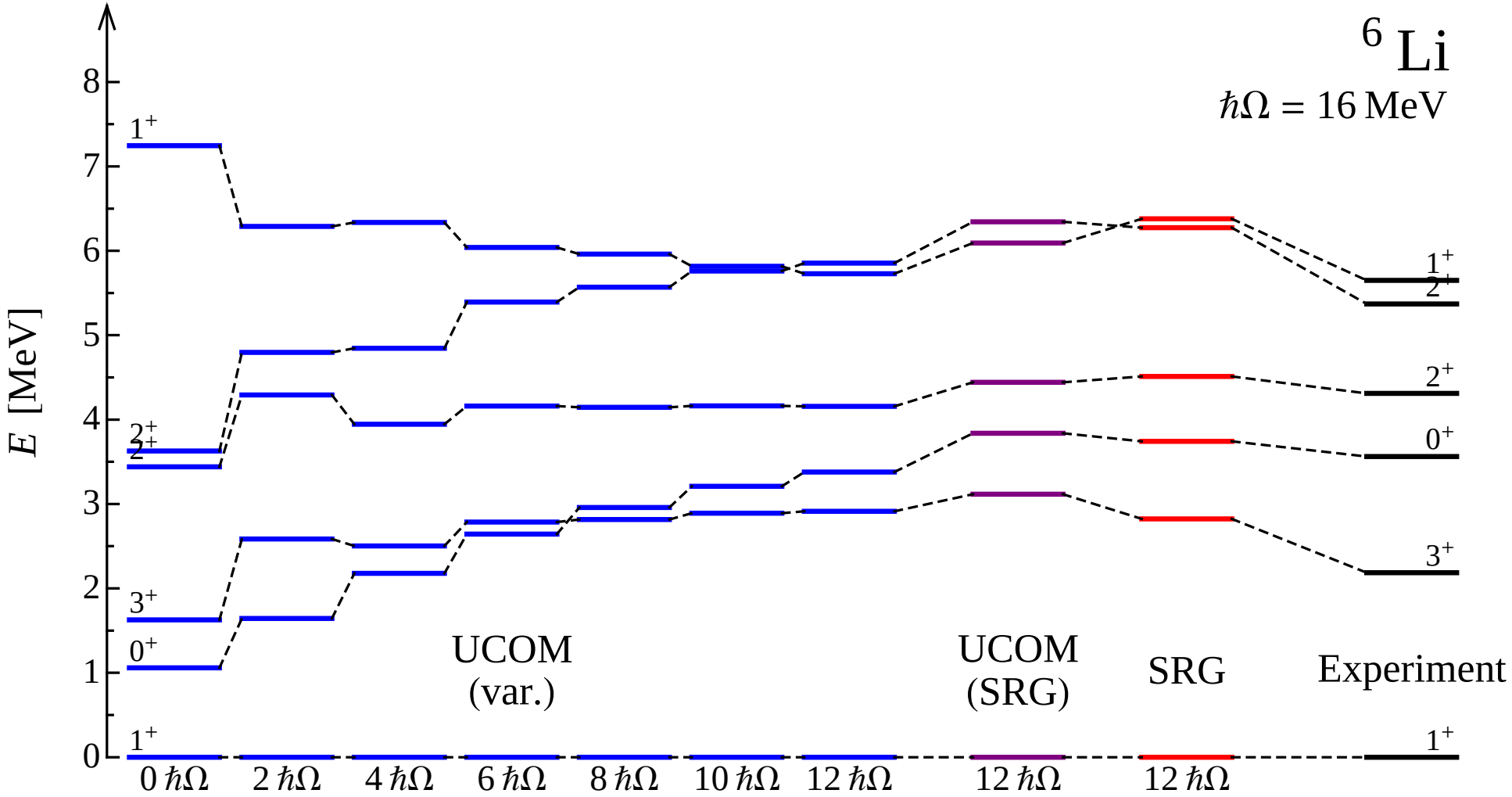

NCSM ^{7}Li spectrum

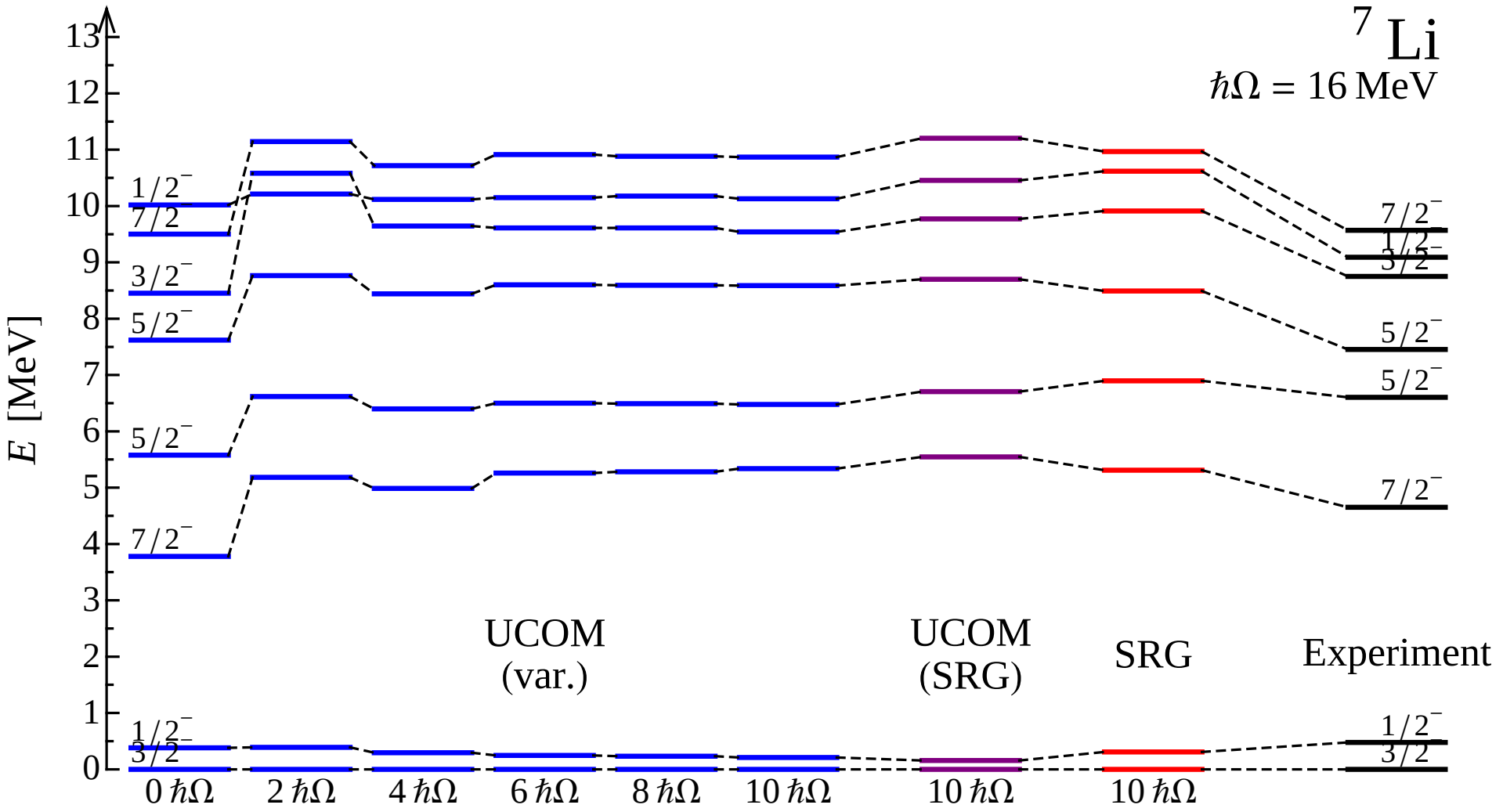

UCOM(SRG)

NCSM ^{6}Li/^{7}Li radii

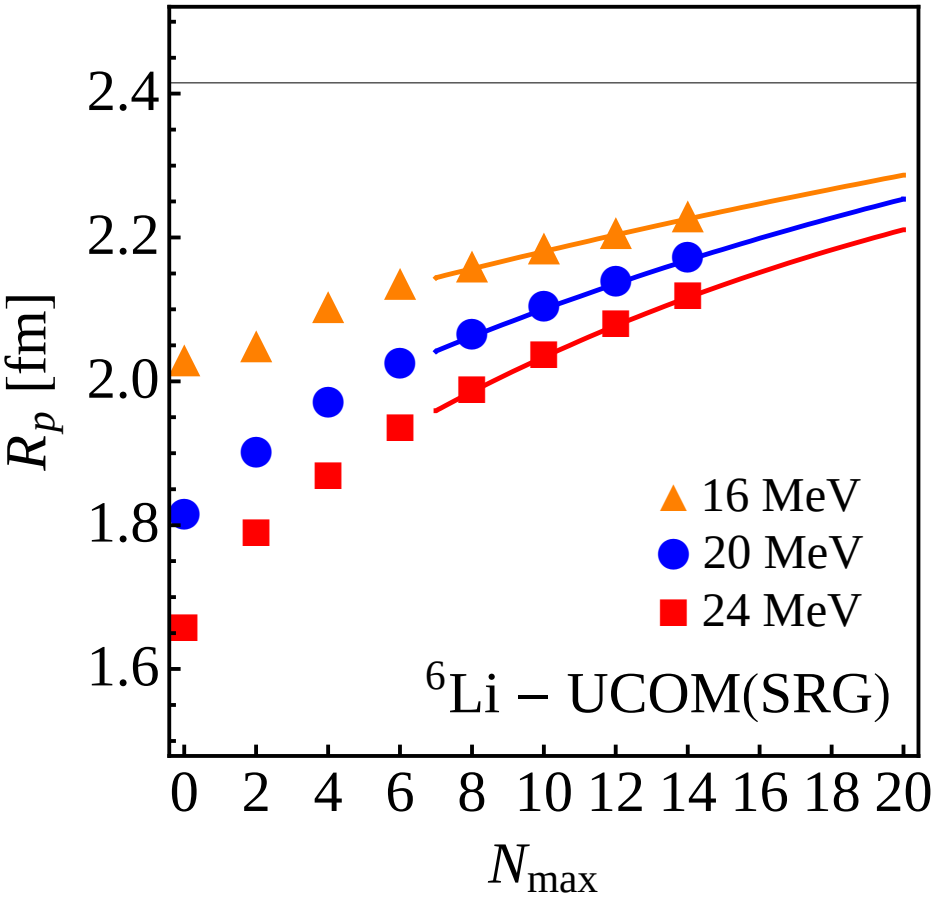

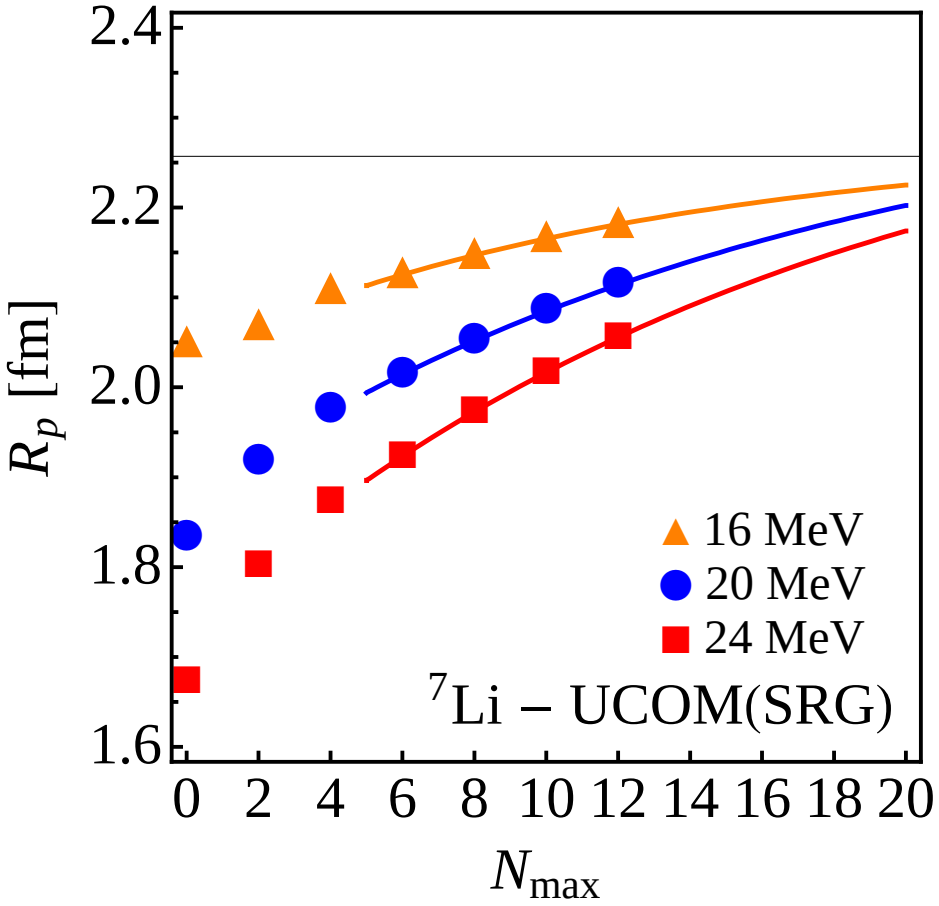

- radii converge worse than energies
- harmonic oscillator basis not well suited to describe tails of weakly bound nuclei

UCOM(SRG)

NCSM ^{6}Li/^{7}Li quadrupole moments

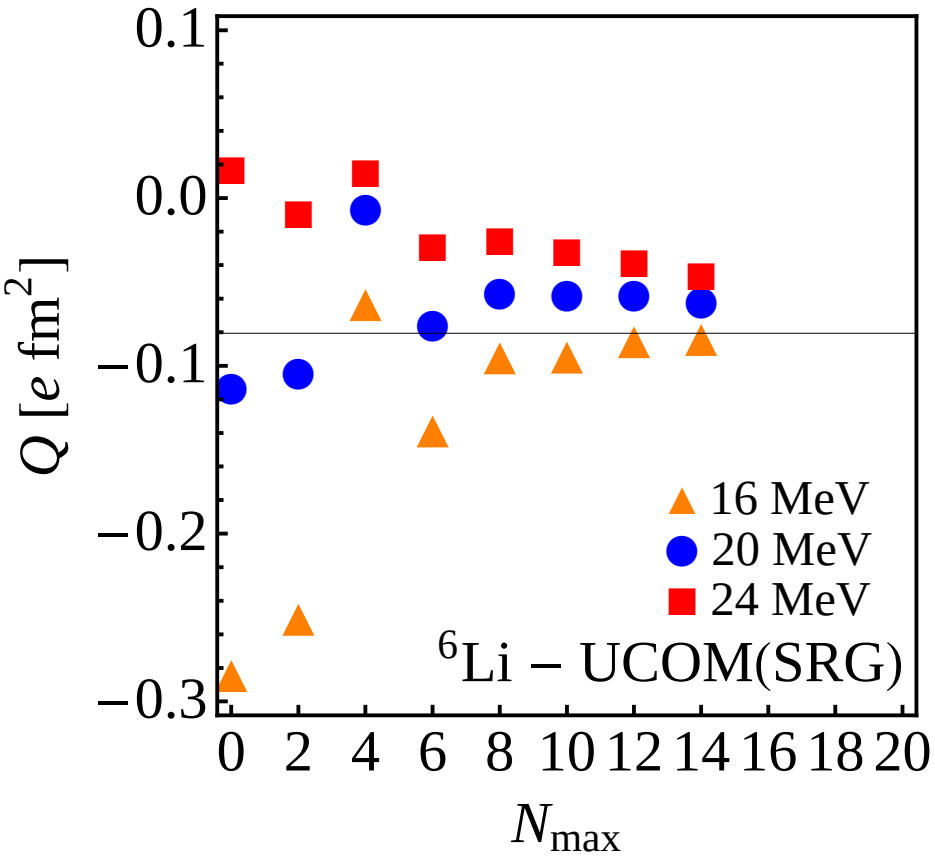

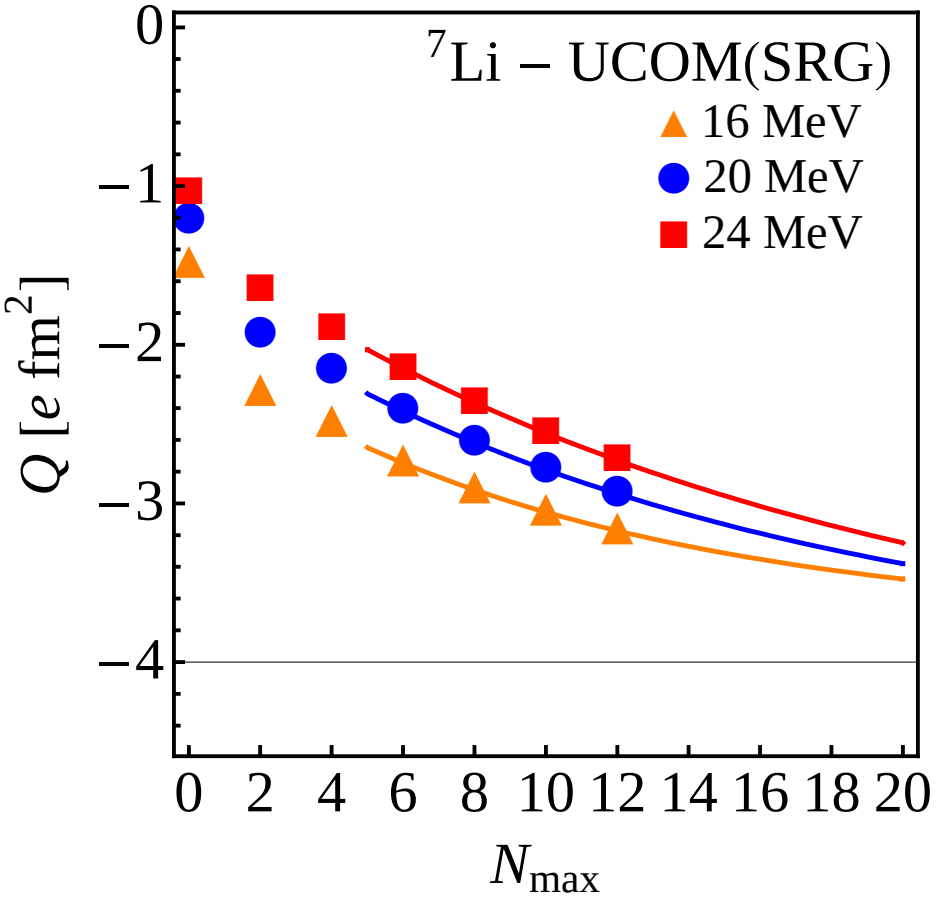

- ^{6}Li quadrupole moment small and negative – essentially $L = 0$ relative motion of deuteron relative to ^{4}He
- ^{3}H-^{4}He cluster structure in ^{7}Li – slow convergence in NCSM model space

Summary: UCOM . . .

- Realistic nucleon-nucleon interactions describe the deuteron and the nucleon-nucleon scattering data
- Realistic nucleon-nucleon interactions induce strong short-range central and tensor correlations
- Short-range correlations can be “absorbed” by unitary transformations (UCOM/SRG)
- Unitarily transformed interactions decouple low- and high-momentum modes
- Such “low-momentum” interactions make many-body calculations possible
- The No-Core Shell is a very powerful many-body approach – but the harmonic oscillator basis is not very suited for loosely bound systems

Overview: FMD

Fermionic Molecular Dynamics (FMD)
Wave Functions

Nucleon-Nucleon Interaction

Mean-Field Calculations

Projection After Variation,
Variation After Projection
and Multiconfiguration Mixing

Clustering and Delocalization

Exotica: Special Challenges

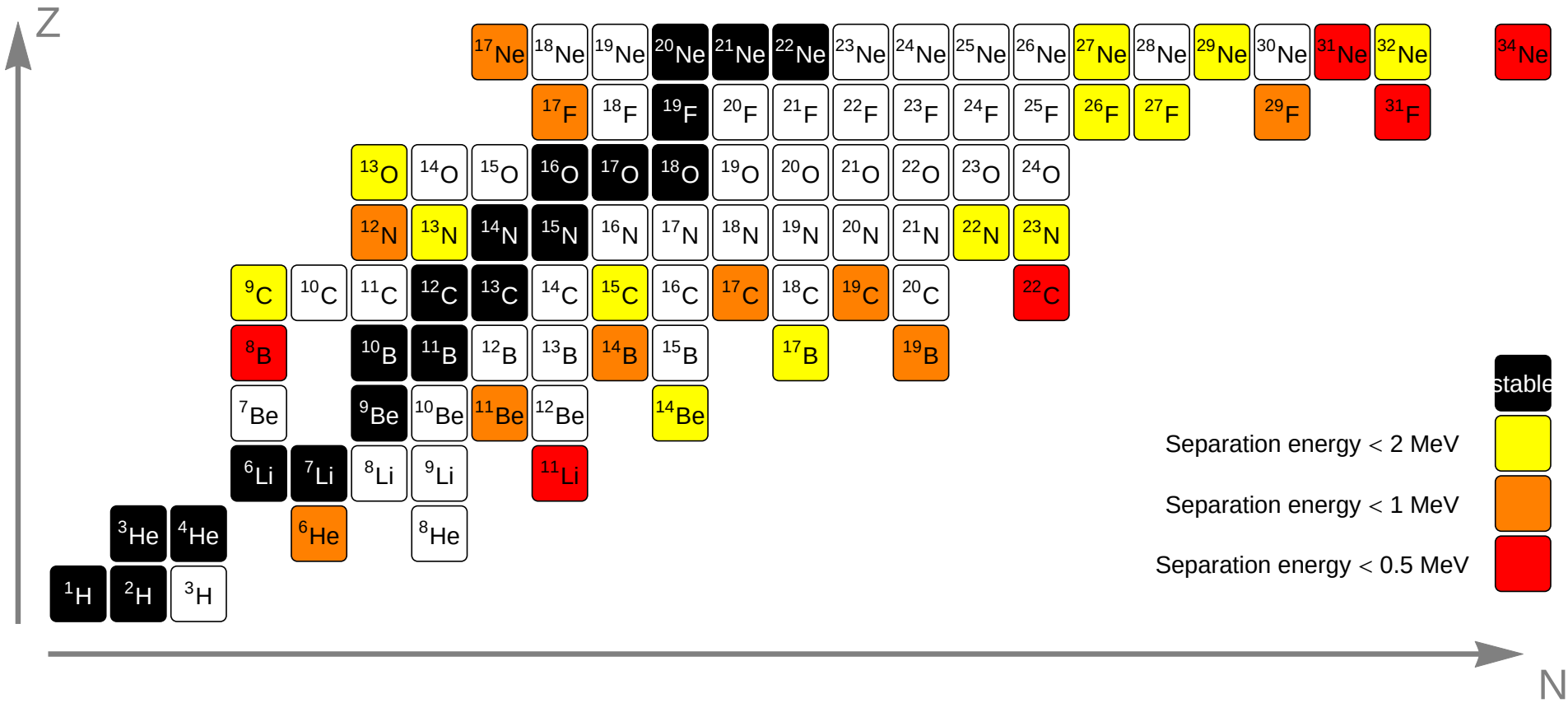

- states close to one-nucleon, two-nucleon or cluster thresholds can have well developed **halo** or **cluster** structure
- these are hard to tackle in the harmonic oscillator basis

Wave Functions

Fermionic

Slater determinant

$$\left| Q \right\rangle = \underset{\sim}{\mathcal{A}} \left(\left| q_1 \right\rangle \otimes \cdots \otimes \left| q_A \right\rangle \right)$$

- antisymmetrized A-body state

Molecular

single-particle states

$$\left\langle \mathbf{x} \middle| q \right\rangle = \sum_i c_i \exp\left\{ -\frac{(\mathbf{x} - \mathbf{b}_i)^2}{2a_i} \right\} \otimes \left| \chi^{\uparrow}_i, \chi^{\downarrow}_i \right\rangle \otimes \left| \xi \right\rangle$$

- Gaussian wave-packets in phase-space (complex parameter $\mathbf{b}_i$ encodes mean position and mean momentum), spin is free, isospin is fixed
- width a_i is an independent variational parameter for each wave packet
- superposition of two wave packets for each single particle state

Gaussian Wave Packets

- Wave Packet

$$\langle \mathbf{x} \,|\, a, \mathbf{b} \rangle = \exp\left\{ -\frac{(\mathbf{x}-\mathbf{b})^2}{2a} \right\}$$

- Norm

$$\langle a, \mathbf{b} \,|\, a, \mathbf{b} \rangle = \left(2\pi \frac{a^\star a}{a^\star + a} \right)^{3/2} \exp\left\{ -\frac{(\mathbf{b}^\star - \mathbf{b})^2}{2(a^\star + a)} \right\}$$

- Mean Position, Mean Momentum

$$\frac{\langle a, \mathbf{b} \,|\, \underset{\sim}{\mathbf{x}} \,|\, a, \mathbf{b} \rangle}{\langle a, \mathbf{b} \,|\, a, \mathbf{b} \rangle} = \frac{a^\star \mathbf{b} + a \mathbf{b}^\star}{a^\star + a}, \qquad \frac{\langle a, \mathbf{b} \,|\, \underset{\sim}{\mathbf{k}} \,|\, a, \mathbf{b} \rangle}{\langle a, \mathbf{b} \,|\, a, \mathbf{b} \rangle} = i \frac{\mathbf{b}^\star - \mathbf{b}}{a^\star + a}$$

- Variance of Position and Momentum

$$\frac{\langle a, \mathbf{b} \,|\, \left(\underset{\sim}{\mathbf{x}} - \langle \underset{\sim}{\mathbf{x}} \rangle \right)^2 \,|\, a, \mathbf{b} \rangle}{\langle a, \mathbf{b} \,|\, a, \mathbf{b} \rangle} = 3 \frac{a^\star a}{a^\star + a} \qquad \frac{\langle a, \mathbf{b} \,|\, \left(\underset{\sim}{\mathbf{k}} - \langle \underset{\sim}{\mathbf{k}} \rangle \right)^2 \,|\, a, \mathbf{b} \rangle}{\langle a, \mathbf{b} \,|\, a, \mathbf{b} \rangle} = 3 \frac{1}{a^\star + a}$$

Gaussian Wave Packets - Transformations

- Translation by $\mathbf{d}$

$$\langle \mathbf{x} \left| \underset{\sim}{T}_{\mathbf{d}} \right| a, \mathbf{b} \rangle = \exp\left\{ -\frac{(\mathbf{x} - (\mathbf{b} + \mathbf{d}))^2}{2a} \right\} = \left| a, \mathbf{b} + \mathbf{d} \right\rangle$$

- Boost with $\mathbf{v}$

$$\begin{aligned} \langle \mathbf{x} \left| \underset{\sim}{B}_{\mathbf{v}} \right| a, \mathbf{b} \rangle &= \exp\left\{ -\frac{(\mathbf{x} - (\mathbf{b} + ima\mathbf{v}))^2}{2a} \right\} \cdot \exp\left\{ im\mathbf{b} \cdot \mathbf{v} - \frac{a}{2} m^2 \mathbf{v}^2 \right\} \\ &= \left| a, \mathbf{b} + ima\mathbf{v} \right\rangle \cdot \exp\left\{ im\mathbf{b} \cdot \mathbf{v} - \frac{a}{2} m^2 \mathbf{v}^2 \right\} \end{aligned}$$

- Parity

$$\langle \mathbf{x} \left| \underset{\sim}{\Pi} \right| a, \mathbf{b} \rangle = \exp\left\{ -\frac{(\mathbf{x} + \mathbf{b})^2}{2a} \right\} = \left| a, -\mathbf{b} \right\rangle$$

- Rotation by $\Omega = (\alpha, \beta, \gamma)$

$$\langle \mathbf{x} \left| \underset{\sim}{R}(\Omega) \right| a, \mathbf{b} \rangle = \exp\left\{ -\frac{(\mathbf{x} - R_3(\Omega) \cdot \mathbf{b})^2}{2a} \right\} = \left| a, R_3(\Omega) \cdot \mathbf{b} \right\rangle$$

Gaussian Wave Packets and Harmonic Oscillator

- Slater determinant invariant under linear transformation of single-particle states
- Harmonic Oscillator wave functions can be obtained by linear combinations of Gaussians

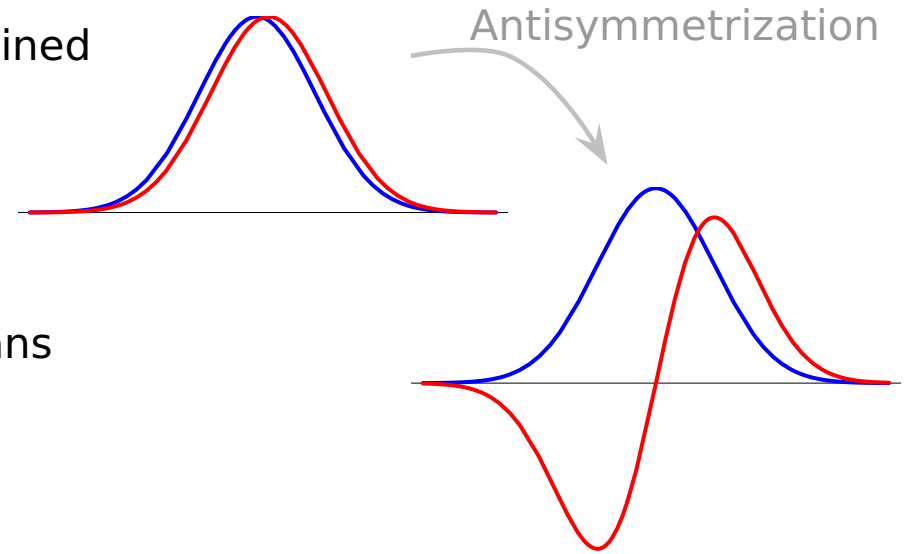

- Create *s*- and *p*-wave Harmonic Oscillator wave functions with two slightly shifted Gaussians

$$\lim_{\Delta\to 0} \frac{1}{2}\left(\langle x \,|\, a, +\Delta\rangle + \langle x \,|\, a, -\Delta\rangle\right) = \langle x \,|\, a, 0\rangle$$

$$\lim_{\Delta\to 0} \frac{1}{2\Delta}\left(\langle x \,|\, a, +\Delta\rangle - \langle x \,|\, a, -\Delta\rangle\right) = x\,\langle x \,|\, a, 0\rangle$$

Dynamics

Time-dependent

Time-dependent variational principle

$$\delta \int dt \frac{\langle Q \left| i\frac{d}{dt} - \underset{\sim}{\hat{H}} \right| Q \rangle}{\langle Q \left| Q \right. \rangle} = 0$$

➻ describe heavy-ion reactions, thermodynamics with ergodic ensembles

Time-independent

Ritz variational principle

$$\delta \frac{\langle Q \left| \underset{\sim}{\hat{H}} - \underset{\sim}{\hat{T}}_{\mathrm{cm}} \right| Q \rangle}{\langle Q \left| Q \right. \rangle} = 0$$

➻ **minimize** expectation value with respect to all the parameters $q_k = \{c_k, a_k, \mathbf{b}_k, \chi_k\}$, $k = 1 \ldots A$

➻ need analytical gradients

$$\frac{\partial}{\partial q_i^\star} \frac{\langle Q \left| \underset{\sim}{\hat{H}} - \underset{\sim}{\hat{T}}_{\mathrm{cm}} \right| Q \rangle}{\langle Q \left| Q \right. \rangle}$$

Rev. Mod. Phys. **72** (2000) 655

Nucl. Phys. **A745** (2004) 3

Non-Orthogonal Basis

- Slater determinant is the antisymmetrized product state

$$\begin{aligned}\left|\, Q \,\right\rangle &= \underset{\sim}{\mathcal{A}}\left(\left|\, q_1 \,\right\rangle \otimes \cdots \otimes \left|\, q_A \,\right\rangle\right) \\ &= \frac{1}{A!}\sum_{\mathcal{P}}(-1)^{\mathcal{P}}\left(\left|\, q_{\mathcal{P}(1)} \,\right\rangle \otimes \cdots \otimes \left|\, q_{\mathcal{P}(A)} \,\right\rangle\right)\end{aligned}$$

- Antisymmetrization operator is a projection operator

$$\underset{\sim}{\mathcal{A}}\underset{\sim}{\mathcal{A}} = \underset{\sim}{\mathcal{A}}$$

- Many-Body Overlap

$$\begin{aligned}\left\langle\, Q \,\middle|\, Q \,\right\rangle &= \left(\left\langle\, q_1 \,\right| \otimes \cdots \otimes \left\langle\, q_A \,\right|\right) \underset{\sim}{\mathcal{A}}^{\dagger}\underset{\sim}{\mathcal{A}} \left(\left|\, q_1 \,\right\rangle \otimes \cdots \otimes \left|\, q_A \,\right\rangle\right) \\ &= \left(\left\langle\, q_1 \,\right| \otimes \cdots \otimes \left\langle\, q_A \,\right|\right) \underset{\sim}{\mathcal{A}} \left(\left|\, q_1 \,\right\rangle \otimes \cdots \otimes \left|\, q_A \,\right\rangle\right) \\ &= \left(\left\langle\, q_1 \,\right| \otimes \cdots \otimes \left\langle\, q_A \,\right|\right) \frac{1}{A!}\sum_{\mathcal{P}}(-1)^{\mathcal{P}}\left(\left|\, q_{\mathcal{P}(1)} \,\right\rangle \otimes \cdots \otimes \left|\, q_{\mathcal{P}(A)} \,\right\rangle\right) \\ &= \frac{1}{A!}\det\left(\left\langle\, q_k \,\middle|\, q_l \,\right\rangle\right)\end{aligned}$$

Non-Orthogonal Basis

- Non-orthogonal basis states $\left| q_k \right\rangle$

$$\left\langle q_k \middle| q_l \right\rangle = n_{kl} \neq \delta_{kl}$$

- Transform into orthogonal basis

$$\left| \phi_\alpha \right\rangle = \sum_{m=1}^{A} \left| q_m \right\rangle (n^{-1/2})_{m\alpha}$$

- Check

$$\begin{aligned} \left\langle \phi_\alpha \middle| \phi_\beta \right\rangle &= \sum_{m,n} (n^{-1/2})_{\alpha m} \left\langle q_m \middle| q_n \right\rangle (n^{-1/2})_{n\beta} \\ &= \sum_{m,n} (n^{-1/2})_{\alpha m}\, n_{mn}\, (n^{-1/2})_{n\beta} \\ &= \delta_{\alpha\beta} \end{aligned}$$

➳ Calculate matrix elements of one- and two-body operators

Evaluation of Matrix Elements

- non-orthogonal basis, use inverse overlap matrix

One-Body Matrix Elements

$$\frac{\langle Q \left| \underset{\sim}{O}^{[1]} \right| Q \rangle}{\langle Q \left| Q \right\rangle} = \sum_{\alpha=1}^{A} \langle \phi_\alpha \left| \underset{\sim}{O}^{[1]} \right| \phi_\alpha \rangle = \sum_{k,l} \langle q_k \left| \underset{\sim}{O}^{[1]} \right| q_l \rangle \, o_{lk}$$

Two-body operators

$$\begin{aligned}\frac{\langle Q \left| \underset{\sim}{O}^{[2]} \right| Q \rangle}{\langle Q \left| Q \right\rangle} &= \sum_{\alpha<\beta}^{A} \left(\langle \phi_\alpha, \phi_\beta \left| \underset{\sim}{O}^{[2]} \right| \phi_\alpha, \phi_\beta \rangle - \langle \phi_\alpha, \phi_\beta \left| \underset{\sim}{O}^{[2]} \right| \phi_\beta, \phi_\alpha \rangle \right) \\ &= \frac{1}{2} \sum_{k,l,m,n}^{A} \langle q_k, q_l \left| \underset{\sim}{O}^{[2]} \right| q_m, q_n \rangle \, (o_{mk} o_{nl} - o_{ml} o_{nk})\end{aligned}$$

$$o = n^{-1} = \left(\langle q_i \left| q_j \right\rangle \right)^{-1}$$

Evaluate Gaussian Integrals

One-dimensional

$$\int_{-\infty}^{\infty} \mathrm{d}x \, \exp\left\{-\frac{x^2}{\alpha}\right\} = \sqrt{\pi\alpha}$$

Three-dimensional

$$\int \mathrm{d}^3 r \exp\left\{-\frac{\mathbf{r}^2}{\alpha}\right\} = \int \mathrm{d}x \int \mathrm{d}y \int \mathrm{d}z \, \exp\left\{-\frac{x^2+y^2+z^2}{\alpha}\right\} = (\pi\alpha)^{3/2}$$

FMD single-particle ovlap

$$\begin{aligned}\left\langle a_k, \mathbf{b}_k \middle| a_l, \mathbf{b}_l \right\rangle &= \int \mathrm{d}^3 x \, \exp\left\{-\frac{(\mathbf{x}-\mathbf{b}_k{}^\star)^2}{2a_k{}^\star}\right\} \exp\left\{-\frac{(\mathbf{x}-\mathbf{b}_l)^2}{2a_l}\right\} \\ &= \left(2\pi\frac{a_k{}^\star a_l}{a_k{}^\star + a_l}\right)^{3/2} \exp\left\{-\frac{(\mathbf{b}_k{}^\star - \mathbf{b}_l)^2}{2(a_k{}^\star + a_l)}\right\}\end{aligned}$$

Interaction Matrix Elements

(One-body) Kinetic Energy

$$\langle q_k \left| \underset{\sim}{T} \right| q_l \rangle = \langle a_k \mathbf{b}_k \left| \underset{\sim}{T} \right| a_l \mathbf{b}_l \rangle \langle \chi_k | \chi_l \rangle \langle \xi_k | \xi_l \rangle$$

$$\langle a_k \mathbf{b}_k \left| \underset{\sim}{T} \right| a_l \mathbf{b}_l \rangle = \frac{1}{2m} \left(\frac{3}{a_k^\star + a_l} - \frac{(\mathbf{b}_k^\star - \mathbf{b}_l)^2}{(a_k^\star + a_l)^2} \right) R_{kl}$$

$$\alpha_{klmn} = \frac{a_k{}^\star a_m}{a_k{}^\star + a_m} + \frac{a_l{}^\star a_n}{a_l{}^\star + a_n}$$

$$\rho_{klmn} = \frac{a_m \mathbf{b}_k{}^\star + a_k{}^\star \mathbf{b}_m}{a_k{}^\star + a_m} - \frac{a_n \mathbf{b}_l{}^\star + a_l{}^\star \mathbf{b}_n}{a_l{}^\star + a_n}$$

$$R_{km} = \langle a_k \mathbf{b}_k \left| a_m \mathbf{b}_m \right. \rangle$$

(Two-body) Potential

- fit radial dependencies by (a sum of) Gaussians

$$G(\mathbf{x}_1 - \mathbf{x}_2) = \exp\left\{ -\frac{(\mathbf{x}_1 - \mathbf{x}_2)^2}{2\kappa} \right\}$$

- perform Gaussian integrals

$$\langle a_k \mathbf{b}_k, a_l \mathbf{b}_l \left| \underset{\sim}{G} \right| a_m \mathbf{b}_m, a_n \mathbf{b}_n \rangle = R_{km} R_{ln} \left(\frac{\kappa}{\alpha_{klmn} + \kappa} \right)^{3/2} \exp\left\{ -\frac{\rho_{klmn}^2}{2(\alpha_{klmn} + \kappa)} \right\}$$

- analytical formulas for matrix elements

Operator Representation of V_{UCOM}

$$\underset{\sim}{C}^{\dagger}(\underset{\sim}{T}+\underset{\sim}{V})\underset{\sim}{C} \;=\; \underset{\sim}{T}$$

one-body kinetic energy

$$+\sum_{ST}\hat{V}_{c}^{ST}(r)+\frac{1}{2}(\underset{\sim}{p_r}^{2}\,\hat{V}_{p^2}^{ST}(r)+\hat{V}_{p^2}^{ST}(r)\,\underset{\sim}{p_r}^{2})+\hat{V}_{l^2}^{ST}(r)\,\underset{\sim}{\mathbf{l}}^{2}$$

central potentials

$$+\sum_{T}\hat{V}_{ls}^{T}(r)\,\underset{\sim}{\mathbf{l}}\cdot\underset{\sim}{\mathbf{s}}+\hat{V}_{l^2ls}^{T}(r)\,\underset{\sim}{\mathbf{l}}^{2}\underset{\sim}{\mathbf{l}}\cdot\underset{\sim}{\mathbf{s}}$$

spin-orbit potentials

$$+\sum_{T}\hat{V}_{t}^{T}(r)\,\underset{\sim}{S}_{12}(\mathbf{r},\mathbf{r})+\hat{V}_{trp_\Omega}^{T}(r)\,\underset{\sim}{p_r}\,\underset{\sim}{S}_{12}(\mathbf{r},\mathbf{p_\Omega})+\hat{V}_{tll}^{T}(r)\,\underset{\sim}{S}_{12}(\mathbf{l},\mathbf{l})+$$
$$\hat{V}_{tp_\Omega p_\Omega}^{T}(r)\,\underset{\sim}{S}_{12}(\mathbf{p_\Omega},\mathbf{p_\Omega})+\hat{V}_{l^2tp_\Omega p_\Omega}^{T}(r)\,\underset{\sim}{\mathbf{l}}^{2}\underset{\sim}{S}_{12}(\mathbf{p_\Omega},\mathbf{p_\Omega})$$

tensor potentials

bulk of tensor force mapped onto central part of correlated interaction

tensor correlations also change the spin-orbit part of the interaction

Nucl. Phys. **A745** (2004) 3

UCOM(var) + phenomenological correction

Effective two-body interaction

- FMD model space can't describe correlations induced by residual medium-long ranged tensor forces
- use **long ranged tensor correlator** to partly account for that
- add phenomenological two-body correction term with a **momentum-dependend** central and (isospin-dependend) **spin-orbit** part
- fit correction term to binding energies and radii of "closed-shell" nuclei (^{4}He, ^{16}O, ^{40}Cα), (^{24}O, ^{34}Si, ^{48}Cα)

➳ in newer calculations we use UCOM(SRG) (with modifications of spin-orbit force)

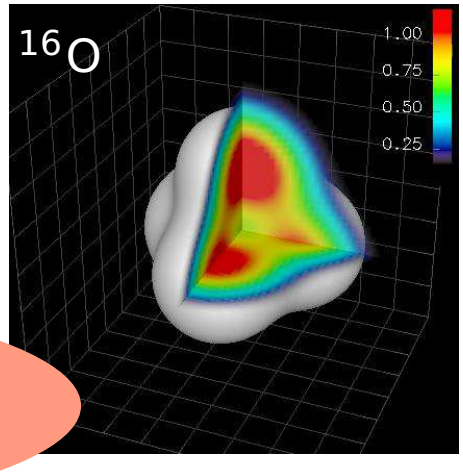

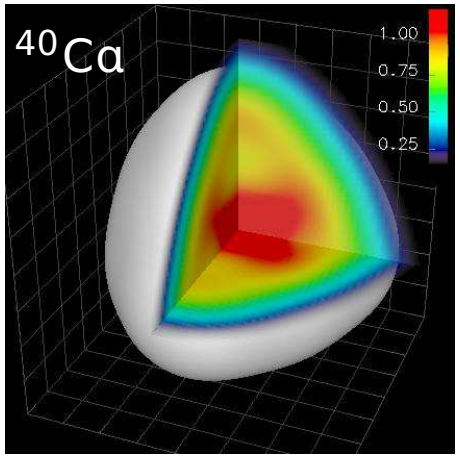

projected tetrahedral configurations are about 6 MeV lower in energy than "closed-shell" configurations

Perform Variation

Minimization

- minimize Hamiltonian with respect to all single-particle parameters q_k

$$\min_{\{q_k\}} \frac{\langle Q | \hat{H} - T_{cm} | Q \rangle}{\langle Q | Q \rangle}$$

- this is a Hartree-Fock calculation in our particular single-particle basis
- mean-field may break the symmetries of the Hamiltonian

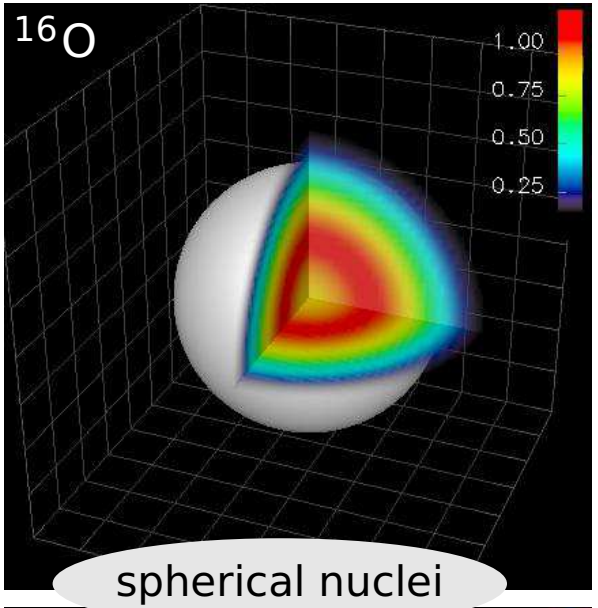

spherical nuclei

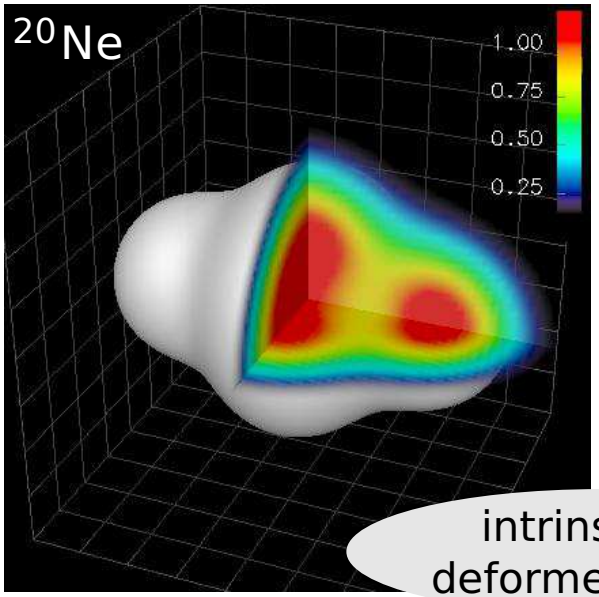

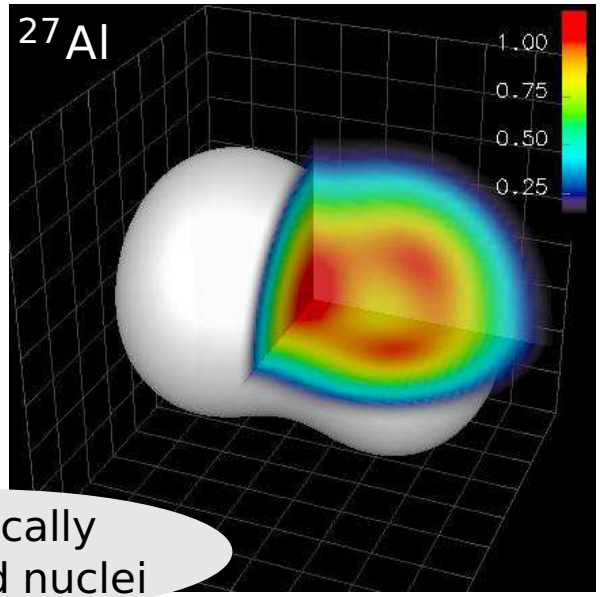

intrinsically deformed nuclei

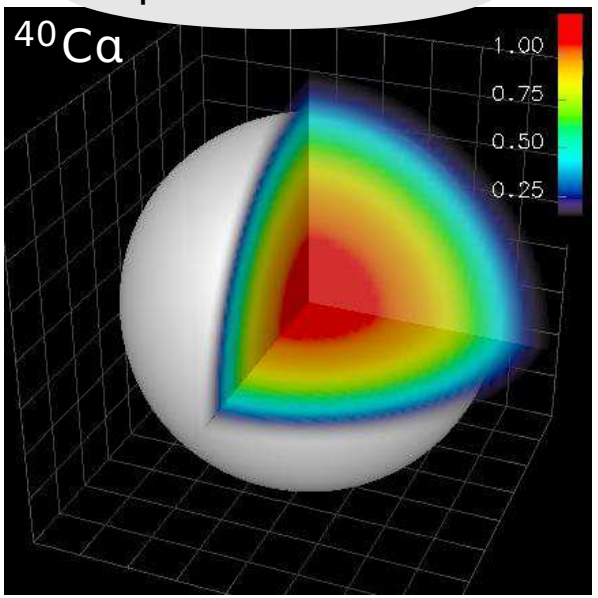

Mean field

Variation

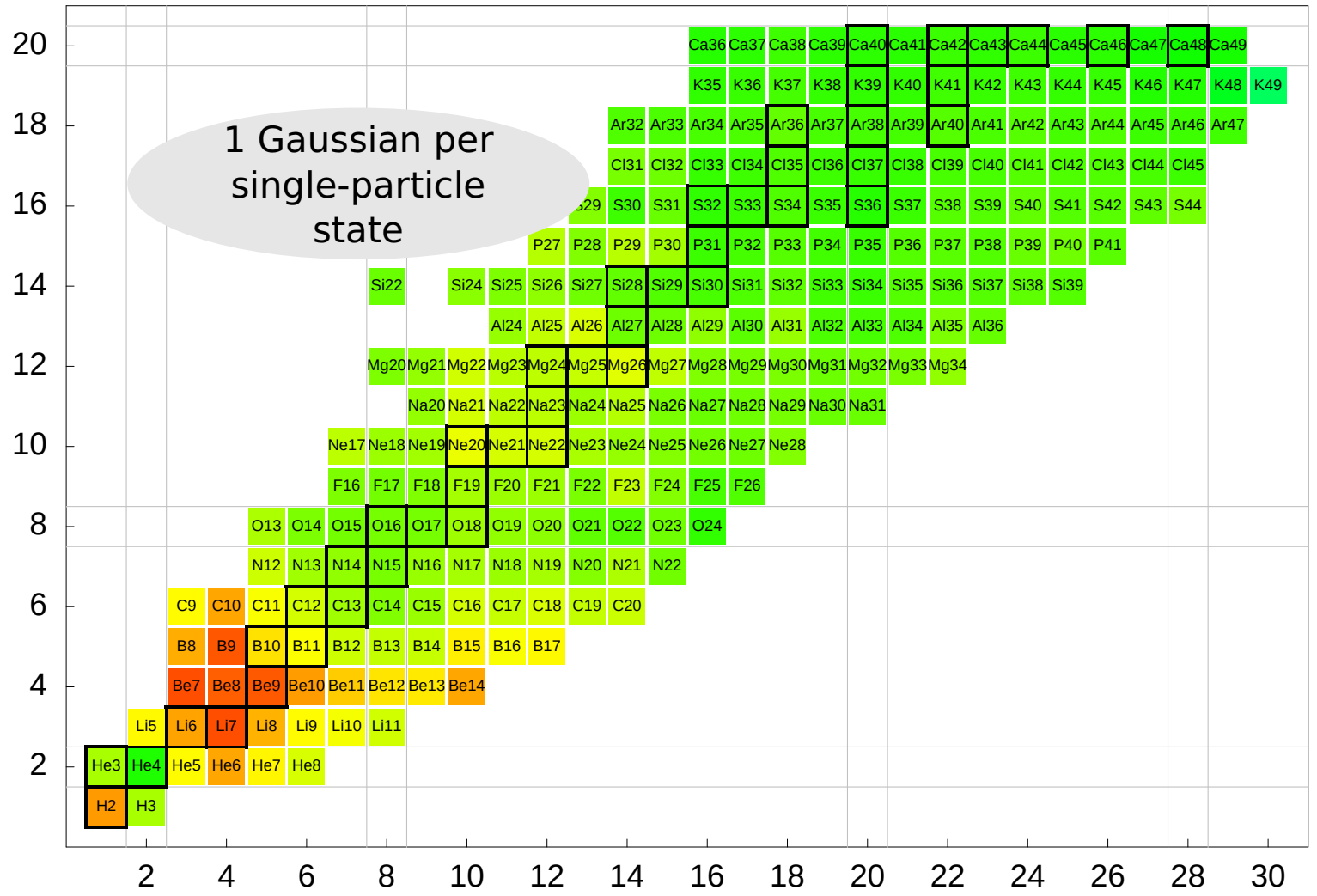

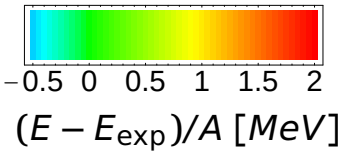

UCOM(var) + phenomenological correction

Mean field

Variation

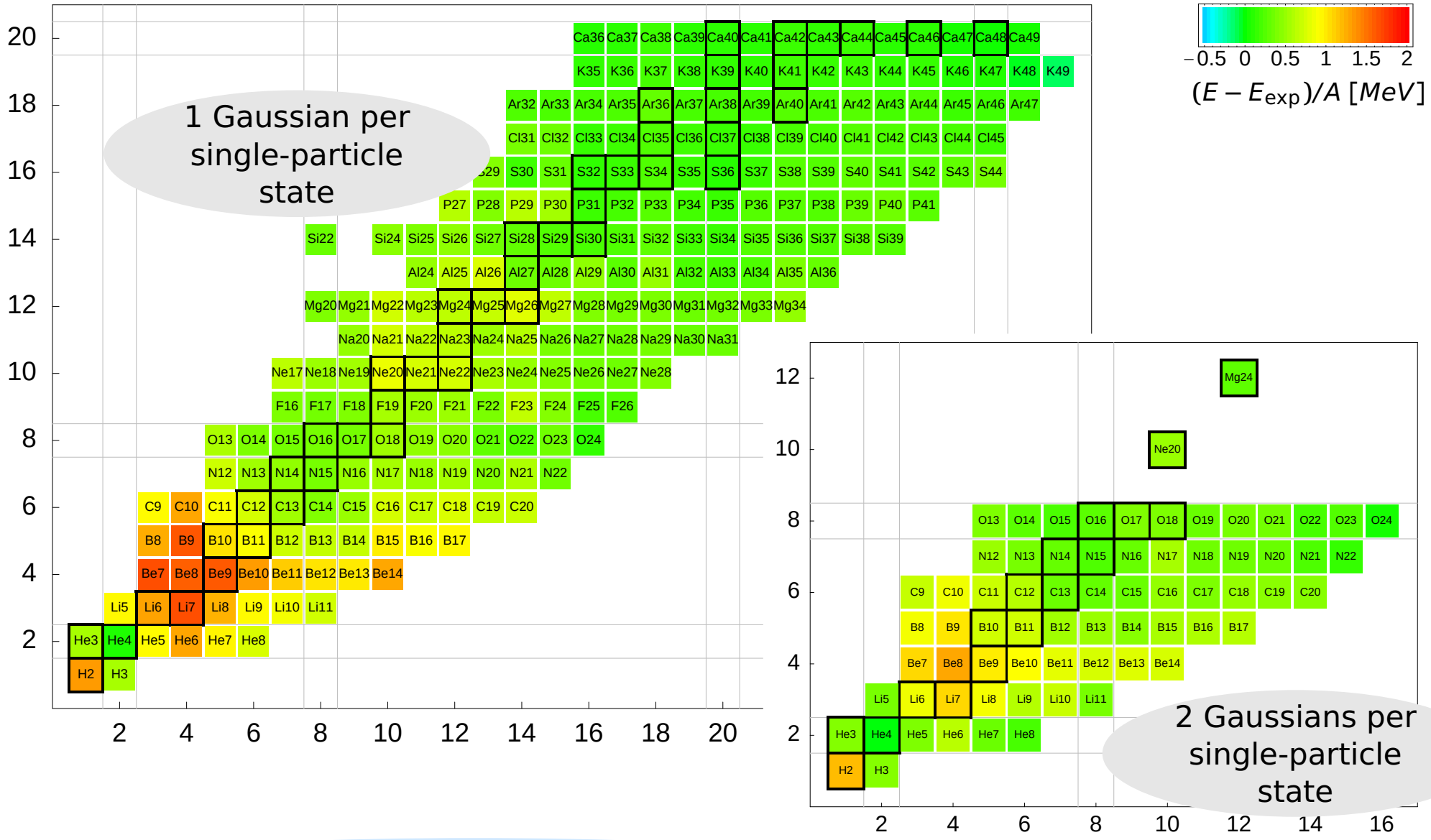

UCOM(var) + phenomenological correction

Beyond Mean-Field

Projection After Variation (PAV)

- mean-field may break symmetries of Hamiltonian
- restore inversion, translational and rotational symmetry by projection on parity, linear and angular momentum

$$\underset{\sim}{P}^{\mathbf{P}} = \frac{1}{(2\pi)^3} \int \mathrm{d}^3X \; \exp\{-i(\underset{\sim}{\mathbf{P}}-\mathbf{P})\cdot\mathbf{X}\}$$

$$\underset{\sim}{P}^{J}_{MK} = \frac{2J+1}{8\pi^2} \int \mathrm{d}^3\Omega \, D^{J}_{MK}{}^{\star}(\Omega) \, \underset{\sim}{R}(\Omega)$$

Variation After Projection (VAP)

- effect of projection can be large
- perform Variation after Parity Projection VAP$^{\pi}$
- perform VAP in GCM sense by applying **constraints** on radius, dipole moment, quadrupole moment or octupole moment and minimize the energy in the projected energy surface

➳ "real" VAP is possible for light nuclei

Multiconfiguration Mixing

- **diagonalize** Hamiltonian in a set of projected intrinsic states

$$\left\{ \left| Q^{(\alpha)} \right\rangle, \quad \alpha = 1, \ldots, N \right\}$$

$$\sum_{K'b} \left\langle Q^{(a)} \right| \underset{\sim}{H} \underset{\sim}{P}^{J^{\pi}}_{KK'} \underset{\sim}{P}^{\mathbf{P}=0} \left| Q^{(b)} \right\rangle \cdot c^{(i)}_{K'b} =$$

$$E^{J^{\pi}}(i) \sum_{K'b} \left\langle Q^{(a)} \right| \underset{\sim}{P}^{J^{\pi}}_{KK'} \underset{\sim}{P}^{\mathbf{P}=0} \left| Q^{(b)} \right\rangle \cdot c^{(i)}_{K'b}$$

Angular Momentum Projection

Intrinsic State

- the intrinsic state is in general not an angular momentum eigenstate
- it is a superposition of angular momentum eigenstates

$$\left|Q\right\rangle = \sum_{JM\alpha} \left|Q;JM\alpha\right\rangle c_{JM\alpha}, \qquad \underset{\sim}{\mathbf{J}}^2 \left|Q;JM\alpha\right\rangle = J(J+1)\left|Q;JM\alpha\right\rangle, \qquad \underset{\sim}{J}_z \left|Q;JM\alpha\right\rangle = M\left|Q;JM\alpha\right\rangle$$

Angular Momentum Projection Operator

$$\underset{\sim}{P}^J_{MK} = \frac{2J+1}{8\pi^2} \int \mathrm{d}^3\Omega \, {D^J_{MK}}^{\star}(\Omega) \, \underset{\sim}{R}(\Omega)$$

- Rotation Operator $\underset{\sim}{R}(\Omega)$ rotates the wave function with the Euler angles $\Omega = (\alpha, \beta, \gamma)$
- Wigner D-matrix

$$D^J_{MK}(\Omega) = \left\langle JM\right| \underset{\sim}{R}(\Omega) \left|JK\right\rangle = \left\langle JM\right| e^{\underset{\sim}{iJ_z}\alpha} e^{\underset{\sim}{iJ_y}\beta} e^{\underset{\sim}{iJ_z}\gamma} \left|JK\right\rangle = \exp\{-iM\alpha\} \, d^J_{MK}(\beta) \, \exp\{iM\gamma\}$$

- not a true projection operator

$$(\underset{\sim}{P}^J_{MK})^{\dagger} \underset{\sim}{P}^{J'}_{M'K'} = \delta_{J,J'} \delta_{M,M'} \underset{\sim}{P}^J_{KK'}$$

Angular Momentum Projection

K-mixing

- angular momentum eigenstates are linear combinations of projected states with different K

$$\left| Q; JM\alpha \right\rangle = \sum_K \underset{\sim}{P}^J_{MK} \left| Q \right\rangle c^{J\alpha}_K$$

- solve the generalized eigenvalue problem to get the eigenstates

$$\sum_{K'} \left\langle Q \right| (\underset{\sim}{P}^J_{MK})^\dagger \underset{\sim}{H} \underset{\sim}{P}^J_{MK'} \left| Q \right\rangle c^{J\alpha}_{K'} = E^{J\alpha} \sum_{K'} \left\langle Q \right| (\underset{\sim}{P}^J_{MK})^\dagger \underset{\sim}{P}^J_{MK'} \left| Q \right\rangle c^{J\alpha}_{K'}$$

- as the Hamiltonian commutes with rotations this simplifies to

$$\sum_{K'} \left\langle Q \right| \underset{\sim}{H} \underset{\sim}{P}^J_{KK'} \left| Q \right\rangle c^{J\alpha}_{K'} = E^{J\alpha} \sum_{K'} \left\langle Q \right| \underset{\sim}{P}^J_{KK'} \left| Q \right\rangle c^{J\alpha}_{K'}$$

Axial Symmetry

- if $\left| Q \right\rangle$ is an eigenstate of $\underset{\sim}{J}_z$ the integrations over α and γ become trivial and only the β integration remains

Matrix Elements of Tensor Operators

- Tensor operator of rank 0

$$\left\langle \underset{\sim}{P}^{J}_{MK} Q^{(a)} \middle| \underset{\sim}{T}^{(0)} \middle| \underset{\sim}{P}^{J}_{MK'} Q^{(b)} \right\rangle = \left\langle Q^{(a)} \middle| \underset{\sim}{T}^{(0)} \underset{\sim}{P}^{J}_{KK'} \middle| Q^{(b)} \right\rangle$$
$$= \frac{2J+1}{8\pi^2} \int d\Omega \, D^{J}_{KK'}{}^{\star}(\Omega) \left\langle Q^{(a)} \middle| \underset{\sim}{T}^{(0)} \underset{\sim}{R}(\Omega) \middle| Q^{(b)} \right\rangle$$

- Tensor operator of rank k

$$\left\langle \underset{\sim}{P}^{J_f}_{M_f K_f} Q^{(a)} \middle| \underset{\sim q}{T}^{(k)} \middle| P^{J_i}_{M_i K_i} Q^{(b)} \right\rangle = \frac{(-1)^{2k}}{\sqrt{2J_f+1}} \mathrm{C} \left(\begin{array}{cc|c} J_i & k & J_f \\ M_i & q & M_f \end{array} \right) \left\langle P^{J_f}_{K_f} Q^{(a)} \middle|\middle| \underset{\sim}{T}^{(k)} \middle|\middle| \underset{\sim}{P}^{J_i}_{K_i} Q^{(b)} \right\rangle$$

with reduced matrix element

$$\left\langle \underset{\sim}{P}^{J_f}_{K_f} Q^{(a)} \middle|\middle| \underset{\sim}{T}^{(k)} \middle|\middle| \underset{\sim}{P}^{J_i}_{K_i} Q^{(b)} \right\rangle =$$
$$\sqrt{2J_f+1} \sum_{K\nu} \mathrm{C} \left(\begin{array}{cc|c} J_i & k & J_f \\ K & \nu & K_f \end{array} \right) \frac{2J_i+1}{8\pi^2} \int d\Omega \, D^{J_i}_{KK_i}{}^{\star}(\Omega) \left\langle Q^{(a)} \middle| \underset{\sim \nu}{T}^{(k)} \underset{\sim}{R}(\Omega) \middle| Q^{(b)} \right\rangle$$

Center-Of-Mass Problem

- Hamiltonian does not couple internal and center-of-mass motion

$$\underset{\sim}{H} = \underset{\sim}{H}_{\text{internal}} + \underset{\sim}{T}_{\text{cm}}$$

- in product states (Slater determinants) the internal motion is entangled with the center-of-mass motion

➳ zero-th order correction: always use internal operators $\underset{\sim}{H}_{\text{internal}} = \underset{\sim}{H} - \underset{\sim}{T}_{\text{cm}}, \ldots$

➳ in the special case where all widths α are equal the wave function factorizes in the internal wave function and the center-of-mass wave function

$$\langle \mathbf{x}_1, \ldots, \mathbf{x}_A \,|\, Q \rangle = \Phi_{\text{internal}}(\boldsymbol{\xi}_1, \ldots, \boldsymbol{\xi}_A)\Phi^{\alpha}_{\text{cm}}(\mathbf{X})$$

with coordinates $\boldsymbol{\xi}_i = \mathbf{x}_i - \mathbf{X}$ and $\mathbf{X} = \frac{1}{A}\sum_i \mathbf{x}_i$

➳ in the general case we project the wave function on total momentum $\mathbf{P} = 0$ with the projection operator

$$\underset{\sim}{P}^{\mathbf{P}} = \frac{1}{(2\pi)^3} \int \mathrm{d}^3X \, \exp\{-i(\underset{\sim}{\mathbf{P}} - \mathbf{P}) \cdot \mathbf{X}\}$$

The projected wave function is then given as

$$\langle \mathbf{x}_1, \ldots, \mathbf{x}_A \,|\, \underset{\sim}{P}^{\mathbf{P}} \,|\, Q \rangle = \frac{1}{(2\pi)^3} \int \mathrm{d}^3X \, e^{i\mathbf{P}\cdot\mathbf{X}} \langle \mathbf{x}_1 - \mathbf{X}, \ldots, \mathbf{x}_A - \mathbf{X} \,|\, Q \rangle$$

Center-Of-Mass Problem

- one-body density calculated with Slater determinant

$$\rho^{(1)}(\mathbf{r}) = \langle \Psi \left| \sum_i \delta(\underset{\sim}{\mathbf{r}}_i - \mathbf{r}) \right| \Psi \rangle$$

- density of internal wave function

$$\rho^{(1)}_{\text{internal}}(\mathbf{r}) = \langle \Psi \left| \sum_i \delta(\underset{\sim}{\mathbf{r}}_i - \underset{\sim}{\mathbf{R}} - \mathbf{r}) \right| \Psi \rangle$$

^{4}He

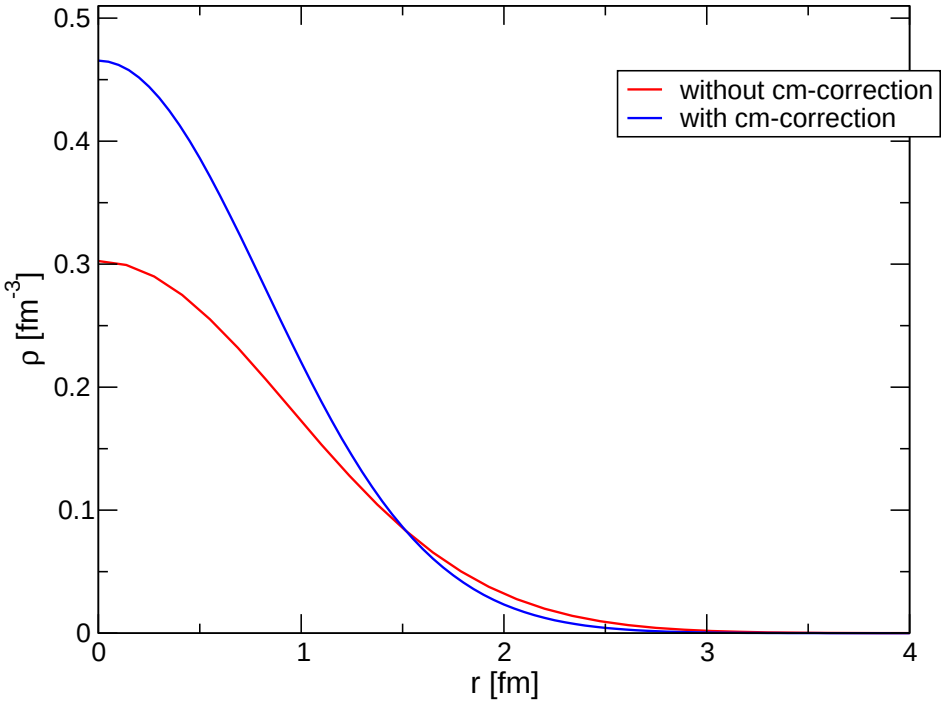

^{16}O

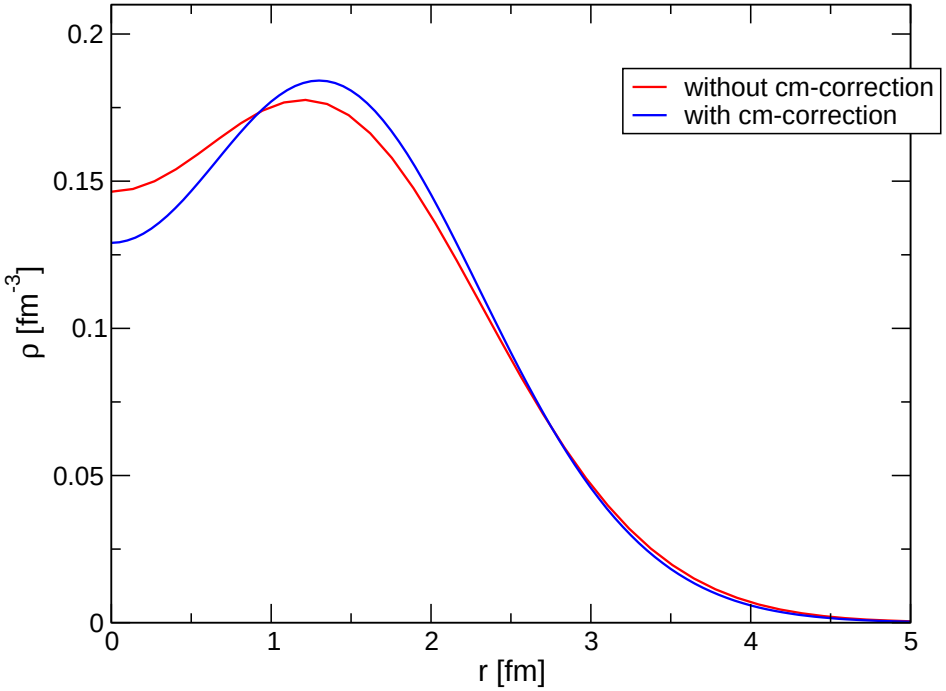

radius and quadrupole constraints

V/PAV

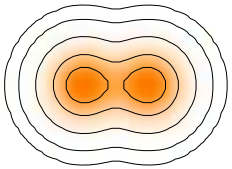

VAP

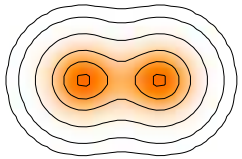

Multiconfig

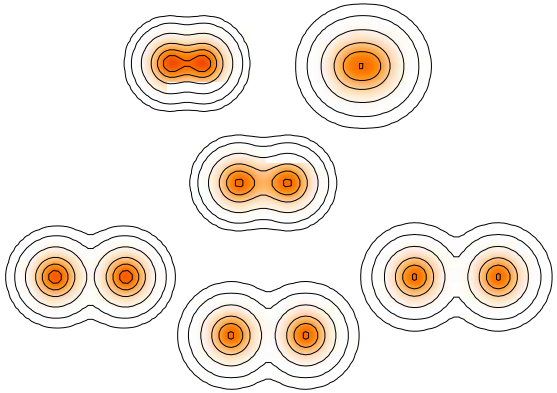

	E_b [MeV]	r_{charge} [fm]	$B(E2)$ [e^2fm^4]
PAV	52.7	2.39	9.31
VAP	54.8	2.49	15.36
Multiconfig	57.2	2.74	30.39
Exp	56.5		

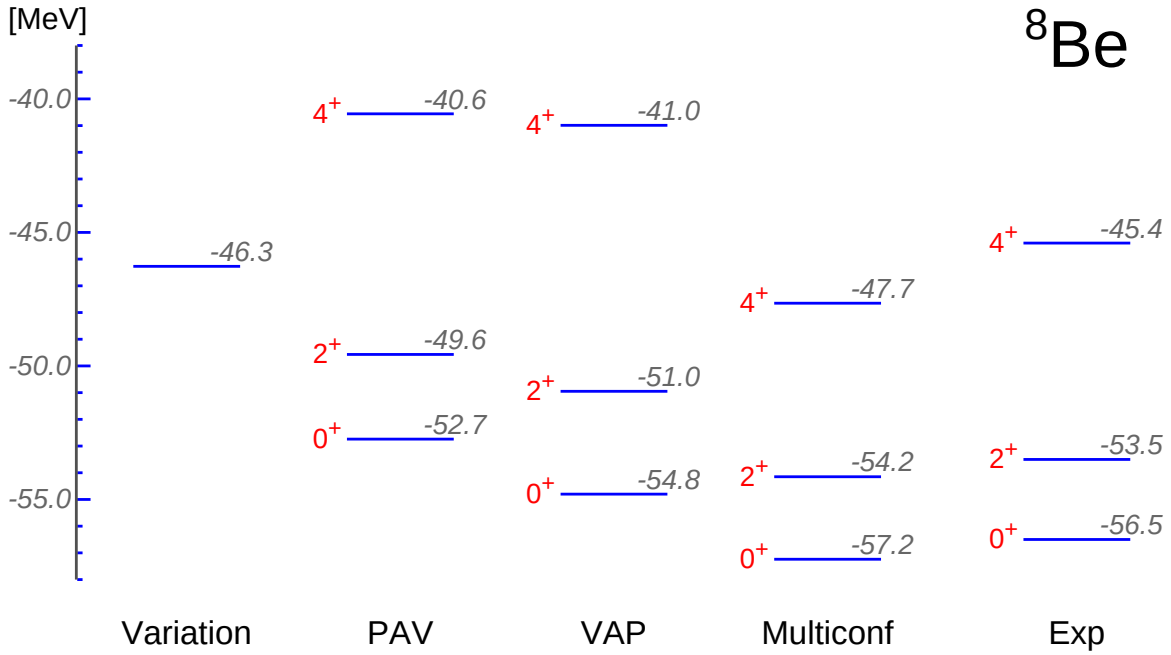

radius and octupole constraints

V/PAV

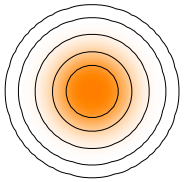

VAP α

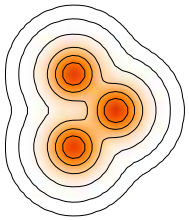

V$^{\pi}$/PAV$^{\pi}$

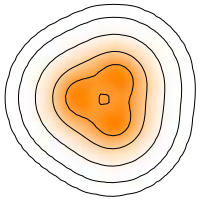

Multiconfig

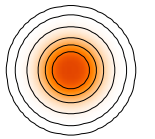

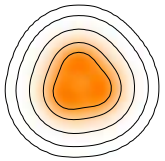

VAP

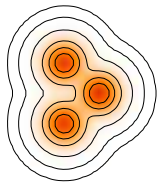

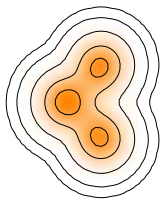

	E_b [MeV]	r_{charge} [fm]	$B(E2)$ [e^2fm^4]
V/PAV	81.4	2.36	-
VAP α-cluster	79.1	2.70	76.9
PAV$^{\pi}$	88.5	2.51	36.3
VAP	89.2	2.42	26.8
Multiconfig	92.2	2.52	42.8
Experiment	92.2	2.47	39.7 ± 3.3

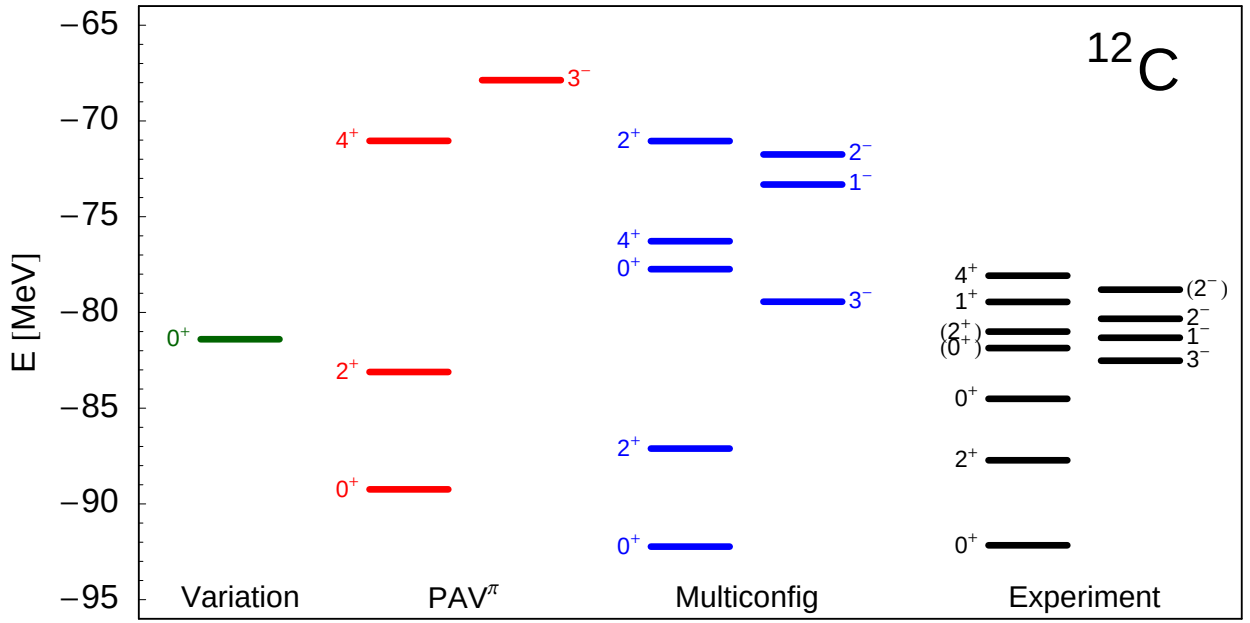

Shell-structure versus Cluster states in ^{12}C

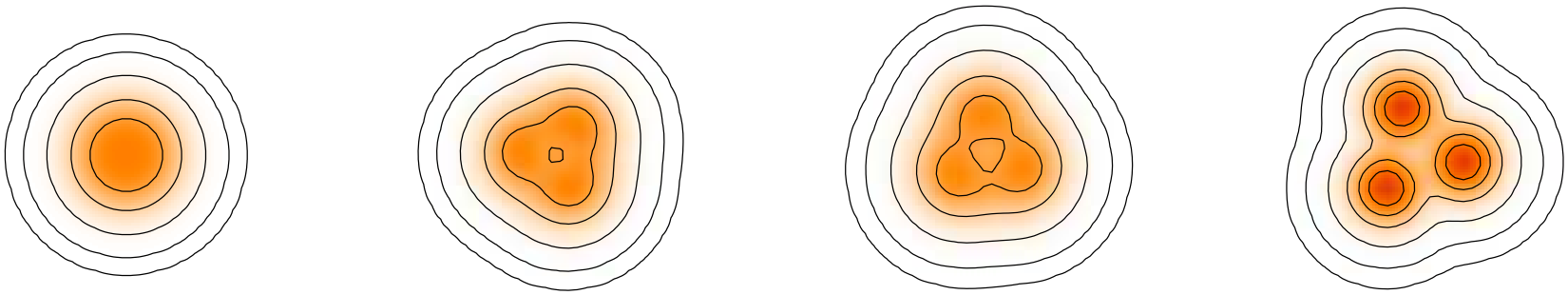

	intrinsic	projected	intrinsic	projected	intrinsic	projected	intrinsic	projected
$\langle \underset{\sim}{H} \rangle$	-81.4	-81.5	-77.0	-88.5	-74.1	-85.5	-57.0	-75.9
$\langle \underset{\sim}{T} \rangle$	212.1	212.1	189.2	186.1	182.8	179.0	213.9	201.4
$\langle \underset{\sim}{V}_{ls} \rangle$	-39.8	-40.2	-12.0	-17.1	-5.8	-8.0	-	-
$\sqrt{\langle \underset{\sim}{r}^2 \rangle}$	2.22	2.22	2.40	2.37	2.45	2.42	2.44	2.42

spin-orbit force
“breaks” clusters

cluster states strongly
“feel” projection

Clustering and Localization/Delocalization

Localization and Kinetic Energy

- **Center-of-mass wave function**
- **Localization in the relative wave function**
- **Localization means large kinetic energy**
- **Delocalization by angular momentum projection and configuration mixing lowers kinetic energy**

➳ **Illustrate for ^{8}Be – ^{4}He-^{4}He example**
Volkov interaction – same width parameter α for all Gaussians

Center-of-Mass

- Slater determinants have a localized center-of-mass
- Center-of-mass wave function (in case of equal width parameters a)

$$\Psi_{\text{cm}}(\mathbf{X}) = \frac{1}{(\pi a_{\text{cm}})^{3/4}} \exp\left\{-\frac{\mathbf{X}^2}{2a_{\text{cm}}}\right\}$$

  with $a_{\text{cm}} = a/A$

- Kinetic energy of center-of-mass motion

$$\langle \underset{\sim}{T}_{\text{cm}} \rangle = \frac{1}{2Am}\frac{3}{2a_{\text{cm}}} = \frac{1}{2m}\frac{3}{2a}$$

$$\left|\Psi\right\rangle = \left|\Psi_{\text{intr}}\right\rangle \otimes \left|\Psi_{\text{cm}}\right\rangle$$

^{4}He

	$\min\langle \underset{\sim}{H} \rangle$	$\min\langle \underset{\sim}{H} - \underset{\sim}{T}_{\text{cm}} \rangle$
$\langle \underset{\sim}{H} - \underset{\sim}{T}_{\text{cm}} \rangle$	-25.42	-27.41
$\langle \underset{\sim}{T} - \underset{\sim}{T}_{\text{cm}} \rangle$	36.76	49.14
$\langle \underset{\sim}{V} \rangle$	-62.18	-76.54
$\langle \underset{\sim}{T}_{\text{cm}} \rangle$	12.26	16.38

^{8}Be

	$\min\langle \underset{\sim}{H} \rangle$	$\min\langle \underset{\sim}{H} - \underset{\sim}{T}_{\text{cm}} \rangle$
$\langle \underset{\sim}{H} - \underset{\sim}{T}_{\text{cm}} \rangle$	-44.05	-45.10
$\langle \underset{\sim}{T} - \underset{\sim}{T}_{\text{cm}} \rangle$	102.62	117.62
$\langle \underset{\sim}{V} \rangle$	-146.68	-162.72
$\langle \underset{\sim}{T}_{\text{cm}} \rangle$	13.03	15.18

- Minimizing $\langle \underset{\sim}{H} - \underset{\sim}{T}_{\text{cm}} \rangle$ corresponds to (approximate) variation after linear momentum projection
- Large effect on the wave function (at least for light nuclei)

Relative Motion of Clusters

- GCM type Slater determinant – localized relative motion
- Relative wave function (in case of equal width parameters a) of two clusters at distance $\mathbf{R}$

$$\Psi_{\text{rel}}(\mathbf{r}) = \frac{1}{(\pi a_{\text{rel}})^{3/4}} \exp\left\{-\frac{(\mathbf{r}-\mathbf{R})^2}{2a_{\text{rel}}}\right\}$$

with $a_{\text{rel}} = a/\mu_A$

- Kinetic energy of relative motion (at large distances)

$$\langle \underset{\sim}{T}_{\text{rel}} \rangle = \frac{1}{2\mu_A m}\frac{3}{2a_{\text{rel}}} = \frac{1}{2m}\frac{3}{2a}$$

$$\left|\Psi\right\rangle = \underset{\sim}{\mathcal{A}}\left\{\left|\Psi_\alpha(-\tfrac{1}{2}\mathbf{R})\right\rangle \otimes \left|\Psi_\alpha(\tfrac{1}{2}\mathbf{R})\right\rangle\right\}$$

$$\left|\Psi_{\text{intr}}\right\rangle = \underset{\sim}{\mathcal{A}}\left\{\left|\Psi_{\text{rel}}\right\rangle \otimes \left|\Phi_\alpha\right\rangle \otimes \left|\Phi_\alpha\right\rangle\right\}$$

^{8}Be – min $\langle \underset{\sim}{H} - \underset{\sim}{T}_{\text{cm}} \rangle$

	intrinsic	projected
$\langle \underset{\sim}{H} - \underset{\sim}{T}_{\text{cm}} \rangle$	-44.32	-51.01
$\langle \underset{\sim}{T} - \underset{\sim}{T}_{\text{cm}} \rangle$	131.05	126.48
$\langle \underset{\sim}{V} \rangle$	-175.37	-177.49
$\langle \underset{\sim}{T}_{\text{cm}} \rangle$	17.11	17.11

^{8}Be – min $\langle 0^+ \left| \underset{\sim}{H} - \underset{\sim}{T}_{\text{cm}} \right| 0^+ \rangle$

	intrinsic	projected
$\langle \underset{\sim}{H} - \underset{\sim}{T}_{\text{cm}} \rangle$	-31.77	-53.05
$\langle \underset{\sim}{T} - \underset{\sim}{T}_{\text{cm}} \rangle$	125.53	113.82
$\langle \underset{\sim}{V} \rangle$	-157.53	-166.87
$\langle \underset{\sim}{T}_{\text{cm}} \rangle$	17.11	17.11

- ➳ angular momentum projection delocalizes relative motion in two directions
- ➳ delocalization in radial direction by configuration mixing

α-α Energy Surface

Kinetic Energy

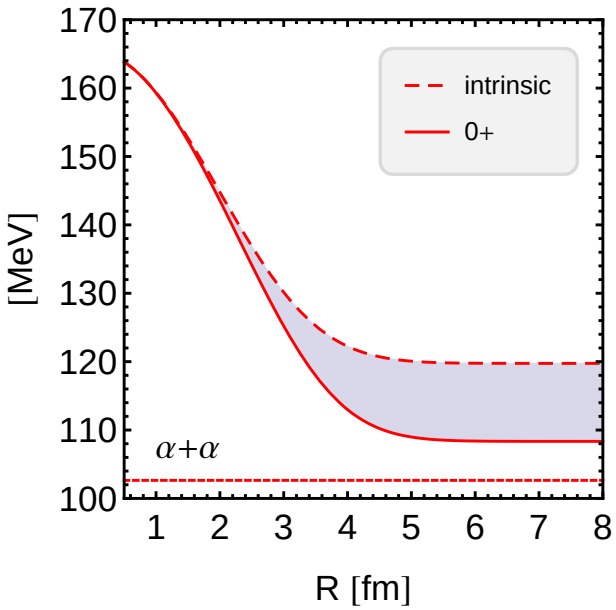

Potential Energy

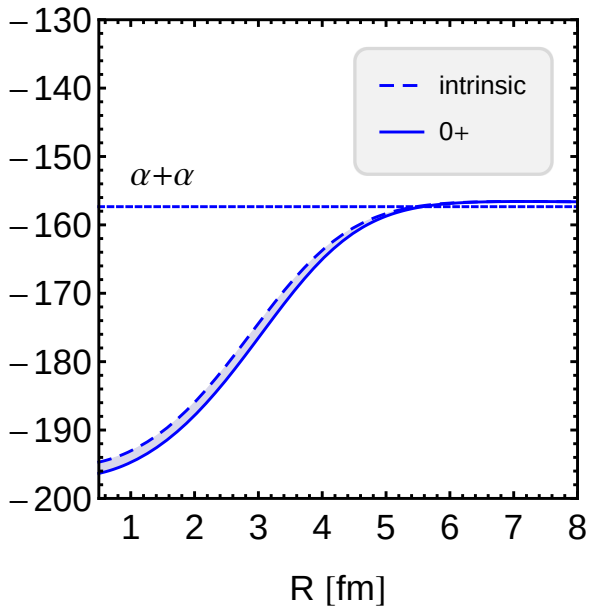

Total Energy

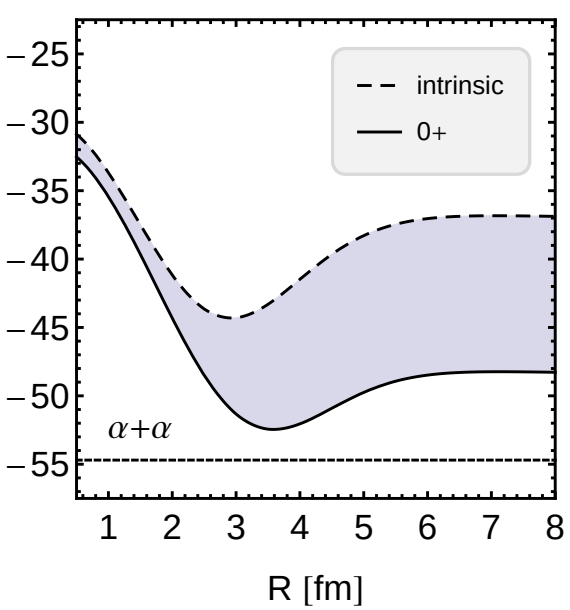

$R = 0.5$fm

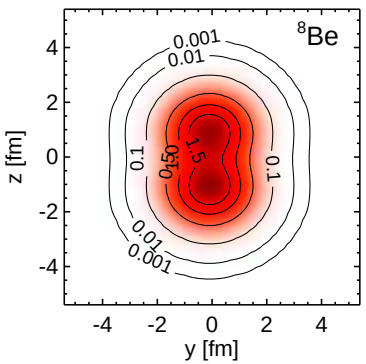

$R = 1.5$fm

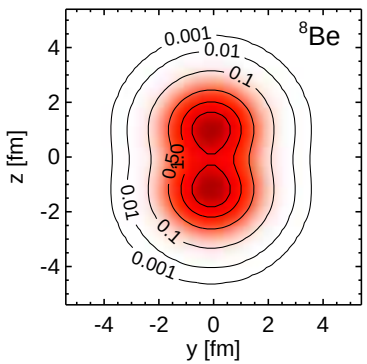

$R = 2.5$fm

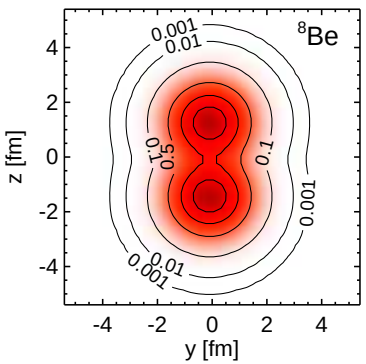

$R = 3.5$fm

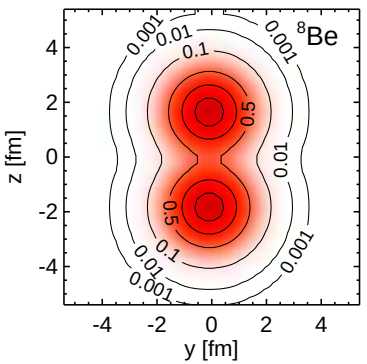

$R = 4.5$fm

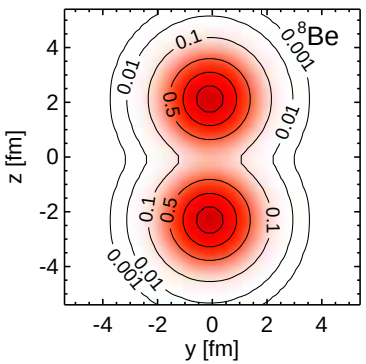

Overview: FMD applications

Neon Isotopes $^{17-22}$Ne

- Halo-candidate ^{17}Ne

Beryllium Isotopes

- $N = 8$ shell closure in ^{12}Be ?

^{3}He(α,γ)^{7}Be Radiative Capture Reaction

- bound and scattering states

Cluster States in ^{12}C

- Microscopic cluster model and FMD
- ^{8}Be+^{4}He continuum

Neon Isotopes ^{17}Ne-^{22}Ne

Structure ?

- s^2/d^2 **competition in** ^{17}Ne **and** ^{18}Ne
- ^{3}He **and** ^{4}He **cluster admixtures**

Observables

- **Charge Radii**
- **Matter Radii**
- **Electromagnetic transitions**
- **Rotational bands**

Calculation

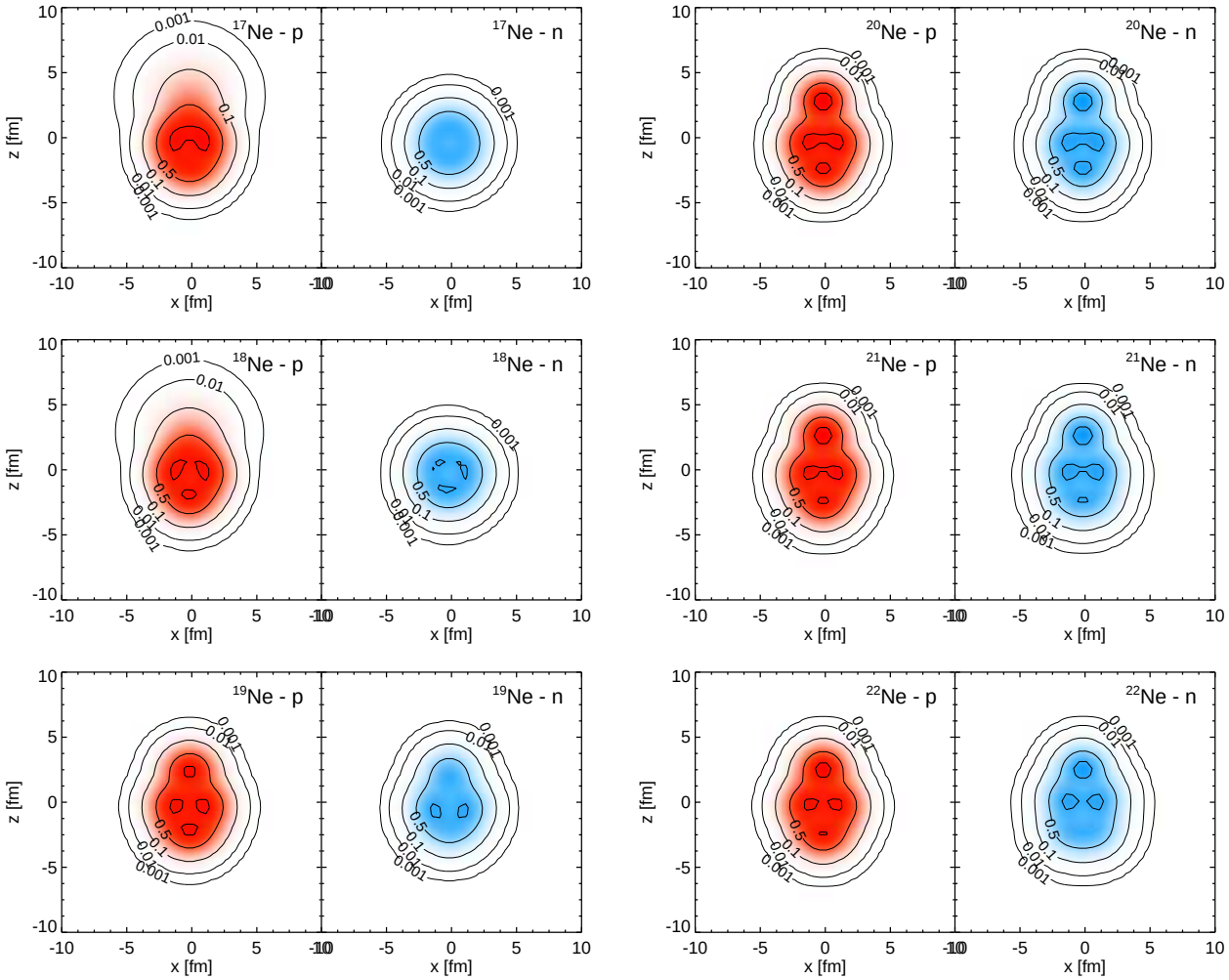

proton/neutron densities of dominant intrinsic FMD configuration

- UCOM(var) + phenomenological correction for saturation and spin-orbit
- Variation after parity projection on positive and negative parity
- Create basis states by cranking strength of spin-orbit force
- ^{15,16}O-“s^2” and ^{15,16}O-“d^2” minima in ^{17,18}Ne
- add explicit cluster configurations:
  ^{17}Ne: ^{14}O-^{3}He
  ^{18}Ne: ^{14}O-^{4}He
  ^{19}Ne: ^{16}O-^{3}He and ^{15}O-^{4}He
  ^{20}Ne: ^{16}O-^{4}He
  ^{21}Ne: “^{17}O”-^{4}He
  ^{22}Ne: “^{18}O”-^{4}He

Separation energies

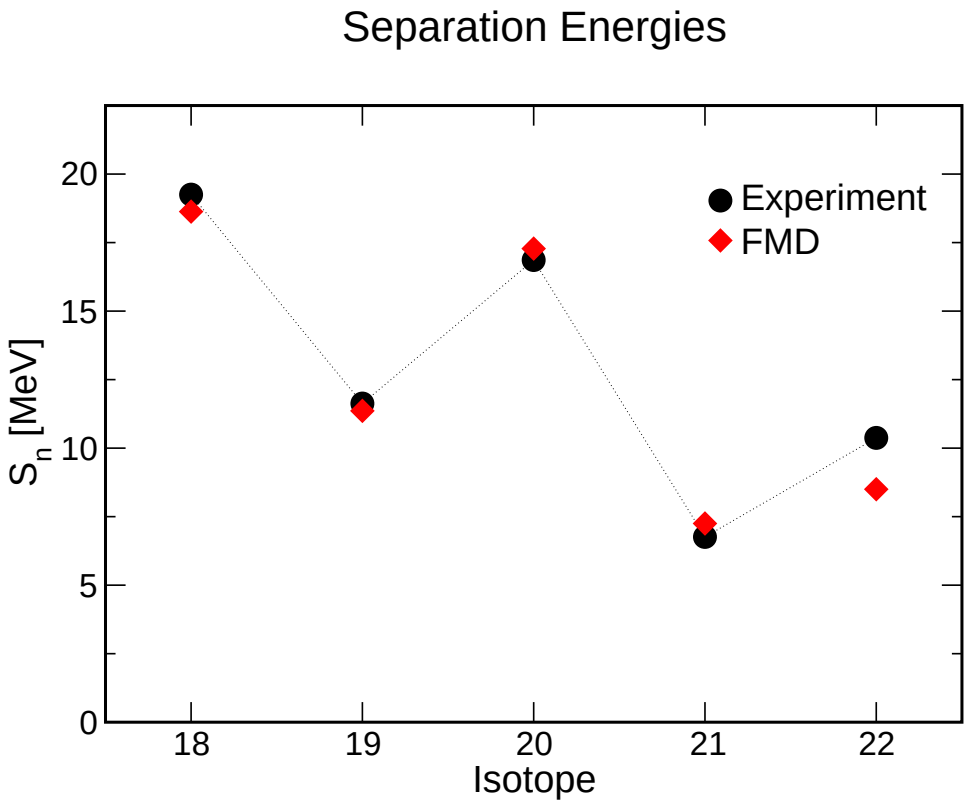

^{17,18}Ne: s^2/d^2 admixture

^{19}Ne: ^{3}He, α clustering

$^{20-22}$Ne: α clustering

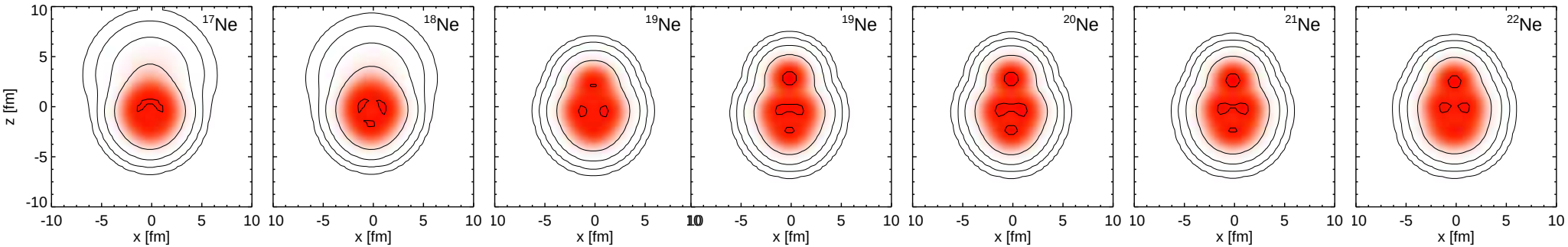

Charge and Matter Radii

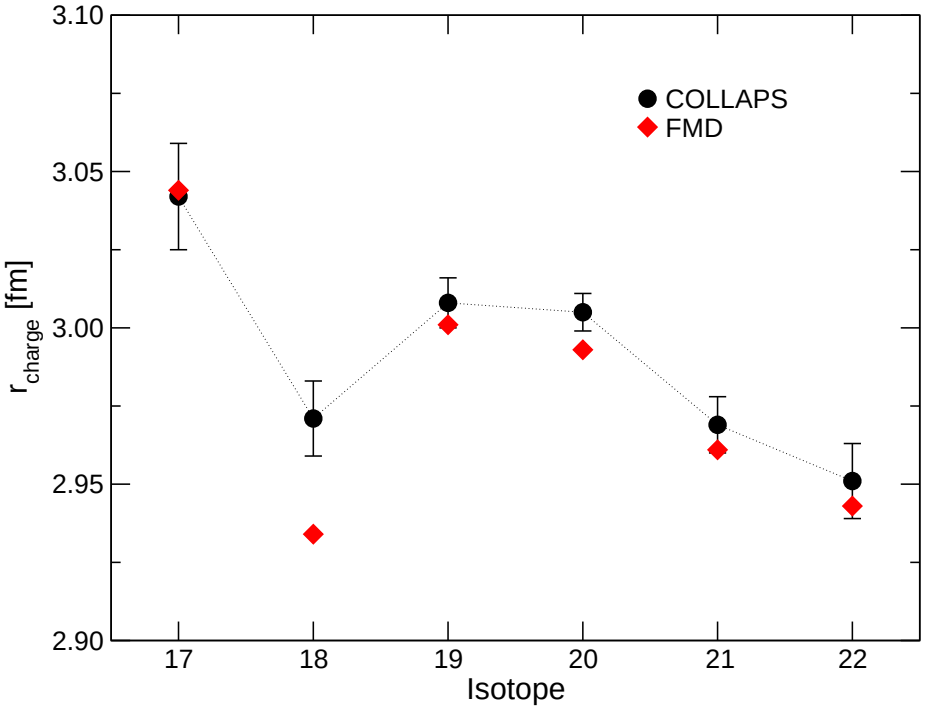

- charge radii of ^{17,18}Ne depend strongly on s^2/d^2 occupations
- cluster admixtures responsible for large charge radii in $^{19-22}$Ne

- measurements of charge radii by COLLAPS@ISOLDE, masses from ISOLTRAP@ISOLDE

W. Geithner, T. Neff *et al.*, Phys. Rev. Lett. **101**, 252502 (2008)

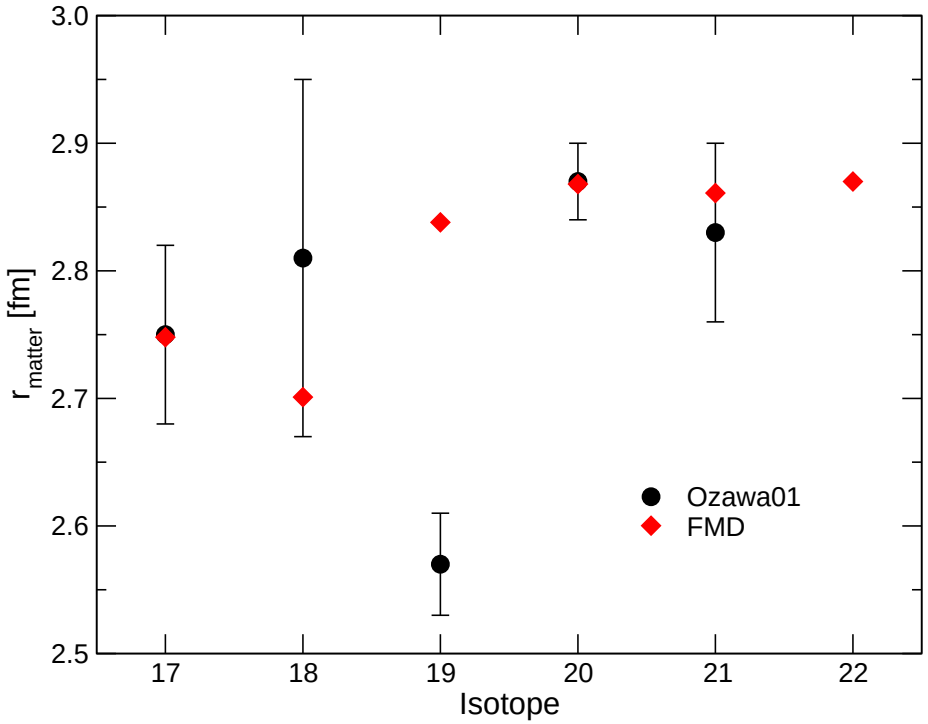

- matter radii from interaction cross sections

  A. Ozawa *et al.*, Nuc. Phys. **A693** (2001) 32

- good agreement with expection of ^{19}Ne

Neon Isotopes

^{17}Ne Halo ?

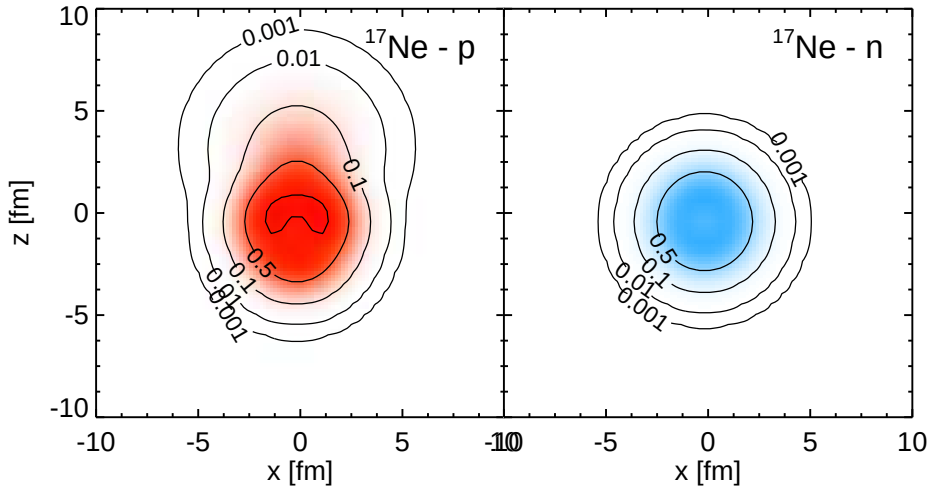

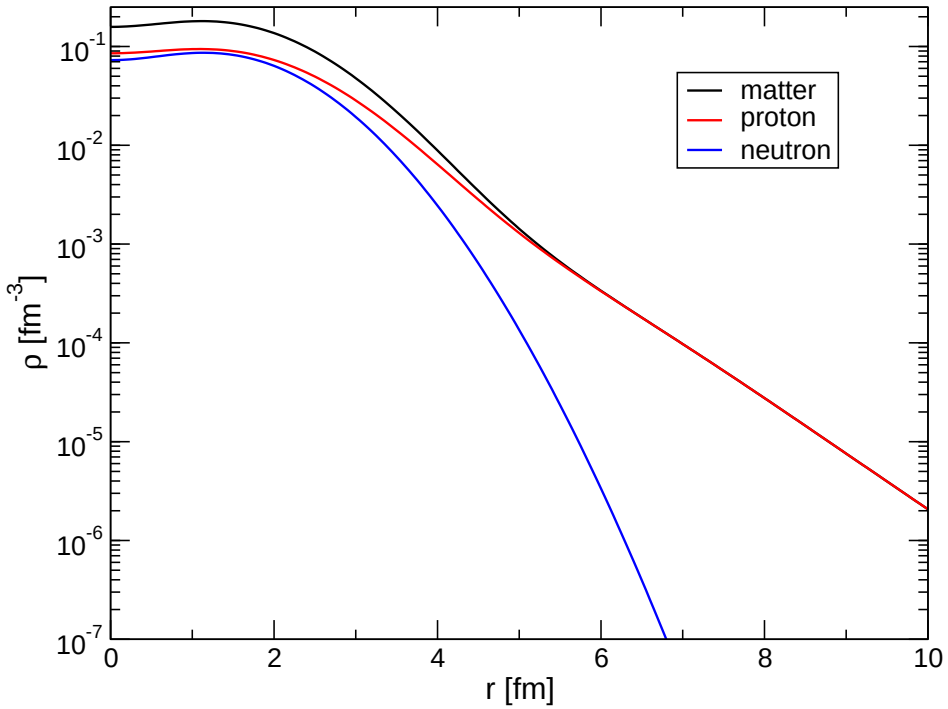

	FMD	Experiment
r_{ch}[fm]	3.04	3.042(21)
r_{mat}[fm]	2.75	2.75(7) [1]
$B(E2; \frac{1}{2}^- \rightarrow \frac{3}{2}^-)[e^2\text{fm}^4]$	76.7	66^{+18}_{-25} [2]
$B(E2; \frac{1}{2}^- \rightarrow \frac{5}{2}^-)[e^2\text{fm}^4]$	119.8	124(18) [2]
occupancy s^2	42%	
occupancy d^2	55%	

- proton skin $r_p - r_n = 0.45$ fm
- 40% probability to find a proton at $r > 5$ fm
- similar results are obtained in a three-body model

  L. Grigorenko *et al.*, Phys. Rev. C **71**, 051604 (2005)

[1] A. Ozawa *et al.*, Nuc. Phys. **A693**, 32 (2001)

[2] M. J. Chromik *et al.*. Phys. Rev. C **66**, 024313 (2002)

Beryllium Isotopes

Questions

- **α-clustering, halos in ^{11}Be and ^{14}Be, $N = 8$ shell closure ?**

Calculation

- **VAP and multiconfiguration-VAP calculations with mean proton distance as generator coordinate**
- **UCOM(SRG) effective spin-orbit strength is too small – modify interaction by multiplying spin-orbit interaction in $S = 1$, $T = 1$ channel with factor $\eta \approx 2$**

Observables

- **energies**
- **charge and matter radii, electromagnetic transitions**

Beryllium Isotopes

Variation (Mean-Field)

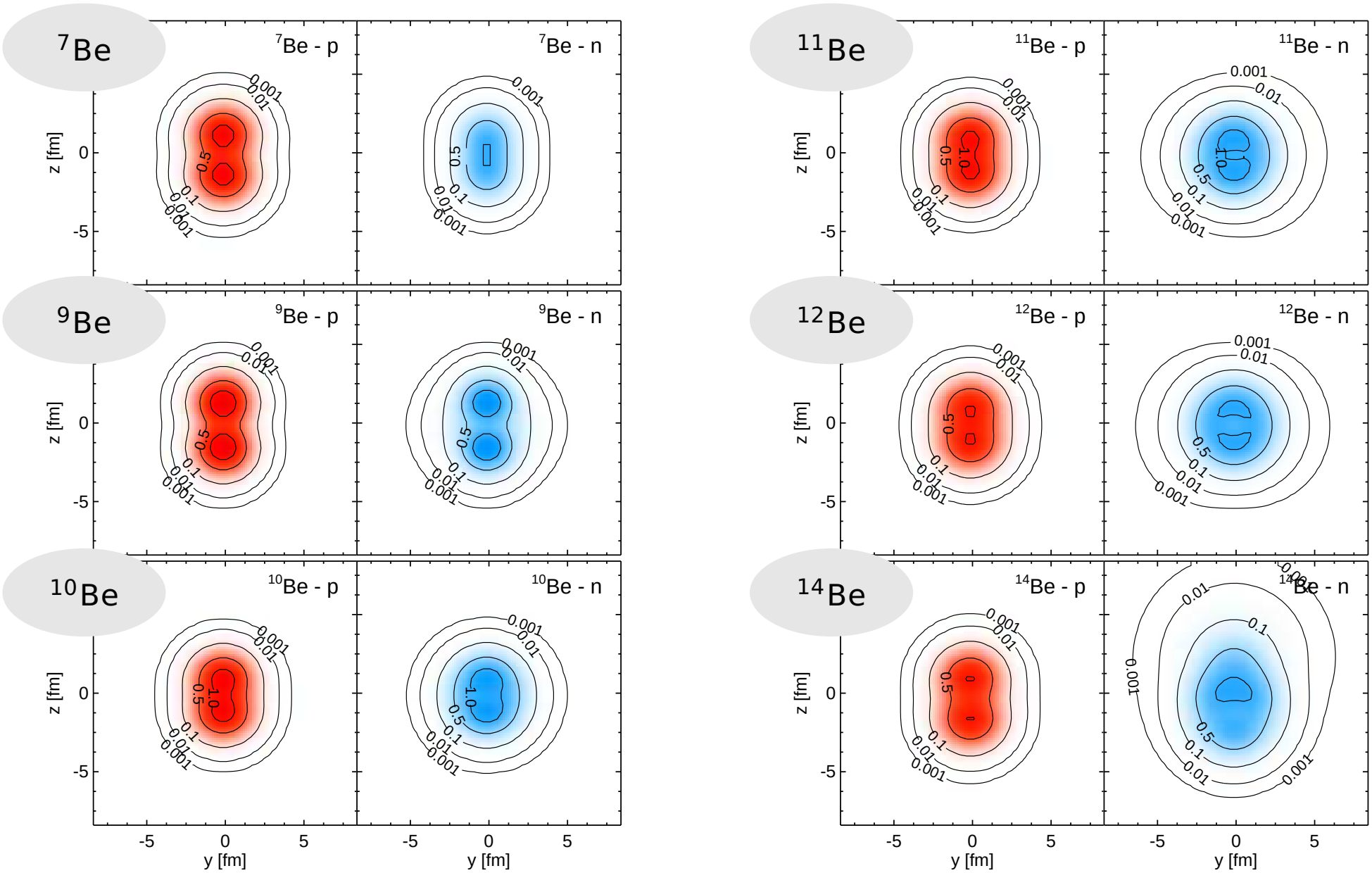

Beryllium Isotopes

Variation after Projection

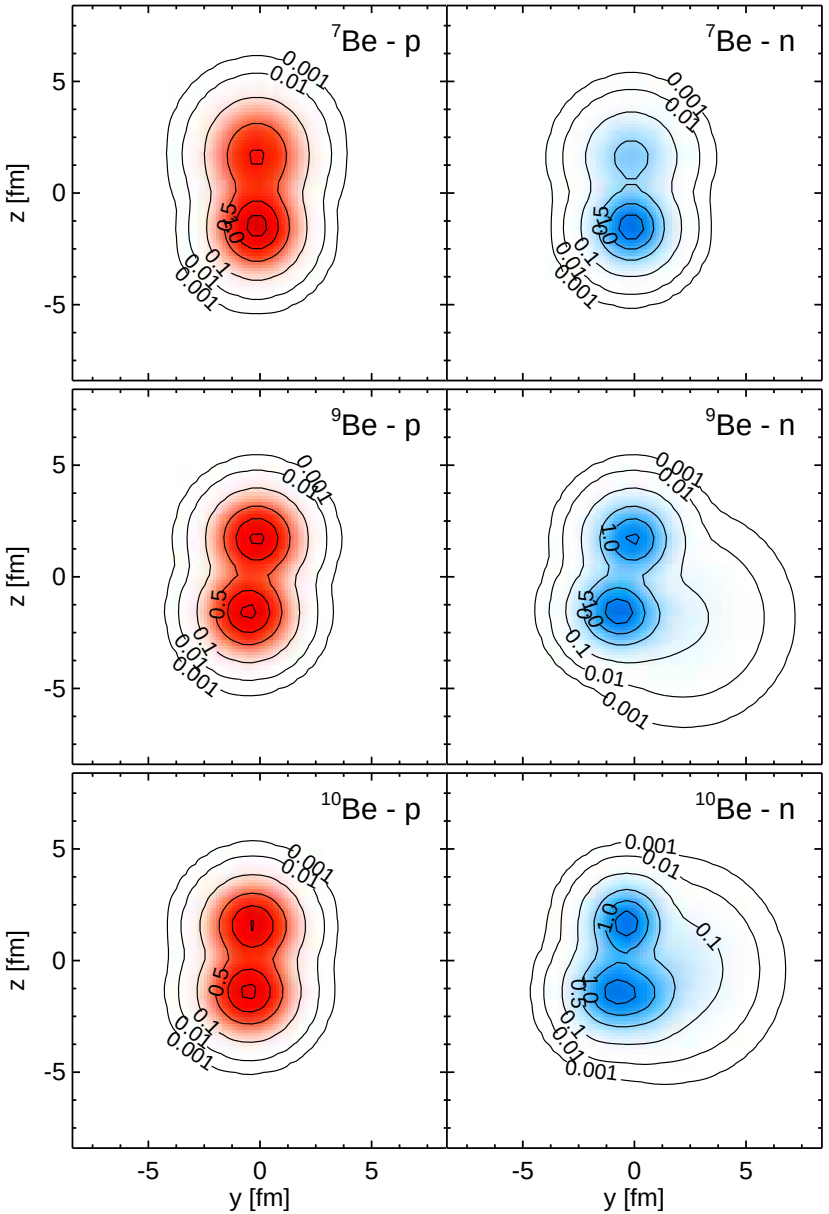

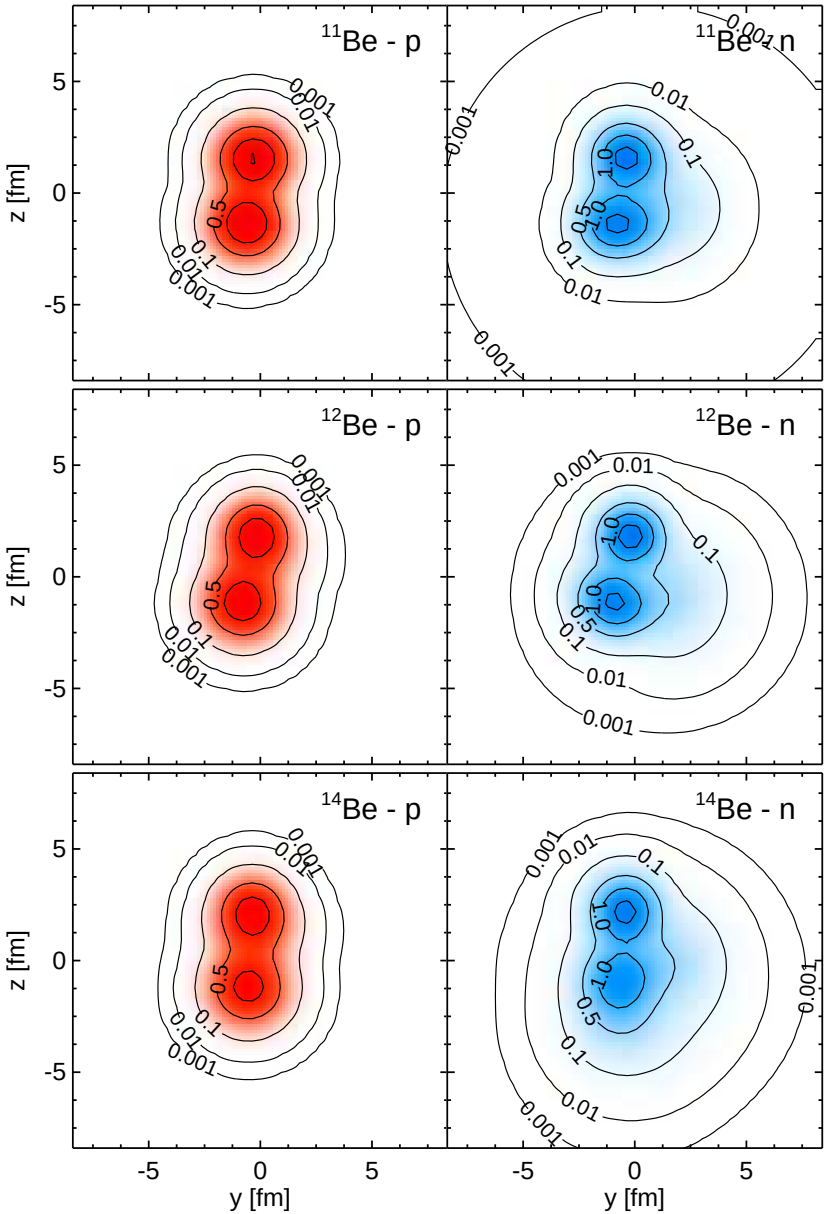

Variation after Projection

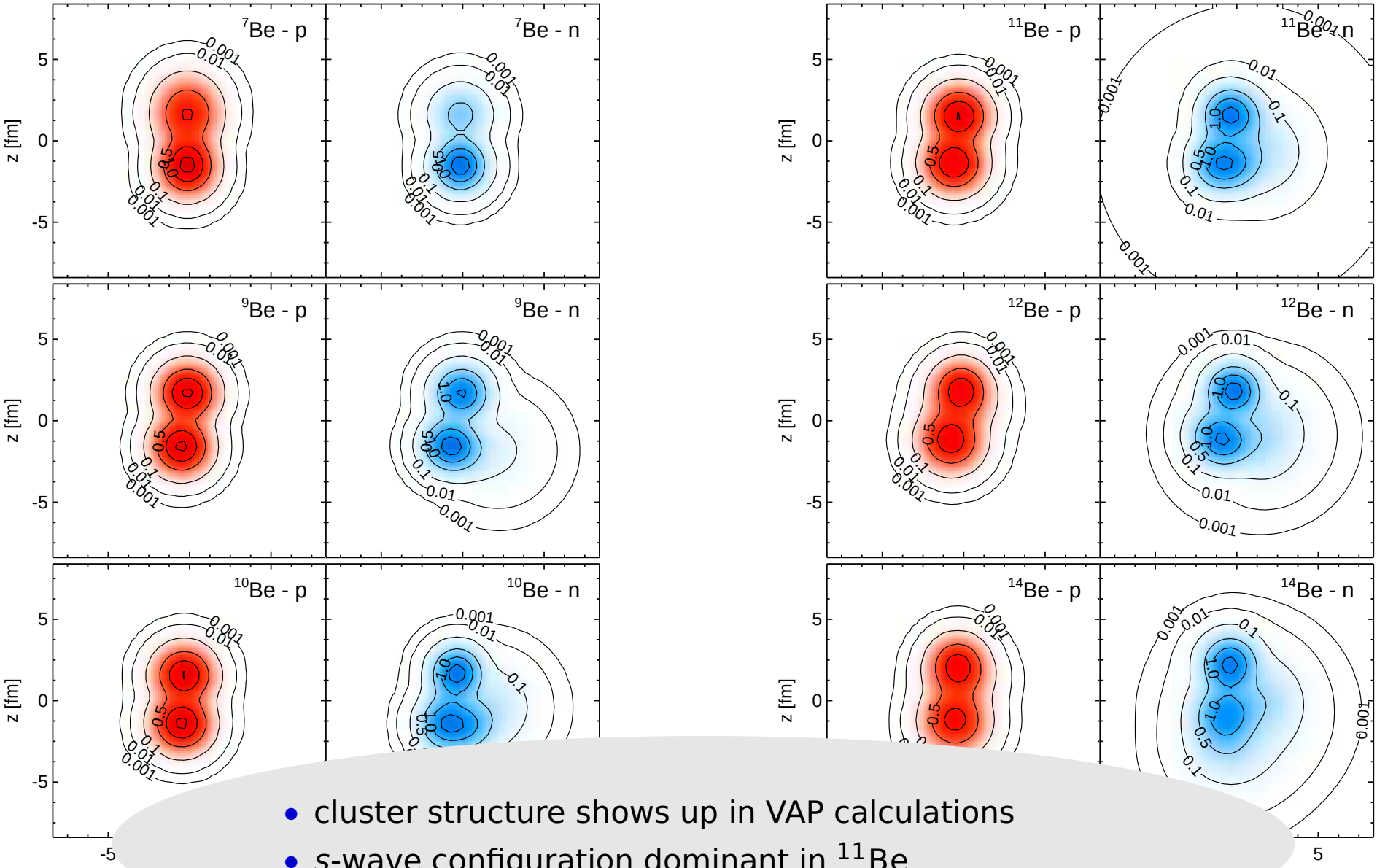

- cluster structure shows up in VAP calculations
- *s*-wave configuration dominant in ^{11}Be

Mean proton distance as generator coordinate

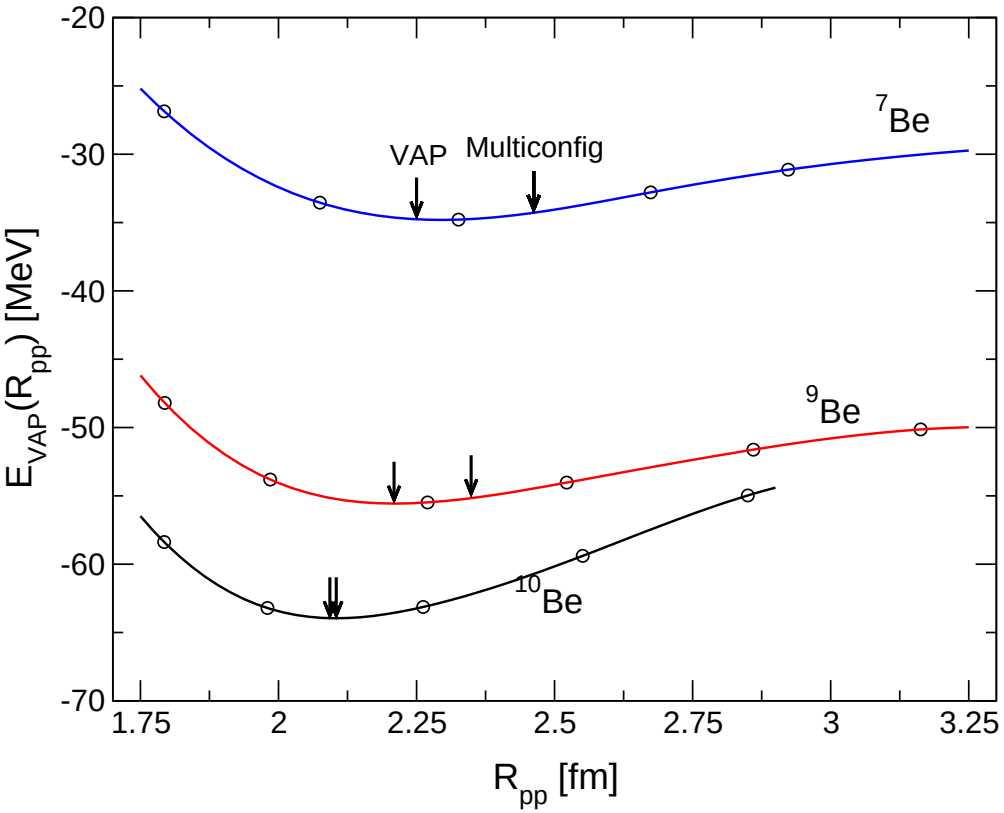

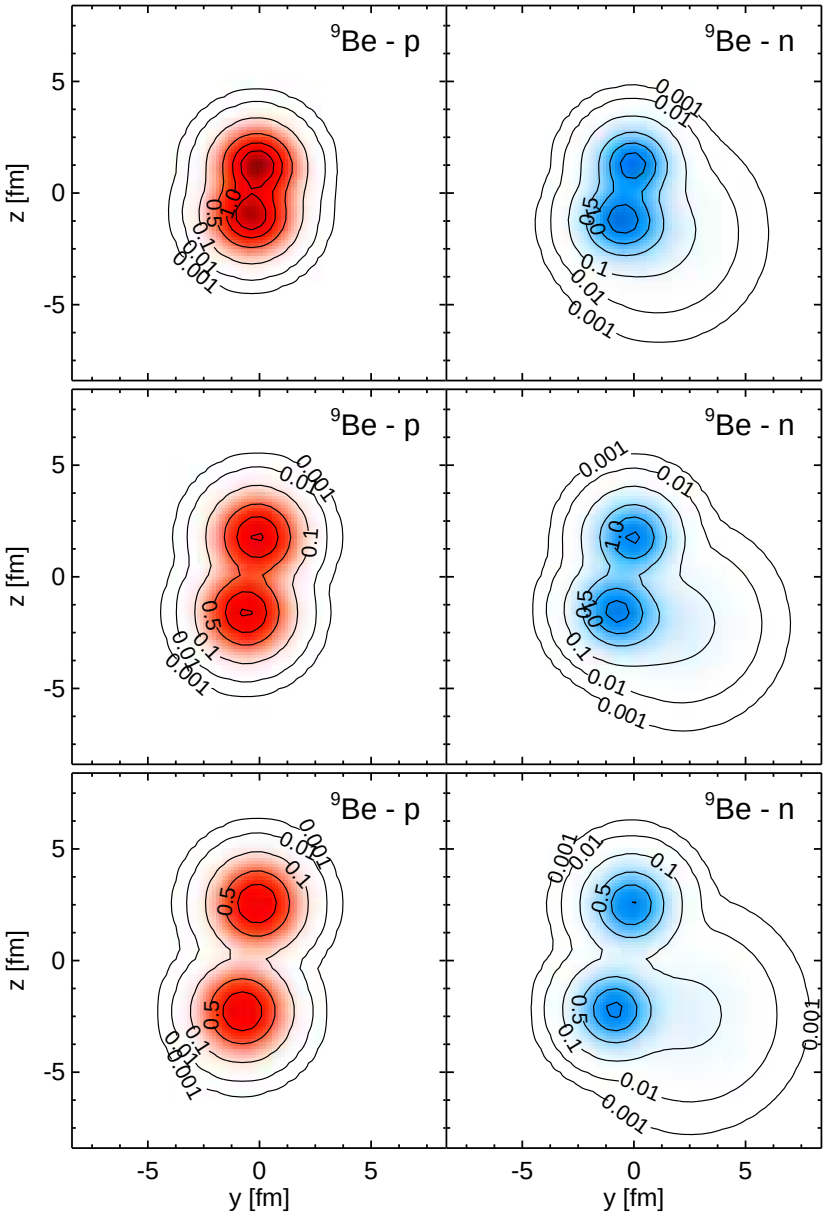

Mean proton distance

$$R_{pp}^2 = \frac{1}{Z^2}\langle \sum_{i<j}^{\text{protons}} (\mathbf{r}_i - \mathbf{r}_j)^2 \rangle$$

R_{pp} as a measure of
α-cluster distance

Mean proton distance as generator coordinate

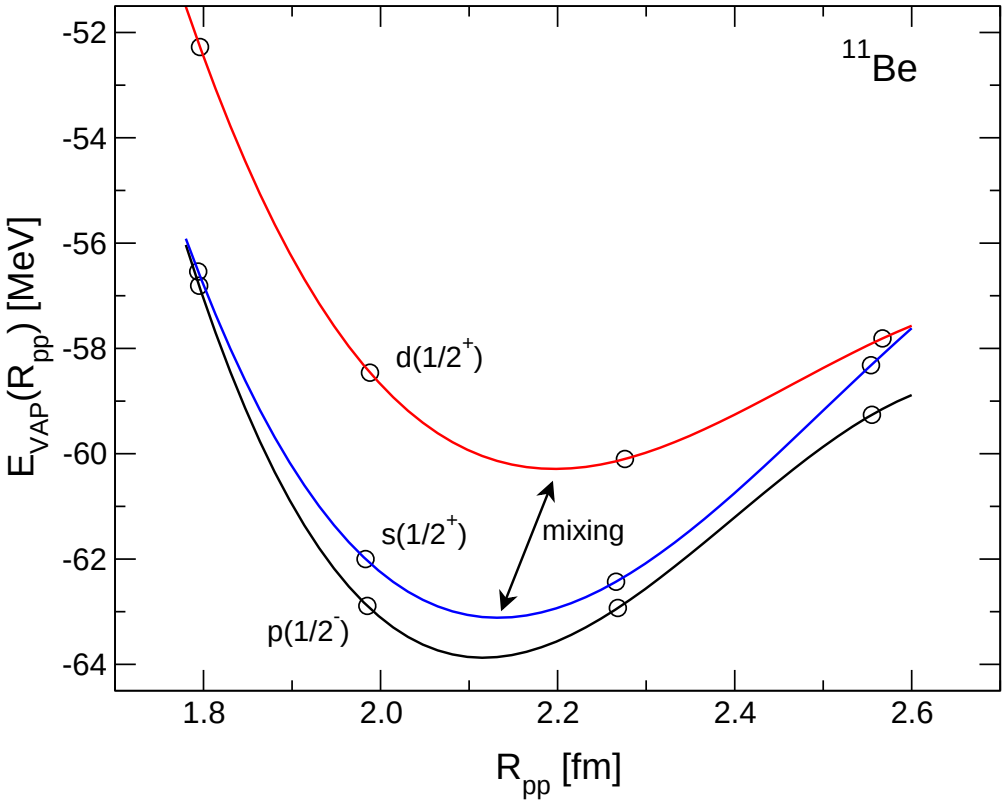

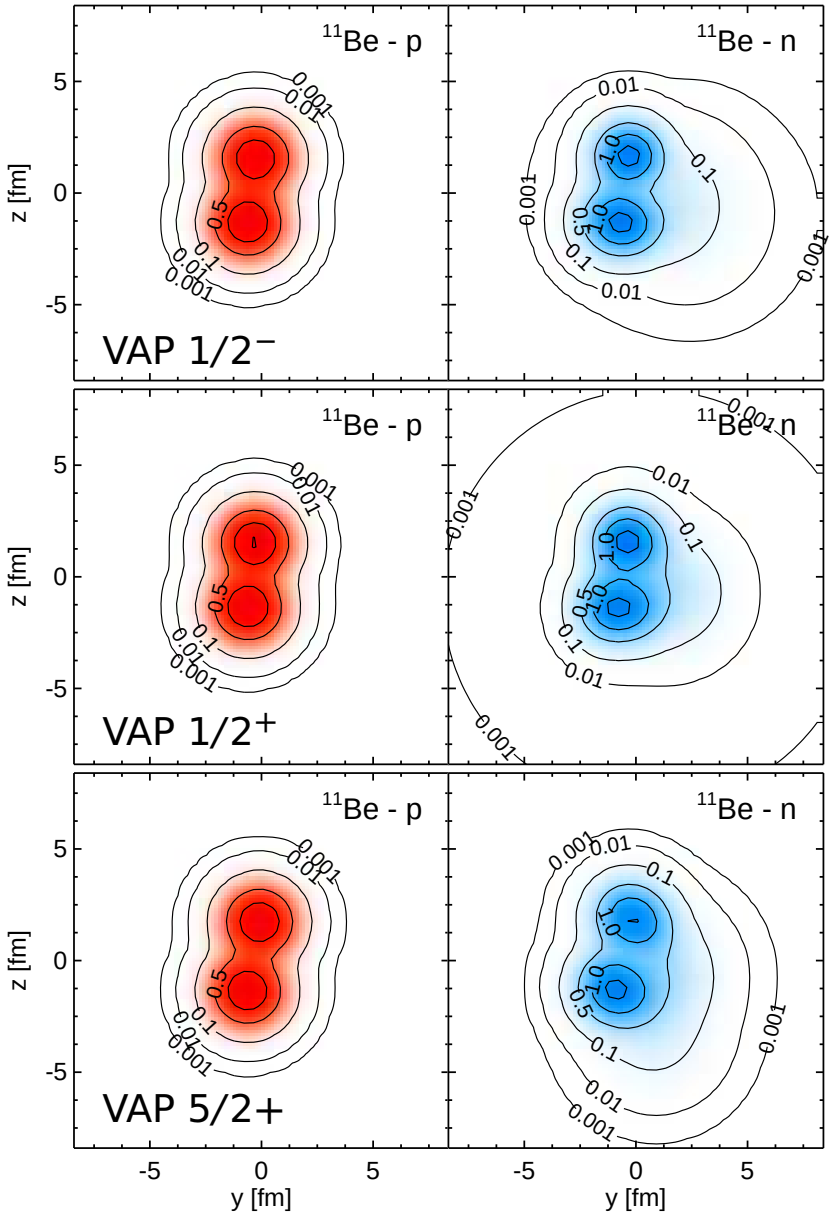

^{11}Be – "*p*", "*s*" and "*d*"-configurations

- "*s*"- and "*d*"-configurations will mix in 1/2$^+$ state
- energy surfaces for "*p*" and "*s*" similar to those in ^{10}Be
- "*d*" surface has minimum at larger cluster distance → *d*-configuration has a polarized ^{10}Be core

Beryllium Isotopes

$N = 8$ shell closure ?

^{10}Be

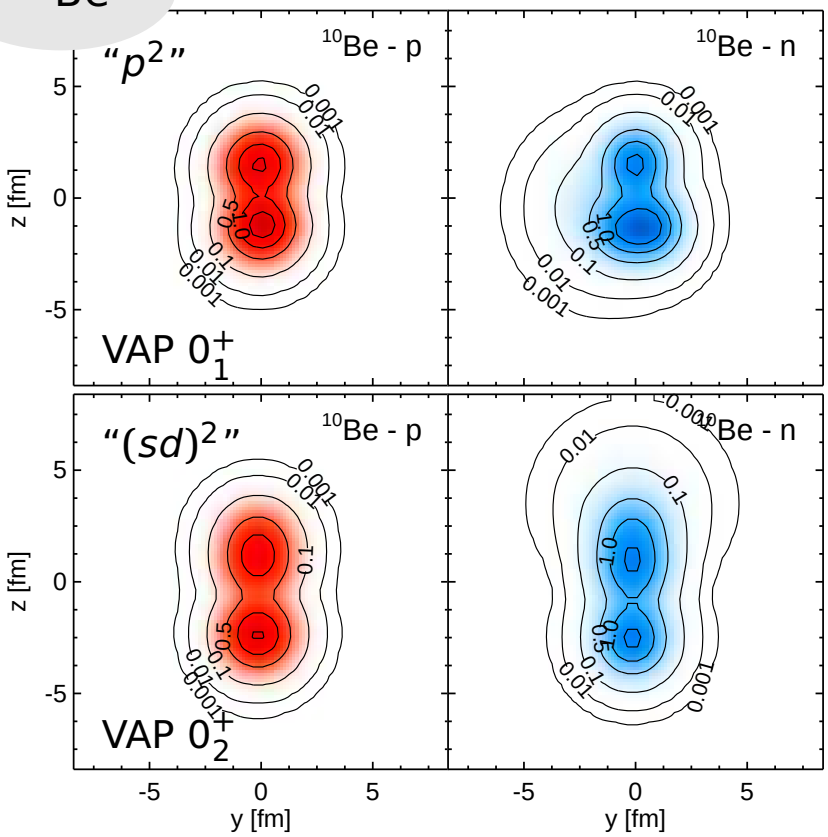

^{12}Be

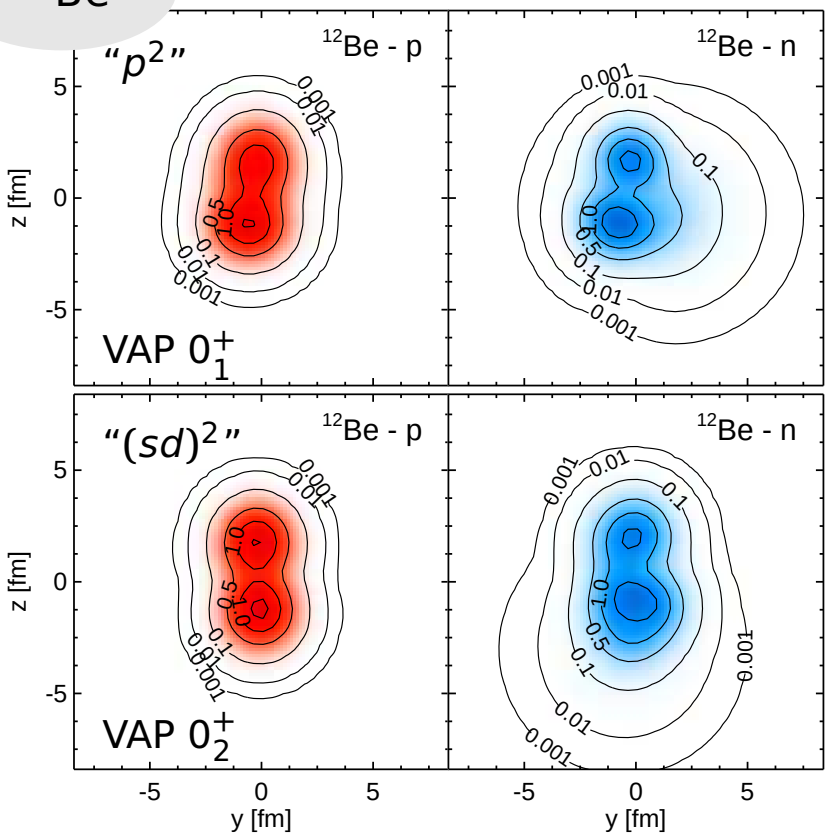

- in ^{12}Be normal and intruder configurations almost degenerate in energy
- contribution of spin-orbit force larger in intruder configuration
- eigenstate composition can be tuned from dominant p^2 to dominant $(sd)^2$ by changing spin-orbit factor from 2.0 to 2.2

Charge Radii

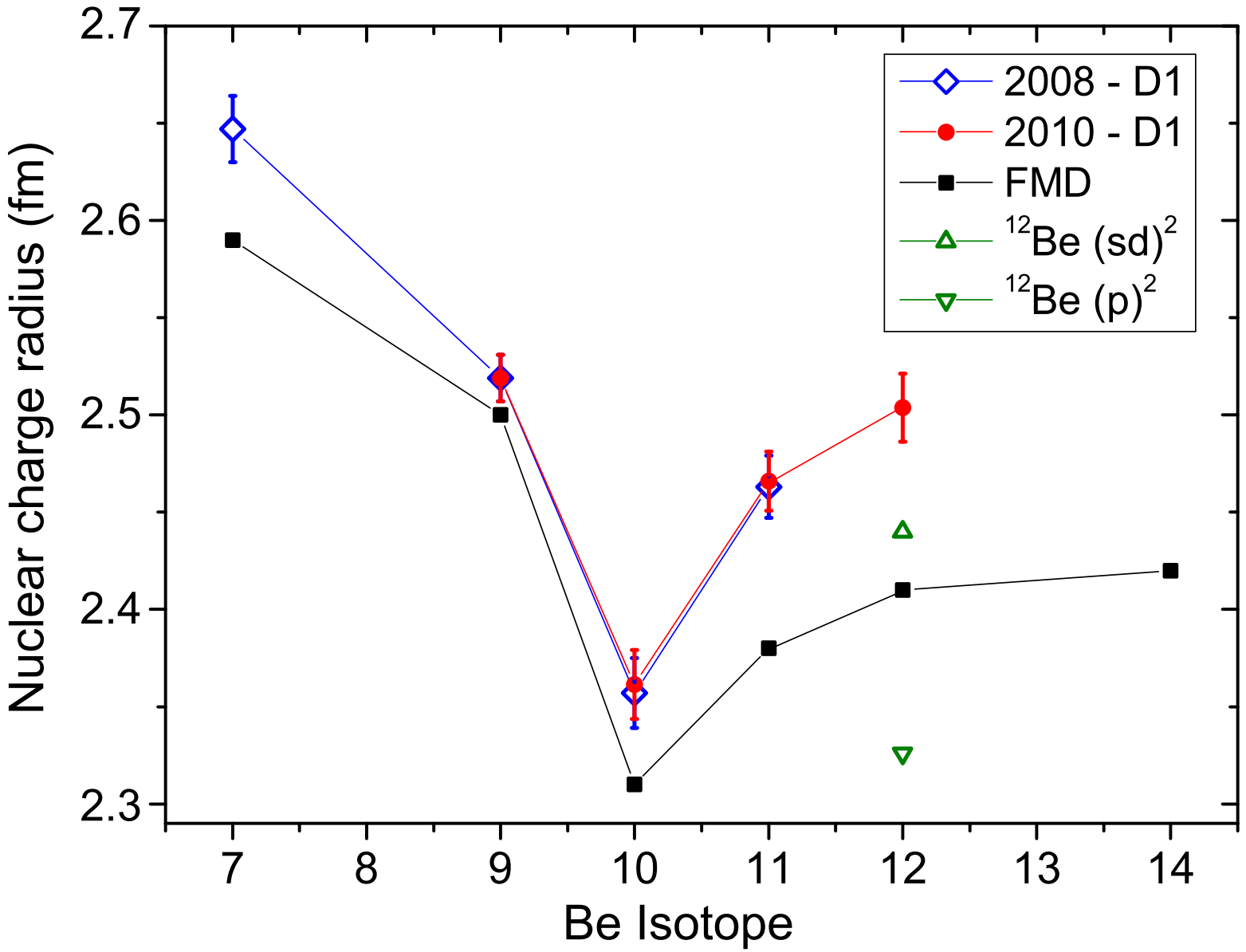

A. Krieger *et al.*, Phys. Rev. Lett. **108**, 142501 (2012)

Electromagnetic transitions

^{10}Be

	FMD(Multiconfig)	Experiment
$B(E2; 2_1^+ \to 0_1^+)$	8.07 e^2fm^4	9.2 ± 0.3 e^2fm^4
$B(E2; 2_2^+ \to 0_1^+)$	0.08 e^2fm^4	0.11 ± 0.02 e^2fm^4
$B(E2; 0_2^+ \to 2_1^+)$	0.17 e^2fm^4	3.2 ± 1.9 e^2fm^4

^{12}Be

	FMD(Multiconfig)	Experiment
$B(E2; 2_1^+ \to 0_1^+)$	8.75 e^2fm^4	8.0 ± 3.0 e^2fm^4
$B(E2; 0_2^+ \to 2_1^+)$	7.45 e^2fm^4	7.0 ± 0.6 e^2fm^4
$M(E0; 0_1^+ \to 0_2^+)$	0.90 $e$fm^2	0.87 ± 0.03 $e$fm^2

- Monopole and Quadrupole transitions directly connected to mixing between normal and intruder configurations
- 2_1^+ state has dominant intruder contribution

McCutchan *et al.*. Phys. Rev. Lett. **103**, 192501 (2009).
Nakamura *et al.*, Phys. Lett. **B394**, 11 (1997).
Shimoura *et al.*, Phys. Lett. **B654**, 87 (2007).
Iwasaki *et al.*, Phys. Lett. **B491**, 8 (2000).

^{3}He(α,γ)^{7}Be radiative capture

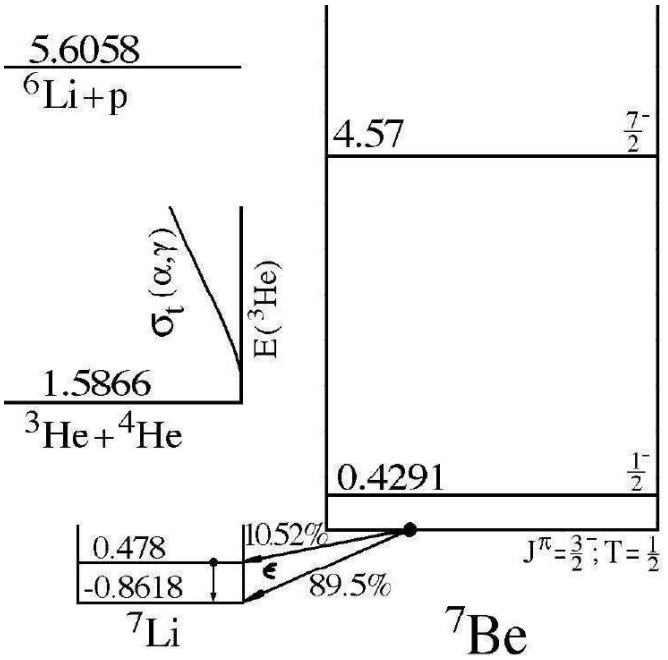

Effective Nucleon-Nucleon interaction:

UCOM(SRG) $\alpha = 0.20$ **fm**^{4} **–** $\lambda \approx 1.5$ **fm**$^{-1}$

Many-Body Approach:

Fermionic Molecular Dynamics

- **Internal region: VAP configurations with radius constraint**
- **External region: Brink-type cluster configurations**
- **Matching to Coulomb solutions: Microscopic *R*-matrix method**

Results:

- ^{7}Be **bound and scattering states**
- **Astrophysical *S*-factor**

T. Neff, Phys. Rev. Lett. **106**, 042502 (2011)

^{3}He(α,γ)^{7}Be

Astrophysical Motivation

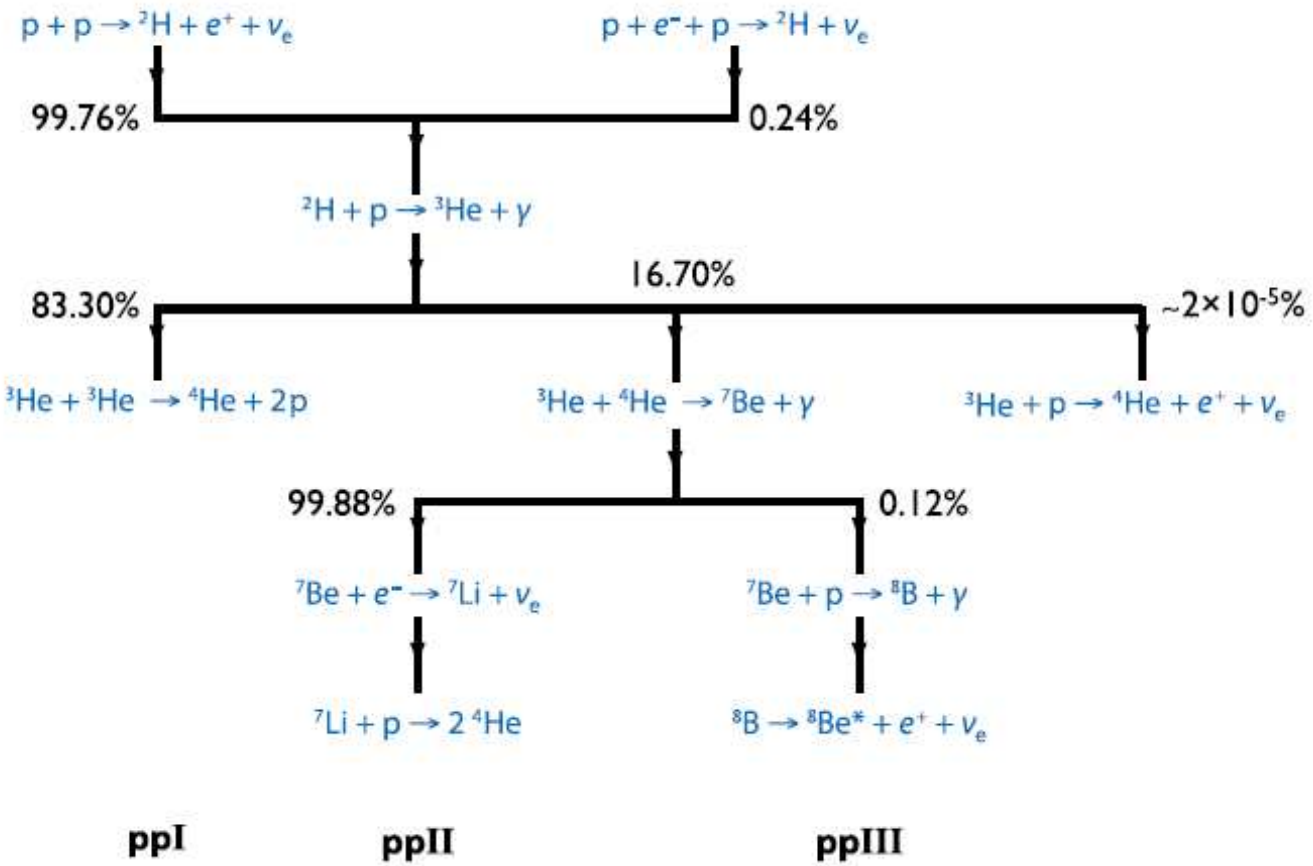

- ^{3}He(α,γ)^{7}Be is one of the key reactions in the solar pp-chains
- in competetion with the ^{3}He(^{3}He,2p)^{4}He reaction it determines production of ^{7}Be and ^{8}B neutrinos

Theoretical Approaches

Potential models (Kim *et al.* 1982, Mohr 2009, . . .)

- ^{4}He and ^{3}He are considered as point-like particles
- interacting via an effective nucleus-nucleus potential fitted to bound state properties and phase shifts
- ANCs calculated from *ab initio* wave functions (Nollett 2001, Navratil *et al.* 2007)

Microscopic Cluster Model (Tang *et al.* 1981, Langanke 1986, Kajino 1986 . . .)

- antisymmetrized wave function built with ^{4}He and ^{3}He clusters
- some attempts to include polarization effects by adding other channels like ^{6}Li plus proton
- interacting via an effective nucleon-nucleon potential, adjusted to describe bound state properties and phase shifts

Our Aim

- fully microscopic wave functions with cluster configurations at large distances and additional polarized A-body configurations in the interaction region
- using a realistic effective interaction

FMD model space

Frozen configurations

- 15 antisymmetrized wave function built with ^{4}He and ^{3}He FMD clusters up to channel radius a=12 fm

Polarized configurations

- 30 FMD wave functions obtained by VAP on $1/2^-$, $3/2^-$, $5/2^-$, $7/2^-$ and $1/2^+$, $3/2^+$ and $5/2^+$ combined with radius constraint in the interaction region

Boundary conditions

- Match relative motion of clusters at channel radius to Whittaker/Coulomb functions with the **microscopic *R*-matrix** method of the Brussels group

D. Baye, P.-H. Heenen, P. Descouvemont

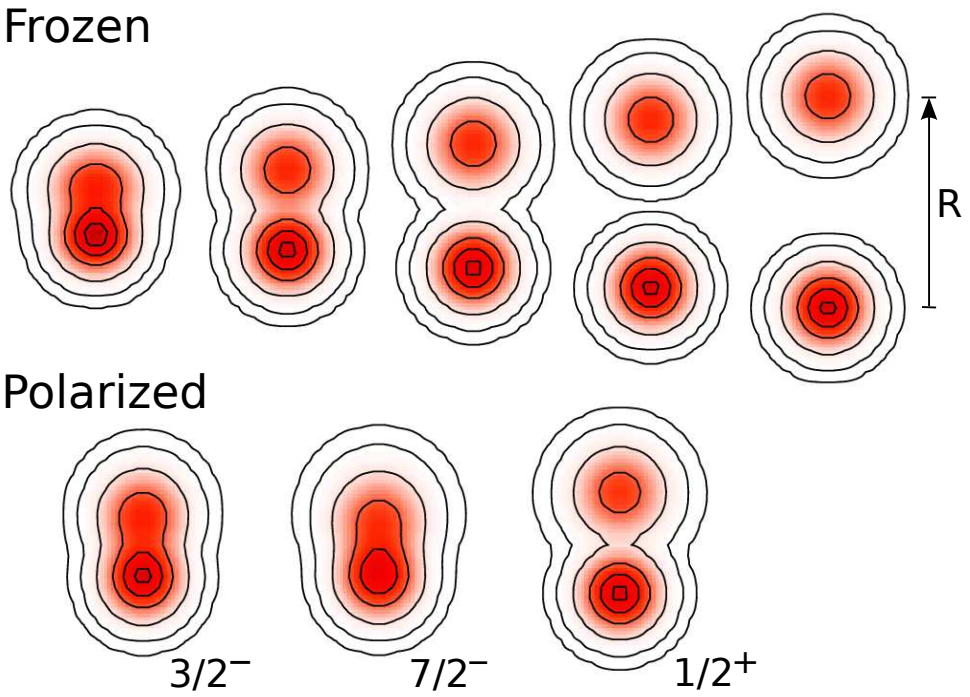

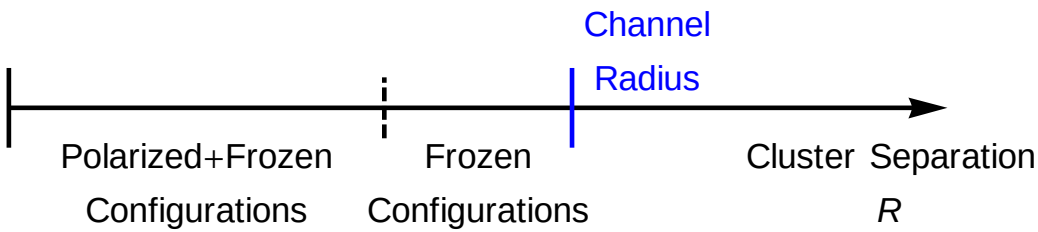

Slater determinants and RGM wave functions

- In internal region wave function is described microscopically with FMD Slater determinants
- In external region wave function is considered as a system of two point-like clusters
- (Microscopic) cluster wave function – Slater determinant

$$\left| Q^{ab}(\mathbf{R}) \right\rangle = \frac{1}{\sqrt{c_{ab}}} \mathcal{A} \left\{ \left| Q^{a}(-\frac{m_b}{m_a+m_b}\mathbf{R}) \right\rangle \otimes \left| Q^{b}(\frac{m_a}{m_a+m_b}\mathbf{R}) \right\rangle \right\}$$

- Projection on total linear momentum decouples intrinsic motion, relative motion of clusters and total center-of-masss

$$\left| Q^{ab}(\mathbf{R}); \mathbf{P}=0 \right\rangle = \int \mathrm{d}^3 r \, \tilde{\Gamma}(\mathbf{r}-\mathbf{R}) \left| \Phi^{ab}(\mathbf{r}) \right\rangle \otimes \left| \mathbf{P}_{cm}=0 \right\rangle$$

using RGM basis states

$$\left\langle \boldsymbol{\rho}, \xi_a, \xi_b \right| \left. \Phi^{ab}(\mathbf{r}) \right\rangle = \frac{1}{\sqrt{c_{ab}}} \mathcal{A} \left\{ \delta(\boldsymbol{\rho}-\mathbf{r}) \Phi^{a}(\xi_a) \Phi^{b}(\xi_b) \right\}$$

RGM norm kernel

$$n^{ab}(\mathbf{r}, \mathbf{r}') = \left\langle \Phi^{ab}(\mathbf{r}) \right| \left. \Phi^{ab}(\mathbf{r}') \right\rangle$$

Slater determinants and RGM wave functions

- Relative motion in Slater determinant described by Gaussian

$$\tilde{\Gamma}(\mathbf{r}-\mathbf{R}) = \left(\frac{\beta_{\text{rel}}}{\pi^2 a_{\text{rel}}}\right)^{3/4} \exp\left(-\frac{(\mathbf{r}-\mathbf{R})^2}{2a_{\text{rel}}}\right)$$

with

$$a_{\text{rel}} = \frac{a_a A_b + a_b A_a}{A_a A_b}, \quad \beta_{\text{rel}} = \frac{a_a a_b}{a_a A_b + a_b A_a}$$

- Overlap of full wave function with RGM cluster basis

$$\psi(\mathbf{r}) = \int \mathrm{d}^3 r'\, n^{-1/2}(\mathbf{r},\mathbf{r}') \left\langle \Phi(\mathbf{r}') \middle| \Psi \right\rangle$$

- Now Angular Momentum and Parity Projected . . .

$$\left| Q^{ab}_{K_a,K_b}(R\mathbf{e}_z); J^\pi MK; \mathbf{P}=0 \right\rangle = \sum_{IL} \int \mathrm{d}r r^2 \tilde{g}^{ab}_{K_a K_b;(LI)J^\pi}(R;r) \left| \Phi^{ab}(r); (LI)J^\pi M \right\rangle \otimes \left| \mathbf{P}_{cm}=0 \right\rangle$$

with the reduced width amplitude

$$\tilde{g}^{ab}_{K_a K_b;(LI)J^\pi}(R;r) = \mathrm{C}\left(\begin{array}{cc|c} I_a & I_b & I \\ K_a & K_b & K \end{array}\right) \mathrm{C}\left(\begin{array}{cc|c} L & I & J \\ 0 & K & K \end{array}\right) \sqrt{\frac{2L+1}{4\pi}} 4\pi \left(\frac{\beta_{\text{rel}}}{\pi^2 a_{\text{rel}}}\right)^{3/4} \exp\left(-\frac{R^2+r^2}{2a_{\text{rel}}}\right) i_L\left(\frac{Rr}{a_{\text{rel}}}\right)$$

R-Matrix Method

- Expand wave function in internal region using (polarized) FMD and two-cluster basis states

$$\left|\,\Psi_{\text{int}};J^\pi M\,\right\rangle_P = \sum_{i\kappa_i}\left|\,Q^{(i)};J^\pi M\kappa_i;\,\mathbf{P}=0\,\right\rangle C^{J^\pi}_{i,\kappa_i} + \sum_j \left|\,Q^{ab}_{K_aK_b}(R_j\mathbf{e}_z);J^\pi M;\,\mathbf{P}=0\,\right\rangle_P C^{J^\pi}_j$$

- Solutions for two-body Hamiltonian in outside region known

$$\underset{\sim}{H}(r) = \underset{\sim}{T}_r + \frac{L(L+1)}{2\mu r^2} + \frac{e^2 Z_a Z_b}{r} + E_a + E_b$$

- Solve the Schrödinger Equation with boundary conditions at $r = a$

$$(\underset{\sim}{H} + \underset{\sim}{\mathcal{L}}(B) - E)\left|\,\Psi_{\text{int}}\,\right\rangle_P = \underset{\sim}{\mathcal{L}}(B)\left|\,\Psi_{\text{ext}}\,\right\rangle$$

with the Bloch operator

$$\underset{\sim}{\mathcal{L}}(B) = \frac{1}{2\mu a}\delta(r-a)\left(\frac{\mathrm{d}}{\mathrm{d}r} - \frac{B}{r}\right),$$

- Evalutating the matrix elements in the internal region

$$\left\langle\, Q^{ab}(R_i)\,\middle|\,\underset{\sim}{H}\,\middle|\,Q^{ab}(R_j)\,\right\rangle_P = \left\langle\, Q^{ab}(R_i)\,\middle|\,\underset{\sim}{H}\,\middle|\,Q^{ab}(R_j)\,\right\rangle - \int_a^\infty \mathrm{d}r\, r^2 \tilde{g}(R_i;r)^\star \underset{\sim}{H}(r)\tilde{g}(R_j;r)\,.$$

R-Matrix Method

- Bound states: Match asymptotics to Whittaker function

$$\psi_{\mathrm{b}}(r) = A\,\frac{1}{r} W_{-\eta,L+1/2}(2\kappa r)$$

with

$$\kappa = \sqrt{-2\mu E_b}, \quad \eta = \mu \frac{Z_a Z_b e^2}{\kappa}$$

➳ This is a self-consistency problem

- Scattering states: Match asymptotics to Coulomb functions with phase shift

$$\psi_{\mathrm{scatt}}(r) = \frac{1}{r}\left\{I_L(\eta, kr) - e^{2i\delta} O_L(\eta, kr)\right\}$$

with

$$k = \sqrt{2\mu E}, \quad \eta = \mu \frac{Z_a Z_b e^2}{k}$$

➳ Determine R-matrix by inversion

p-wave Bound and Scattering States

Bound states

		Experiment	FMD
^{7}Be	$E_{3/2-}$	-1.59 MeV	-1.49 MeV
	$E_{1/2-}$	-1.15 MeV	-1.31 MeV
	r_{ch}	2.647(17) fm	2.67 fm
	Q	–	-6.83 e fm^2
^{7}Li	$E_{3/2-}$	-2.467 MeV	-2.39 MeV
	$E_{1/2-}$	-1.989 MeV	-2.17 MeV
	r_{ch}	2.444(43) fm	2.46 fm
	Q	-4.00(3) e fm^2	-3.91 e fm^2

- centroid of bound state energies well described if polarized configurations included
- tail of wave functions tested by charge radii and quadrupole moments

Phase shift analysis:

Spiger and Tombrello, PR **163**, 964 (1967)

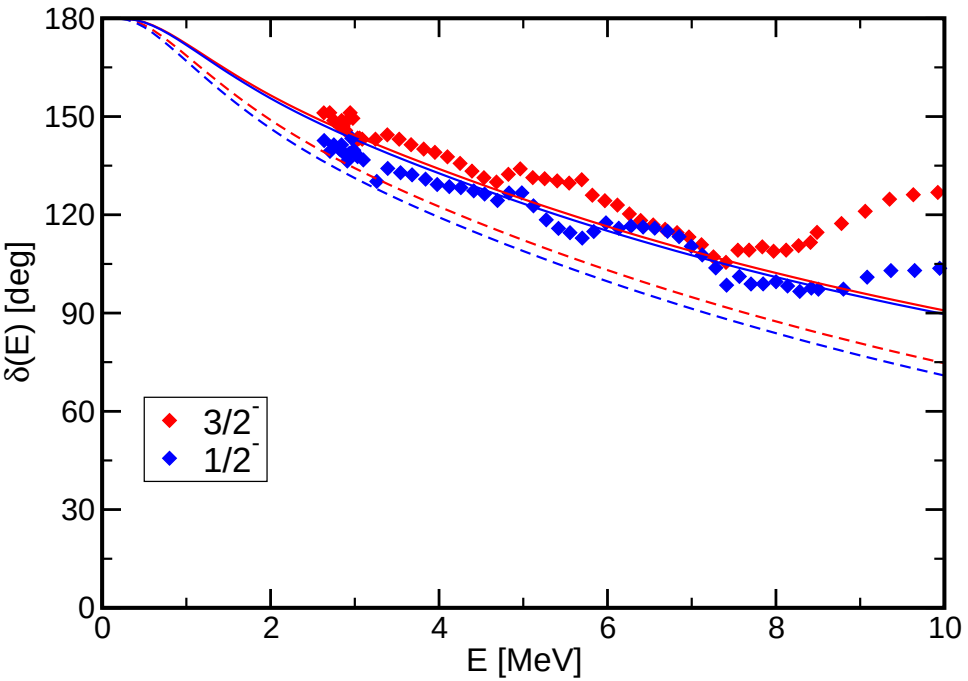

dashed lines – frozen configurations only
solid lines – polarized configurations in interaction region included

- Scattering phase shifts well described, polarization effects important

^{3}He$(\alpha,\gamma)^7$Be

s-, d- and f-wave Scattering States

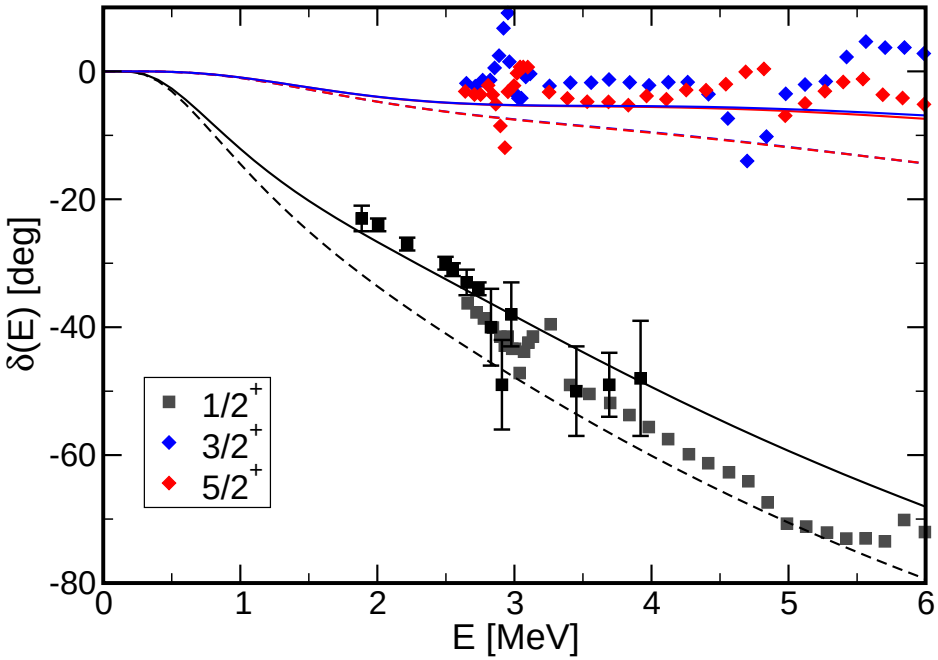

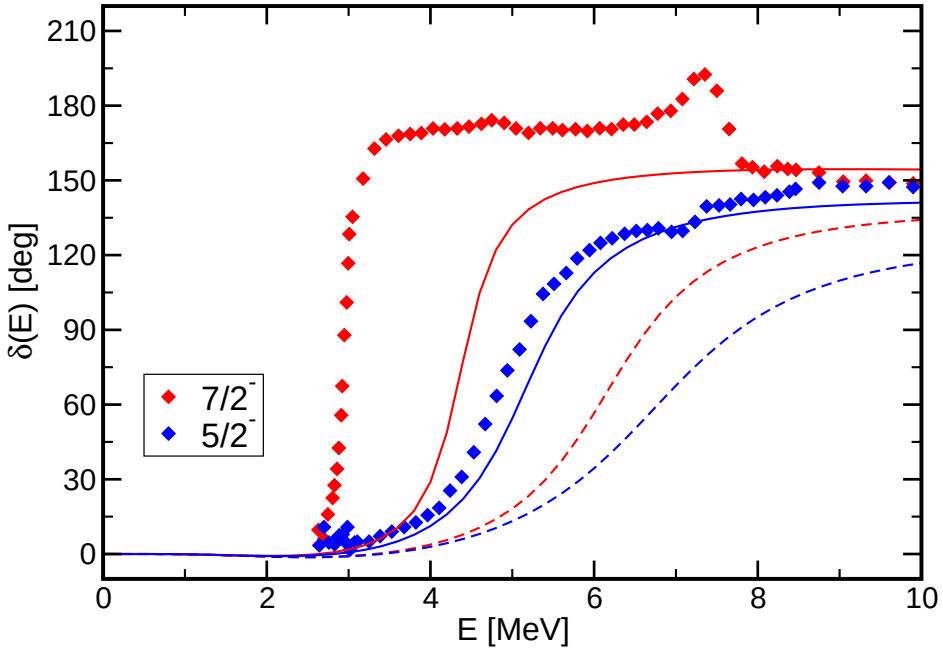

dashed lines – frozen configurations only – solid lines – FMD configurations in interaction region included

- polarization effects important
- s- and d-wave scattering phase shifts well described
- $7/2^-$ resonance too high, $5/2^-$ resonance roughly right, consistent with no-core shell model calculations

$^3He(\alpha,\gamma)^7Be$
S-Factor

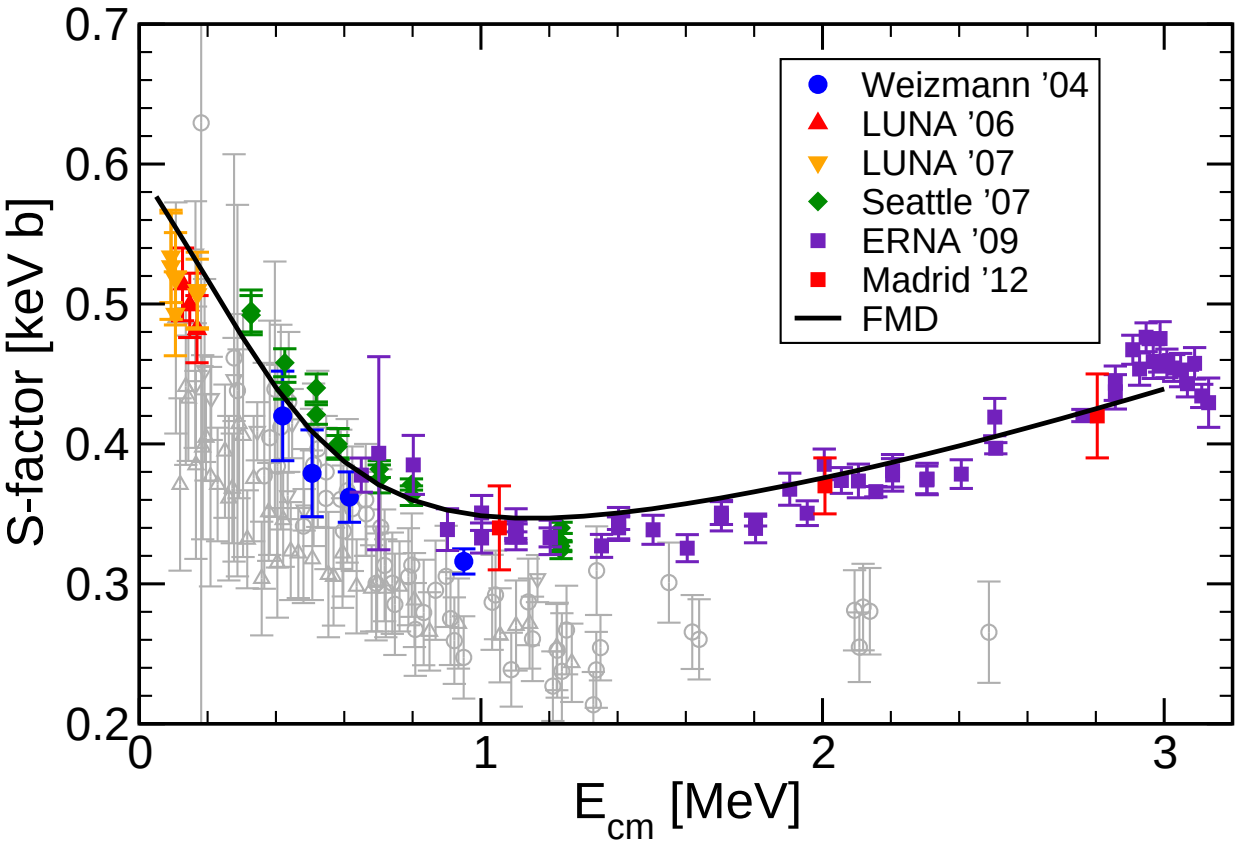

S-factor:

$$S(E) = \sigma(E) E \exp\{2\pi\eta\}$$

$$\eta = \frac{\mu Z_1 Z_2 e^2}{k}$$

Nara Singh *et al.*, PRL **93**, 262503 (2004)
Bemmerer *et al.*, PRL **97**, 122502 (2006)
Confortola *et al.*, PRC **75**, 065803 (2007)
Brown *et al.*, PRC **76**, 055801 (2007)
Di Leva *et al.*, PRL **102**, 232502 (2009)
Carmona-Gallardo *et al.*,
PRC **86**, 032801(R) (2012)

- dipole transitions from $1/2^+$, $3/2^+$, $5/2^+$ scattering states into $3/2^-$, $1/2^-$ bound states
- ➳ FMD is the only model that describes well the energy dependence and normalization of new high quality data
- ➳ fully microscopic calculation, bound and scattering states are described consistently

T. Neff, Phys. Rev. Lett. **106** (2011) 042502

$^3He(\alpha,\gamma)^7Be$

Overlap Functions and Dipole Matrixelements

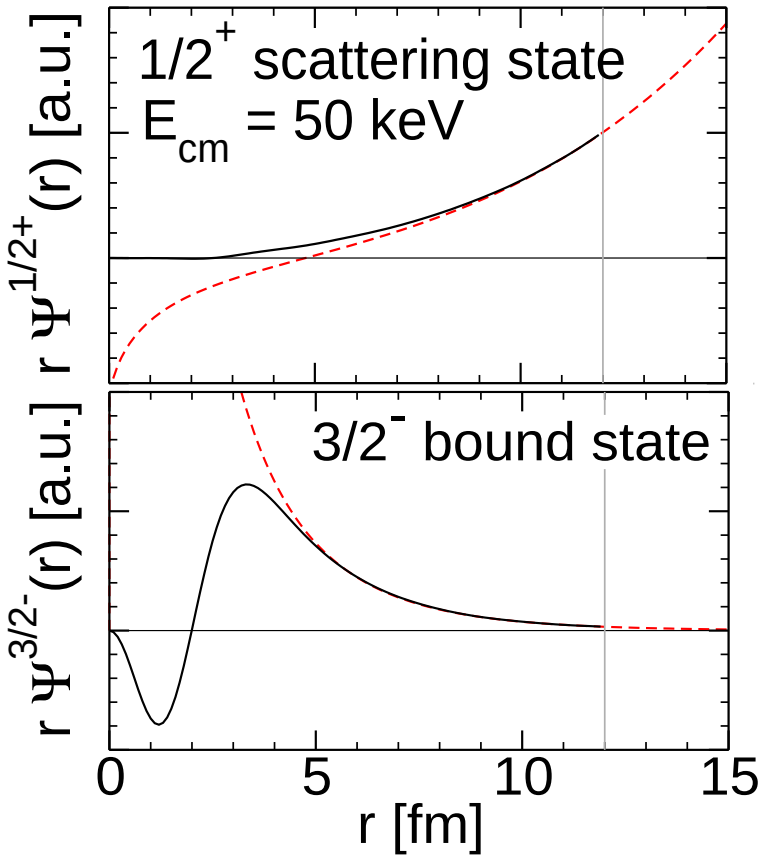

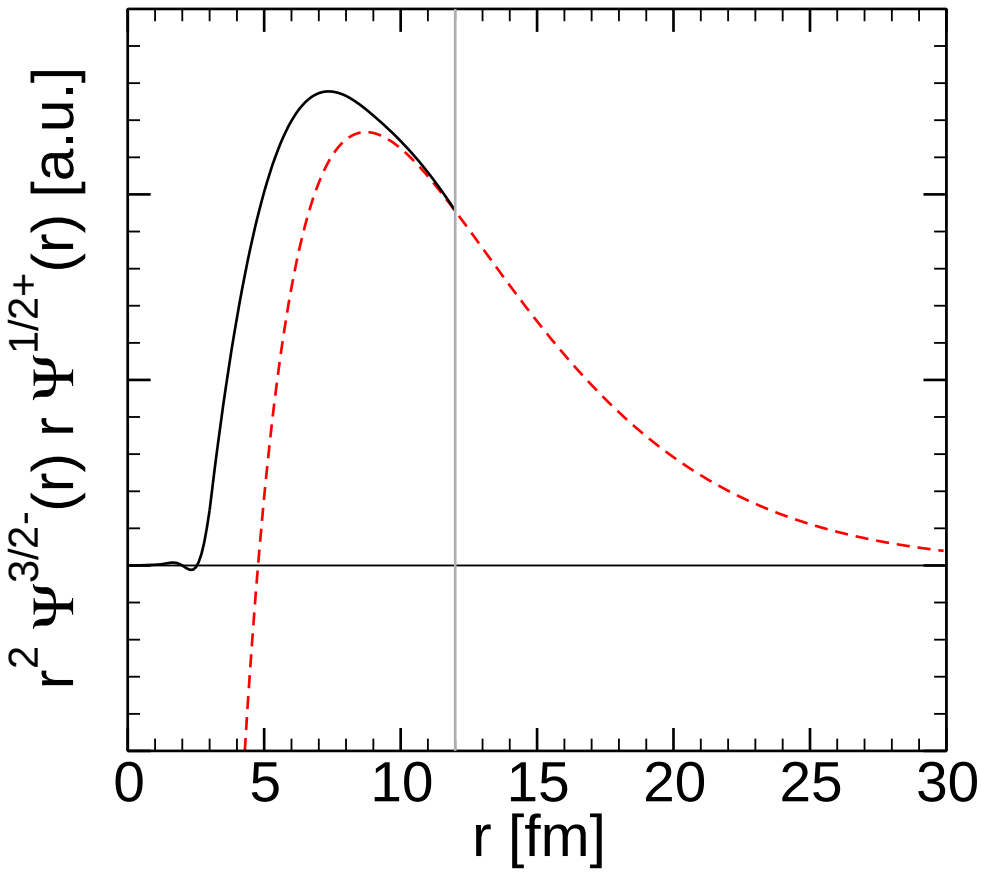

- Overlap functions from projection on RGM-cluster states
- Coulomb and Whittaker functions matched at channel radius a=12 fm
- Dipole matrix elements calculated from overlap functions reproduce full calculation within 2%
- cross section depends significantly on internal part of wave function, description as an “external” capture is too simplified

^{3}H(α,γ)^{7}Li

S-Factor

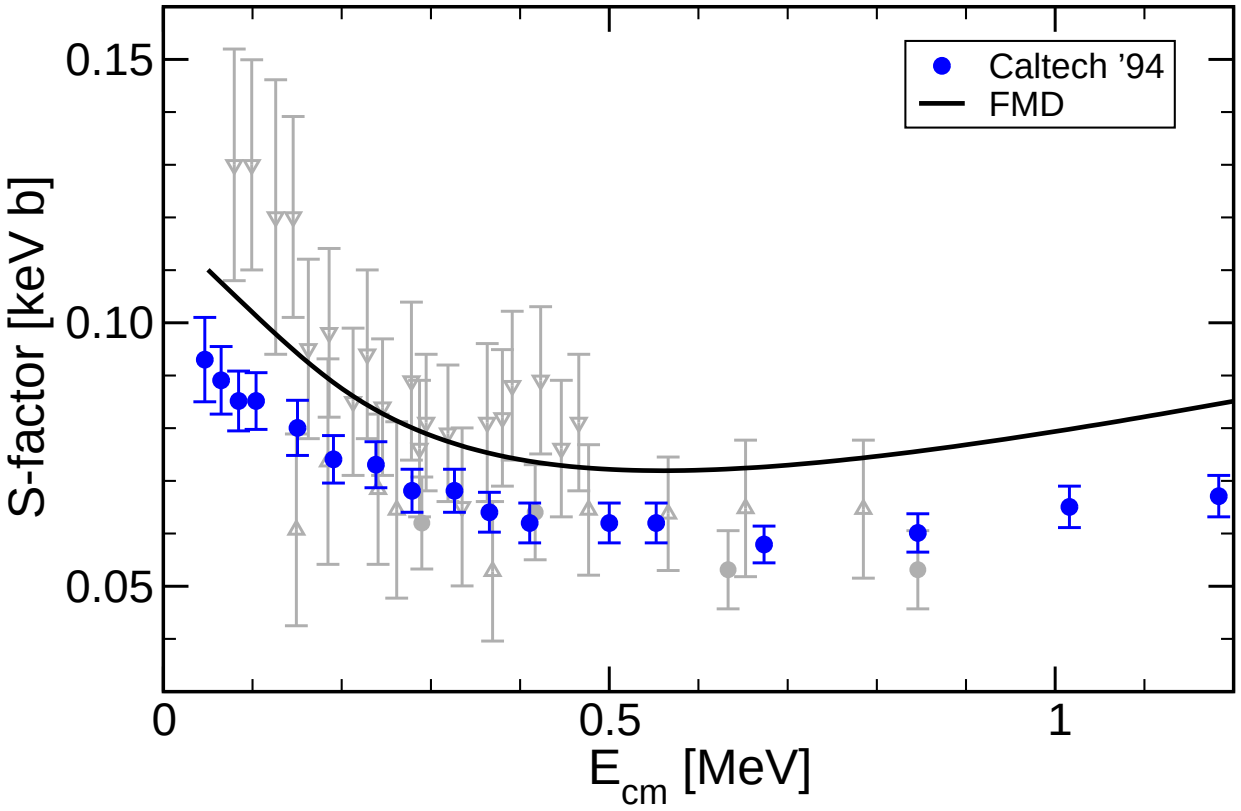

S-factor:

$$S(E) = \sigma(E) E \exp\{2\pi\eta\}$$

$$\eta = \frac{\mu Z_1 Z_2 e^2}{k}$$

Brune *et al.*, PRC **50**, 2205 (1994)

- isospin mirror reaction of ^{3}He(α,γ)^{7}Be
- ^{7}Li bound state properties and phase shifts well described

➳ FMD calculation describes energy dependence of Brune *et al.* data but cross section is larger by about 15%

$^3He(\alpha,\gamma)^7Be$ and $^3H(\alpha,\gamma)^7Li$ S-Factors consistent ?

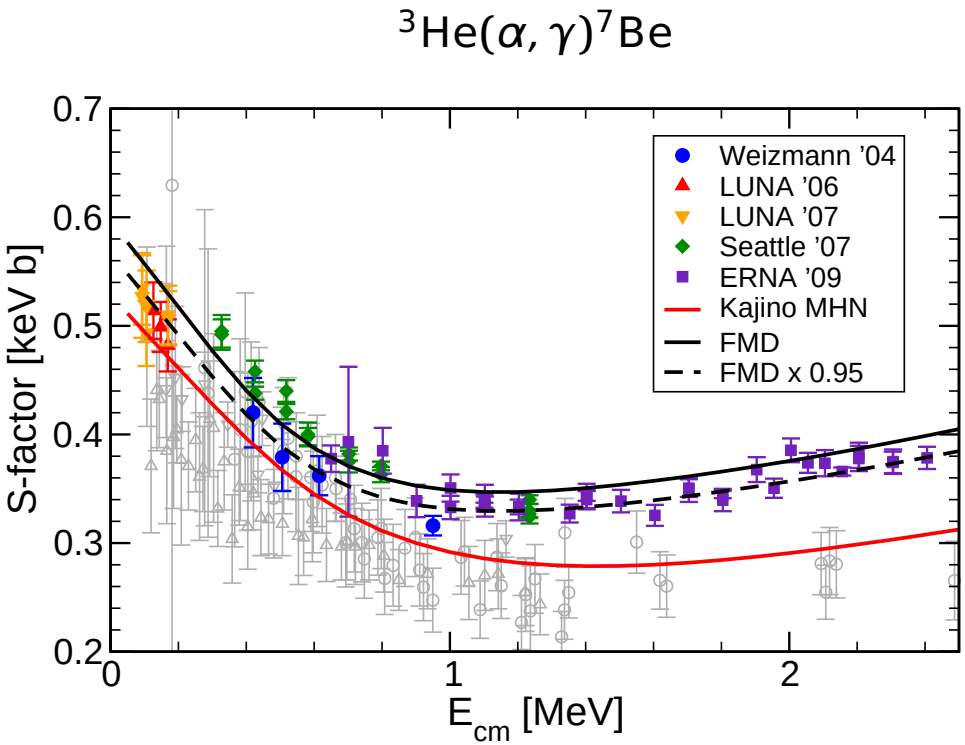

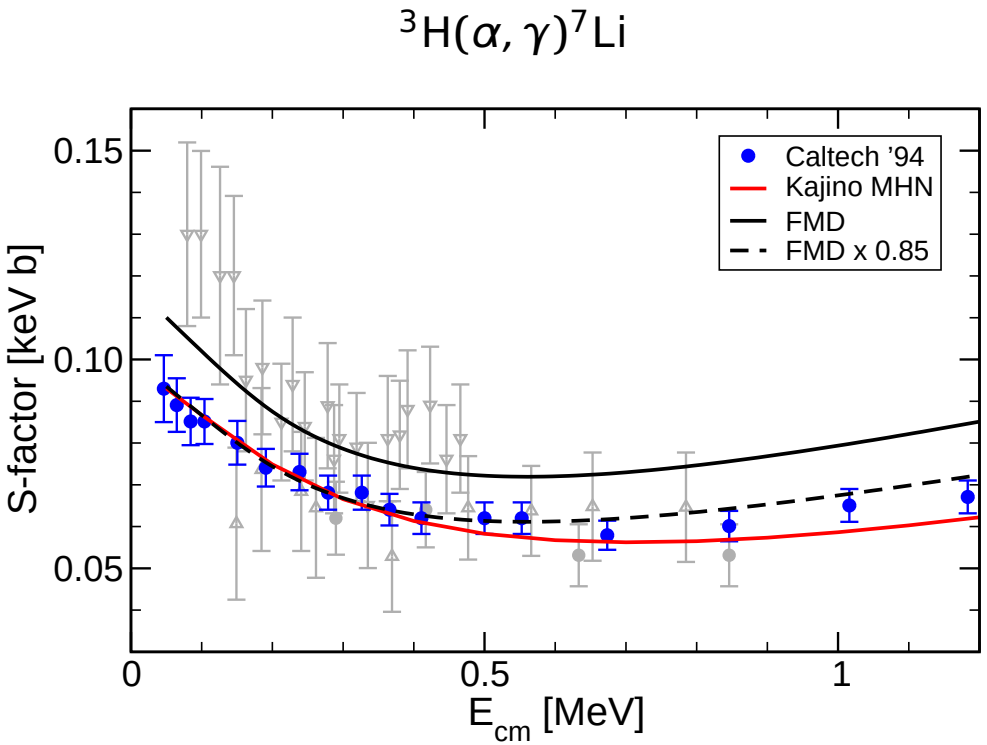

- FMD calculation agrees with normalization and energy dependence of $^3He(\alpha,\gamma)^7Be$ data
- FMD calculation agrees with energy dependence but not normalization of $^3H(\alpha,\gamma)^7Li$ data
- similar inconsistency observed in other models

Cluster States in ^{12}C

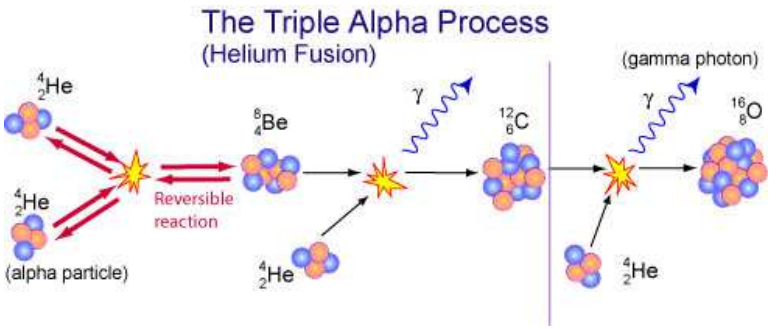

Structure

- **Is the Hoyle state a pure α-cluster state ?**
- **Second 2^+ state**
  Zimmermann *et al.*, Phys. Rev. Lett. 110, 152502 (2013)
- **Second 4^+ state**
  Freer *et al.*, Phys. Rev. C 83, 034314 (2011)
- **Other states in the continuum**
  Fynbo *et al.*, . . .

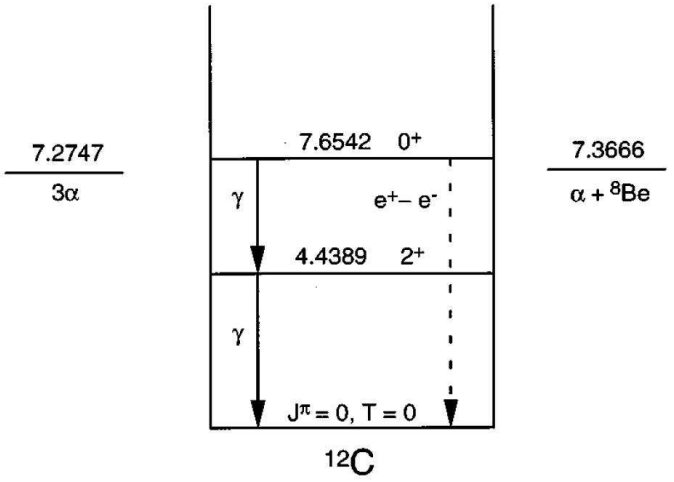

➳ **Include continuum in the calculation!**

➳ **Compare microscopic α-cluster model and FMD**

Chernykh, Feldmeier, Neff, von Neumann-Cosel, Richter,
Phys. Rev. Lett. (2007) 032501 (2007); Phys. Rev. Lett 105, 022501 (2010)
Neff, Feldmeier, arXiv:1409.3726

Microscopic α-cluster model

What are the degrees of freedom ?

- **^{12}C is described as a system of three α-particles**
- **α-particles are given by HO $(0s)^4$ wave functions**
- **wave function is fully antisymmetrized**
- **effective nucleon-nucleon interaction adjusted to reproduce α-α and ^{12}C ground state properties**

➳ **include ^{8}Be-α channels for continuum**

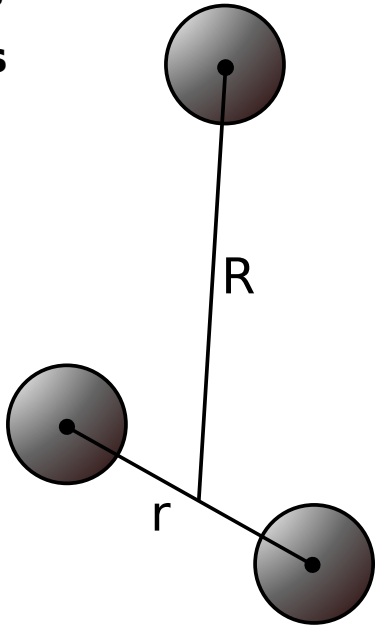

Model space in internal region

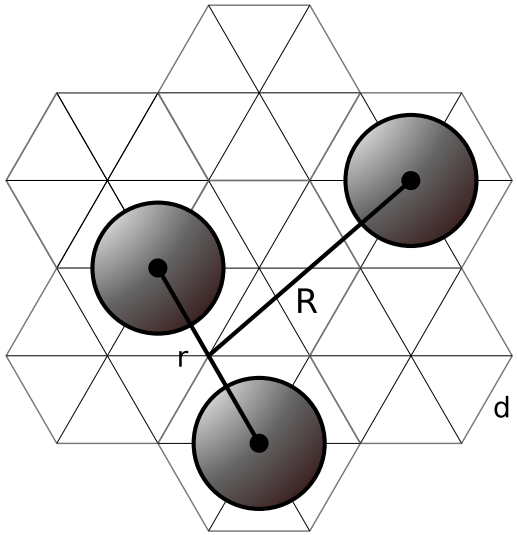

$$\rho^2 = \frac{1}{2}\mathbf{r}^2 + \frac{2}{3}\mathbf{R}^2$$

Hyperradius

Model Space

- include all possible configurations on triangular grid ($d = 1.4\,\mathrm{fm}$) up to a certain hyperradius ρ
- no restriction on relative angular momenta

Basis States

- Intrinsic states are projected on parity and angular momentum

$$\left|\Psi^{3\alpha}_{JMK\pi}(\mathbf{R}_1,\mathbf{R}_2,\mathbf{R}_3)\right\rangle = \underset{\sim}{P}^{\pi}\underset{\sim}{P}^{J}_{MK}\underset{\sim}{\mathcal{A}}\left\{\left|\Psi^{^4\mathrm{He}}(\mathbf{R}_1)\right\rangle \otimes \left|\Psi^{^4\mathrm{He}}(\mathbf{R}_2)\right\rangle \otimes \left|\Psi^{^4\mathrm{He}}(\mathbf{R}_3)\right\rangle\right\}$$

Volkov Interaction

- simple central interaction
- parameters adjusted to give reasonable α binding energy and radius, $\alpha-\alpha$ scattering data, adjusted to reproduce ^{12}C ground state energy

✘ only reasonable for ^{4}He, ^{8}Be and ^{12}C nuclei

Kamimura, Nuc. Phys. **A351** (1981) 456
Funaki et al., Phys. Rev. C **67** (2003) 051306(R)

Model space in external region

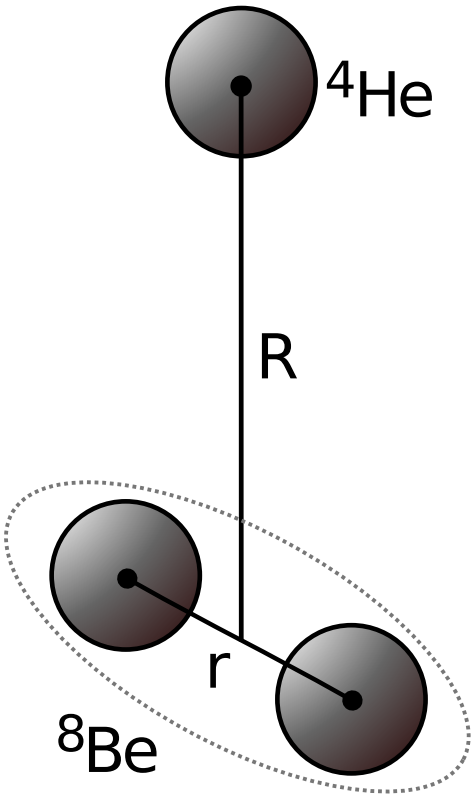

Model Space

- ^{8}Be-^{4}He cluster configurations with generator coordinate R
- ^{8}Be ground state (0^+_1) and pseudo states (2^+_1, 0^+_2, 2^+_2, 4^+_1) obtained by diagonalizing α-α configurations up to $r = 10\,\mathrm{fm}$

Basis States

- ^{12}C basis states are obtained by **double projection**:

Project first ^{8}Be

$$\left| \Psi^{^8\mathrm{Be}}_{IK} \right\rangle = \sum_i \underset{\sim}{P}^I_{K0} \underset{\sim}{\mathcal{A}} \left\{ \left| \Psi^{^4\mathrm{He}}(-\tfrac{r_i}{2}\mathbf{e}_z \right\rangle \otimes \left| \Psi^{^4\mathrm{He}}(+\tfrac{r_i}{2}\mathbf{e}_z \right\rangle \right\} c^I_i$$

then the combined wave function

$$\left| \Psi^{^8\mathrm{Be},^4\mathrm{He}}_{IK;JM\pi}(R_j) \right\rangle = \underset{\sim}{P}^{\pi} \underset{\sim}{P}^{J}_{MK} \underset{\sim}{\mathcal{A}} \left\{ \left| \Psi^{^8\mathrm{Be}}_{IK}(-\tfrac{R_j}{3}\mathbf{e}_z) \right\rangle \otimes \left| \Psi^{^4\mathrm{He}}(+\tfrac{2R_j}{3}\mathbf{e}_z \right\rangle \right\}$$

- will allow to match to Coulomb asymptotics

Descouvemont, Baye, Phys. Rev. C **36** (1987) 54

Arai, Phys. Rev. C **74** (2006) 064311

Include ^{8}Be-α continuum

How to treat the ^{12}C continuum above the 3-α threshold ?

- **In principle it should be described as a three-body continuum**
- **However ^{8}Be+α configurations are lower in energy than 3-α configurations up to pretty large hyperradii**
- **Approximation: consider ^{8}Be(0^{+}) and ^{8}Be(2^{+}) (and additional ^{8}Be pseudo states) as bound states**
- **Could be considered as a microscopic CDCC approach**

^{8}Be-α wave functions

alpha-cluster model calculations with continuum:

Descouvemont, Baye, Phys. Rev. **C36**, 54 (1987)
Arai, Phys. Rev. **C74**, 064311 (2006)
Vasilevsky *et al.*, Phys. Rev. **C85**, 034318 (2012)

^{8}Be wave functions

- α-α configurations up to 9 fm distance, project on 0^+ and 2^+, $M = 0, 1, 2$

$$\left| {}^8\mathrm{Be}_{I,K} \right\rangle = P^I_{K0} \sum_i \left\{ \left| {}^4\mathrm{He}(-R_i/2\mathbf{e}_z) \right\rangle \otimes \left| {}^4\mathrm{He}(R_i/2\mathbf{e}_z \right\rangle \right\} c^J_i$$

- reproduces ground state energy within 50 keV compared to full calculation

^{12}C configurations

- ^{8}Be(0^+,2^+) and α at distance R
- ^{8}Be(2^+) can have different orientations with respect to distance vector
- ^{8}Be(0^+,2^+)+α configurations have to be projected on total angular momentum

$$\left| {}^8\mathrm{Be}_{I,K}, {}^4\mathrm{He}; R; JM \right\rangle = P^J_{MK} \left\{ \left| {}^8\mathrm{Be}_{I,K}(-1/3R\mathbf{e}_z) \right\rangle \otimes \left| {}^4\mathrm{He}(2/3R\mathbf{e}_z) \right\rangle \right\}$$

^{8}Be-α Energy Surfaces

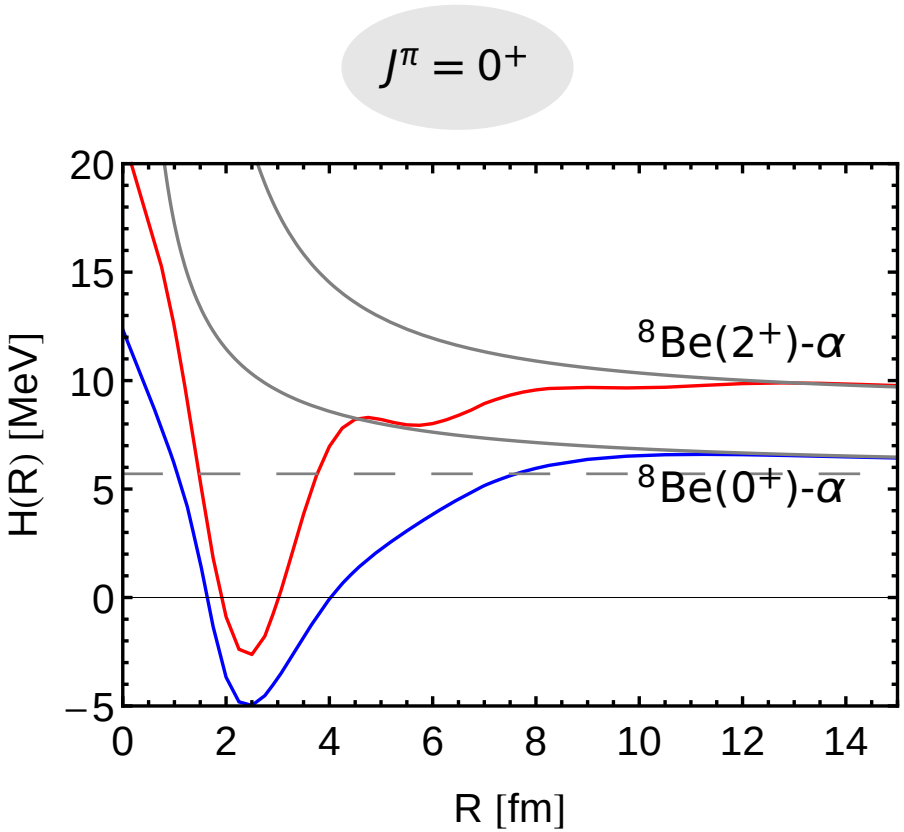

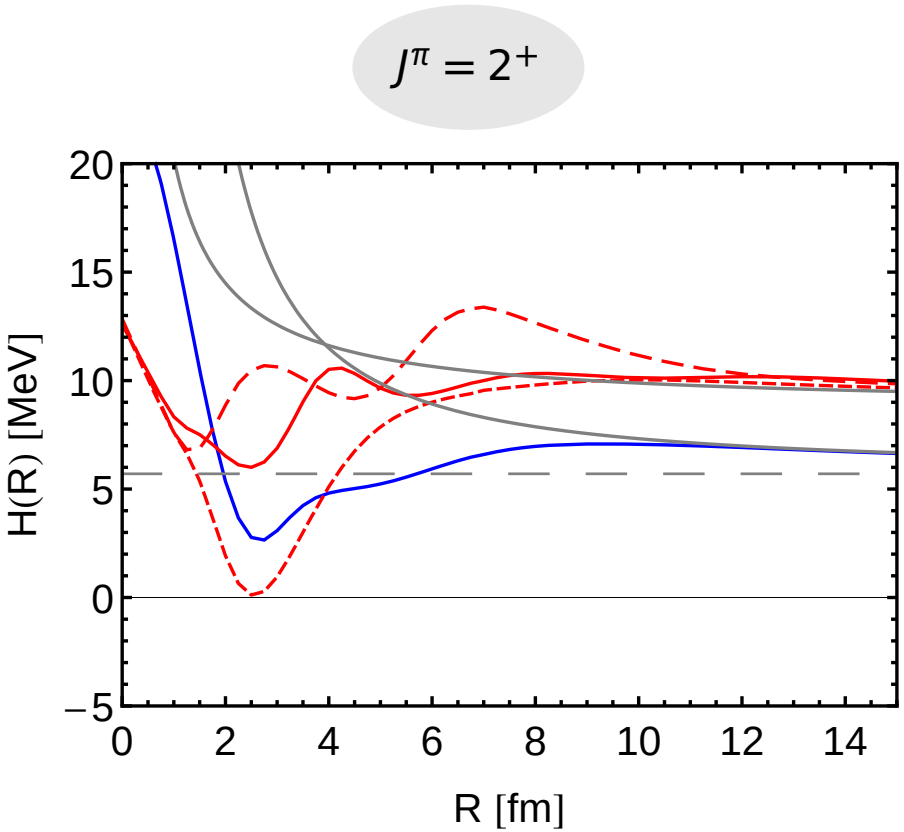

- energy surfaces contain localization energy for relative motion of ^{8}Be and α
- 2^+ energy surface depends strongly on orientation of ^{8}Be 2^+ state: $K = 2$ most attractive

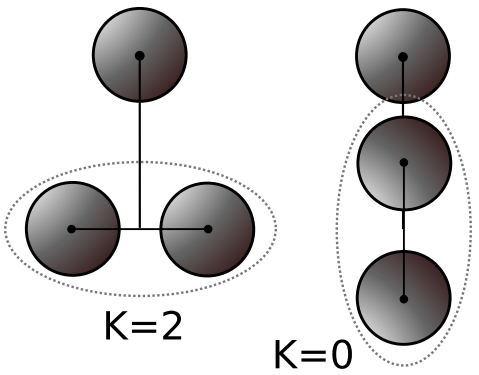

Bound state approximation – Convergence ?

	$\rho < 6\,\mathrm{fm}$	$\rho < 6\,\mathrm{fm}$, $R < 9\,\mathrm{fm}$	$\rho < 6\,\mathrm{fm}$, $R < 12\,\mathrm{fm}$	$\rho < 6\,\mathrm{fm}$, $R < 15\,\mathrm{fm}$	Experiment	
$E(0_1^+)$	-89.63	-89.64	-89.64	-89.64	-92.16	
$E^*(2_1^+)$	2.53	2.54	2.54	2.54	4.44	
$E^*(0_2^+)$, $\Gamma_\alpha(0_2^+)$	8.53	7.82	7.78	7.76	7.65, $(8.5 \pm 1.0)10^{-6}$	
$E^*(2_2^+)$, $\Gamma_\alpha(2_2^+)$	10.11	9.18	9.08	8.93	10.03(11), 0.80(13)	[3]
$r_{\mathrm{charge}}(0_1^+)$	2.53	2.53	2.53	2.53	2.47(2)	
$r(0_1^+)$	2.39	2.39	2.39	2.39	–	
$r(0_2^+)$	3.21	3.68	3.78	3.89	–	
$B(E2, 2_1^+ \rightarrow 0_1^+)$	9.03	9.12	9.08	9.08	7.6(4)	
$M(E0, 0_1^+ \rightarrow 0_2^+)$	7.20	6.55	6.40	6.27	5.47(9)	[2]
$B(E2, 2_2^+ \rightarrow 0_1^+)$	3.65	2.48	2.09	1.33	0.73(13)	[3]

- properties of resonances (Hoyle state and second 2^+ state) can not be determined in bound state approximation in an unambigouos way

[1] Ajzenberg-Selove, Nuc. Phys. **A506**, 1 (1990)
[2] Chernykh et al., Phys. Rev. Lett. **105**, 022501 (2010)
[3] Zimmermann et al., Phys. Rev. Lett. **110**, 152502 (2013); these numbers are under discussion

Matching to Coulomb asymptotics

Model Space

- Internal region: 3-α configurations on a grid
- External region: ^{8}Be$(0^+, 2^+, 4^+)$-α configurations
- Asymptotically: only Coulomb interaction between ^{8}Be and ^{4}He clusters

GCM basis state expressed in RGM basis

- Microscopic GCM wave functions are functions of single-particle coordinates: internal wave functions of cluster, the relative motion of the clusters and the total center-of-mass motion are entangled
- Write GCM basis state in external region with RGM basis states

$$\left| \Psi^{^8\mathrm{Be},^4\mathrm{He}}_{IK;JM\pi}(R_j) \right\rangle = \sum_L \mathrm{C} \left(\begin{array}{cc|c} I & L & J \\ K & 0 & K \end{array} \right) \int dr r^2 \, \Gamma_L(R_j; r) \left| \Phi^{^8\mathrm{Be},^4\mathrm{He}}_{(IL)JM\pi}(r) \right\rangle \otimes \left| \Phi^{\mathrm{cm}} \right\rangle$$

with $(\pi = (-1)^L)$

$$\left\langle \boldsymbol{\rho}, \xi_a, \xi_b \left| \Phi^{^8\mathrm{Be},^4\mathrm{He}}_{(IL)JM\pi}(r) \right\rangle = \sum_{M_I, M_L} \mathrm{C} \left(\begin{array}{cc|c} I & L & J \\ M_I & M_L & M \end{array} \right) \underset{\sim}{\mathcal{A}} \left\{ \frac{\delta(\rho - r)}{r^2} \Phi^{^8\mathrm{Be}}_{IM_I}(\xi_a) \, \Phi^{^4\mathrm{He}}(\xi_b) \, Y_{LM_L}(\hat{\rho}) \right\}$$

- asymptotically RGM states have good channel spin I and orbital angular momentum L

Matching to Coulomb asymptotics

RGM norm kernel and Overlap functions

- RGM norm kernel reflects effects of antisymmetrization, channel $c = (IL)J$

$$N_{c,c'}(r,r') = \left\langle \Phi_c(r) \middle| \Phi_{c'}(r') \right\rangle \overset{r,r'\to\infty}{\longrightarrow} \delta_{cc'} \frac{\delta(r-r')}{rr'}$$

- Overlap functions can be interpreted as wave functions for point-like clusters

$$\psi_c(r) = \int dr' r'^2 \, N^{-1/2}_{c,c'}(r,r') \left\langle \Phi_{c'}(r') \middle| \Psi \right\rangle$$

Matching to the asymptotic solution

- Use multichannel microscopic R-matrix approach
  Descouvemont, Baye, Phys. Rept. 73, 036301 (2010)
- Check that results are independent from channel radius: used $a = 16.5$ fm here

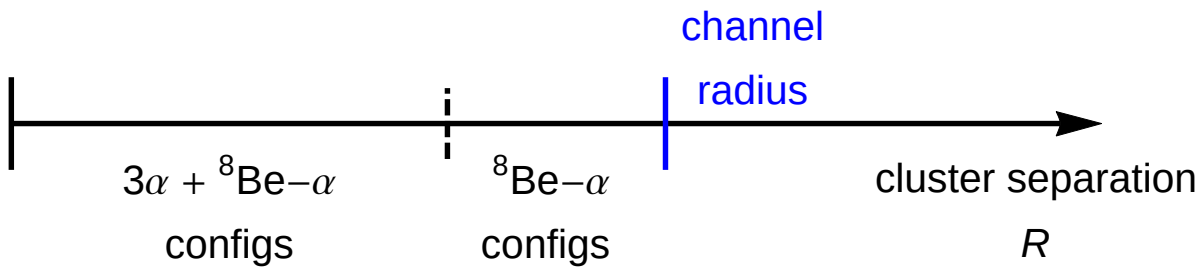

Matching to Coulomb asymptotics

Bound states

- Whittaker functions

$$\psi_c(r) = A_c \frac{1}{r} W_{-\eta_c, L_c+1/2}(2\kappa_c r), \qquad \kappa_c = \sqrt{-2\mu(E-E_c)}$$

Resonances

- purely outgoing Coulomb, k complex

$$\psi_c(r) = A_c \frac{1}{r} O_{L_c}(\eta_c, k_c r), \qquad k_c = \sqrt{2\mu(E-E_c)}$$

Scattering states

- in- and outgoing Coulomb (incoming channel c_0)

$$\psi_c(r) = \frac{1}{r}\left\{\delta_{L_c,L_0} I_{L_c}(\eta_c, k_c r) - S_{c,c_0} O_{L_c}(\eta_c, k_c r)\right\}, \qquad k_c = \sqrt{2\mu(E-E_c)}$$

- Diagonal phase shifts and inelasticity parameters: $S_{cc} = \eta_c \exp\{2i\delta_c\}$
- Eigenphases: $S = U^{-1} D U, D_{\alpha\alpha} = \exp\{2i\delta_\alpha\}$

Cluster Model: ^{8}Be(0^+_1,2^+_1)-α Continuum

0^+ Phase shifts

Eigenphaseshifts

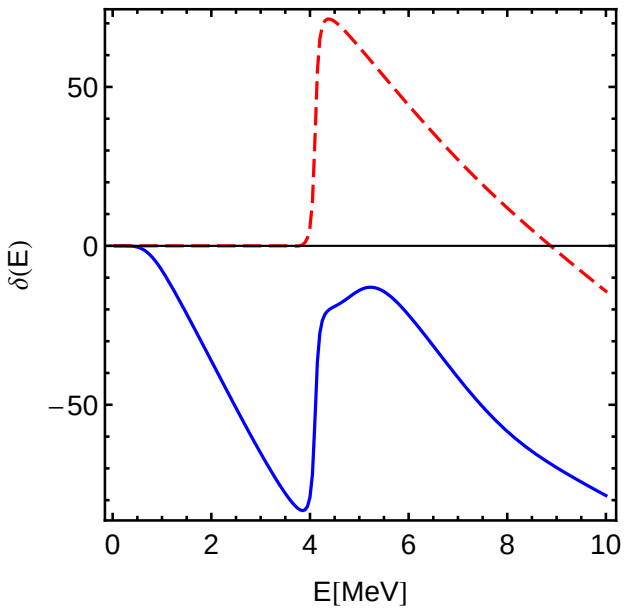

Phaseshifts

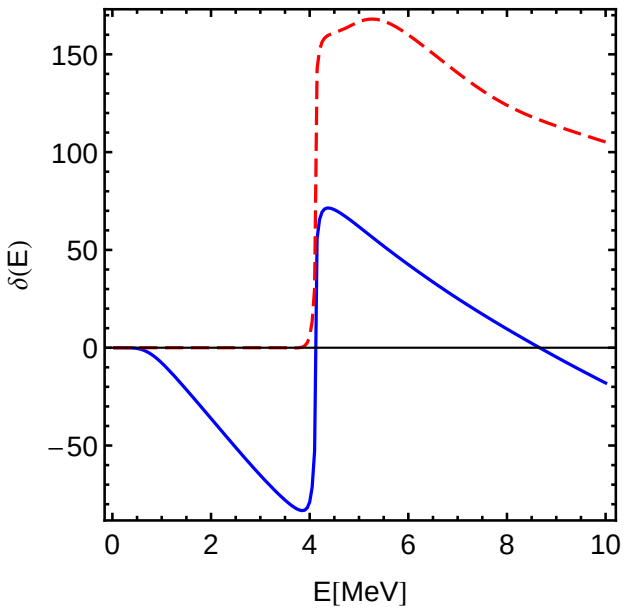

Inelasticities

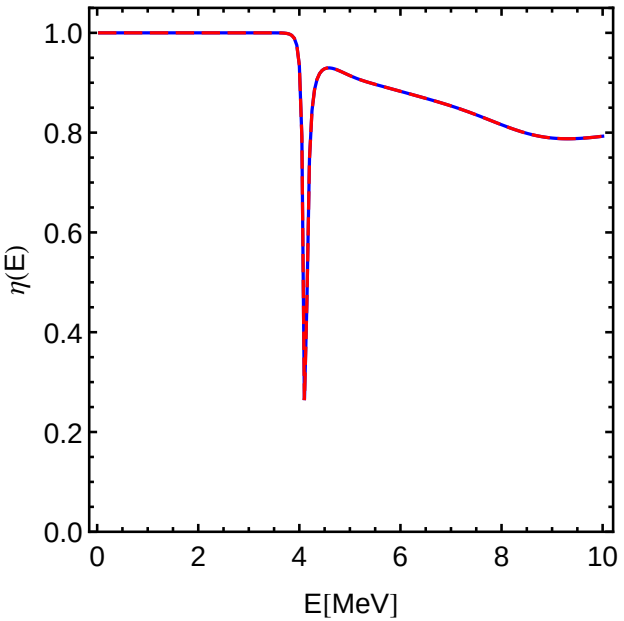

Gamow states

	E [MeV]	Γ_α [MeV]
0^+_2	0.29	$1.78 \cdot 10^{-5}$
0^+_3	4.11	0.12
0^+_4	4.76	1.57

- Hoyle state missed when scanning the phase shifts
- non-resonant background
- strong coupling between ^{8}Be(0^+) and ^{8}Be(2^+) channel at 4.1 MeV

Cluster Model: ^{8}Be(0^+_1,2^+_1)-α Continuum

2^+ Phase shifts

Eigenphaseshifts

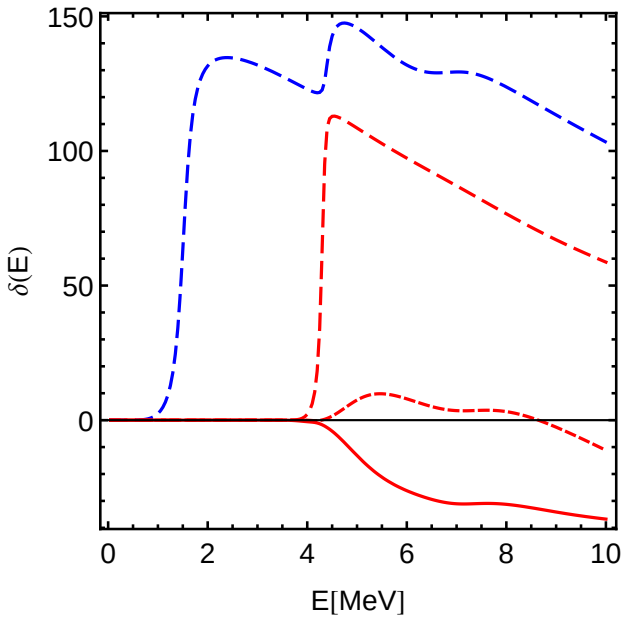

Phaseshifts

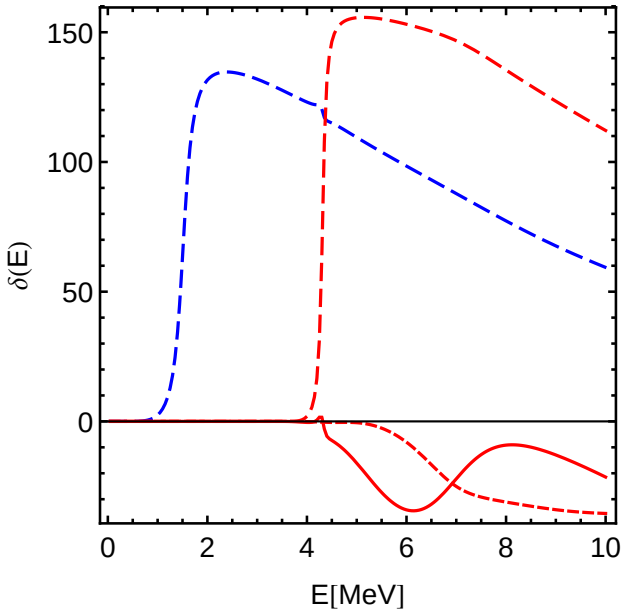

Inelasticities

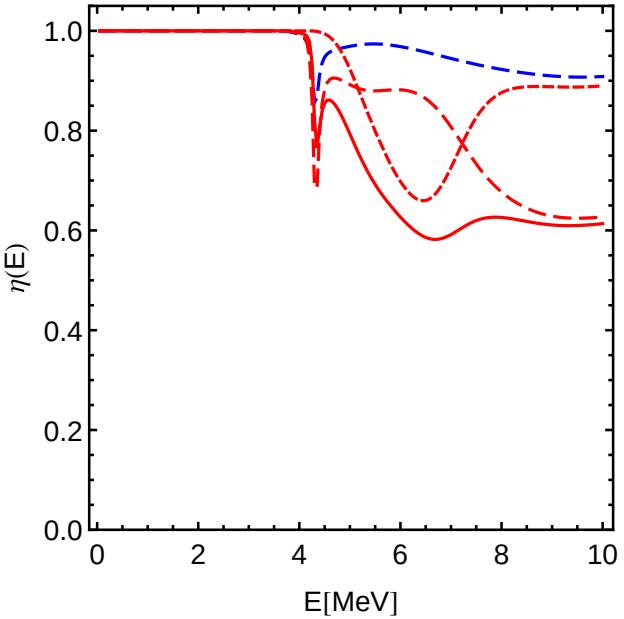

Gamow states

	E [MeV]	Γ_α [MeV]
2^+_2	1.51	0.32
2^+_3	4.31	0.14
...		

- non-resonant background
- $L = 2$ ^{8}Be(0^+) and ^{8}Be(2^+) resonances

Cluster Model: ^{8}Be(0^+_1,2^+_1)-α Continuum
4^+ Phase shifts

Eigenphaseshifts

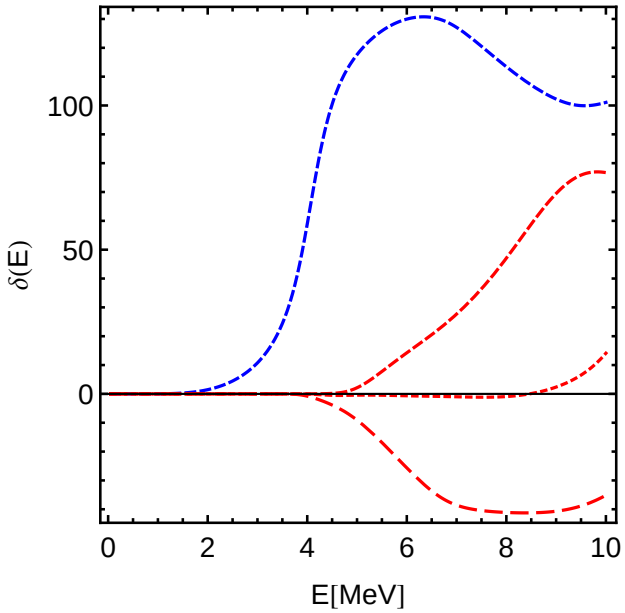

Phaseshifts

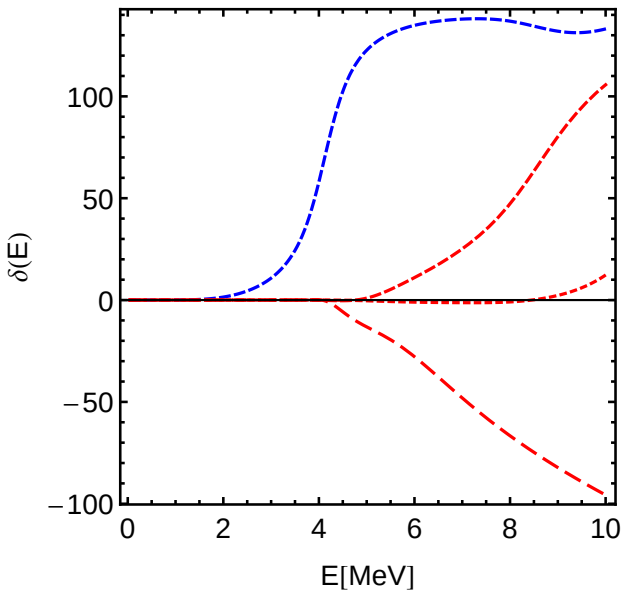

Inelasticities

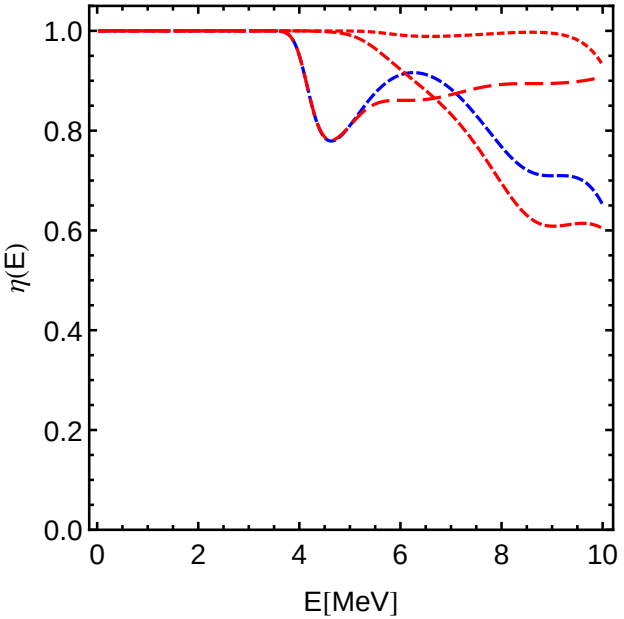

Gamow states

	E [MeV]	Γ_α [MeV]
4^+_1	1.17	$8.07 \cdot 10^{-6}$
4^+_2	4.06	0.98
...		

- 4_1 state (ground state band) very narrow, missed when scanning phase shifts
- 4^+_2 state mostly ^{8}Be(0+) but some mixing

Observables with proper treatment of Continuum

	$\rho < 6\,\mathrm{fm}$ $R < 9\,\mathrm{fm}$	$\rho < 6\,\mathrm{fm}$ $R < 12\,\mathrm{fm}$	$\rho < 6\,\mathrm{fm}$ $R < 15\,\mathrm{fm}$	$\rho < 6\,\mathrm{fm}$ Continuum	Experiment
$E(0_1^+)$	-89.64	-89.64	-89.64	-89.64	-92.16
$E^*(2_1^+)$	2.54	2.54	2.54	2.54	4.44
$E^*(0_2^+), \Gamma_\alpha(0_2^+)$	7.82	7.78	7.76	7.76, $3.04 \cdot 10^{-3}$	7.65, $(8.5 \pm 1.0) \cdot 10^{-6}$
$E^*(2_2^+), \Gamma_\alpha(2_2^+)$	9.18	9.08	8.93	8.98, 0.46	10.03(11), 0.80(13)
$r_{\mathrm{charge}}(0_1^+)$	2.53	2.53	2.53	2.53	2.47(2)
$r(0_1^+)$	2.39	2.39	2.39	2.39	–
$r(0_2^+)$	3.68	3.78	3.89	4.08 + 0.07i	–
$B(E2, 2_1^+ \to 0_1^+)$	9.12	9.08	9.08	9.08	7.6(4)
$M(E0, 0_1^+ \to 0_2^+)$	6.55	6.40	6.27	6.15 + 0.01i	5.47(9)
$B(E2, 2_2^+ \to 0_1^+)$	2.48	2.09	1.33	2.14 + 1.45i	0.73(13)

- Resonances are calculated as Gamow states
- Matrix elements including resonances are regulated according to Berggren and Gyarmati
- Imaginary part provides information about uncertainty of matrix elements

Berggren, Nucl. Phys. **A109**, 265 (1968)
Gyarmati, Krisztinkovics, Vertse, Phys. Lett. **B41**, 475 (1972)
Berggren, Phys. Lett. **B373**, 1 (1996)

Overlap functions

$$\psi_{(IL)J}(r) = \int dr' r'^2 \, N^{-1/2}_{(IL)J,(I'L')J}(r,r') \langle \, \Phi_{(I'L')J}(r') \, | \, \Psi \, \rangle$$

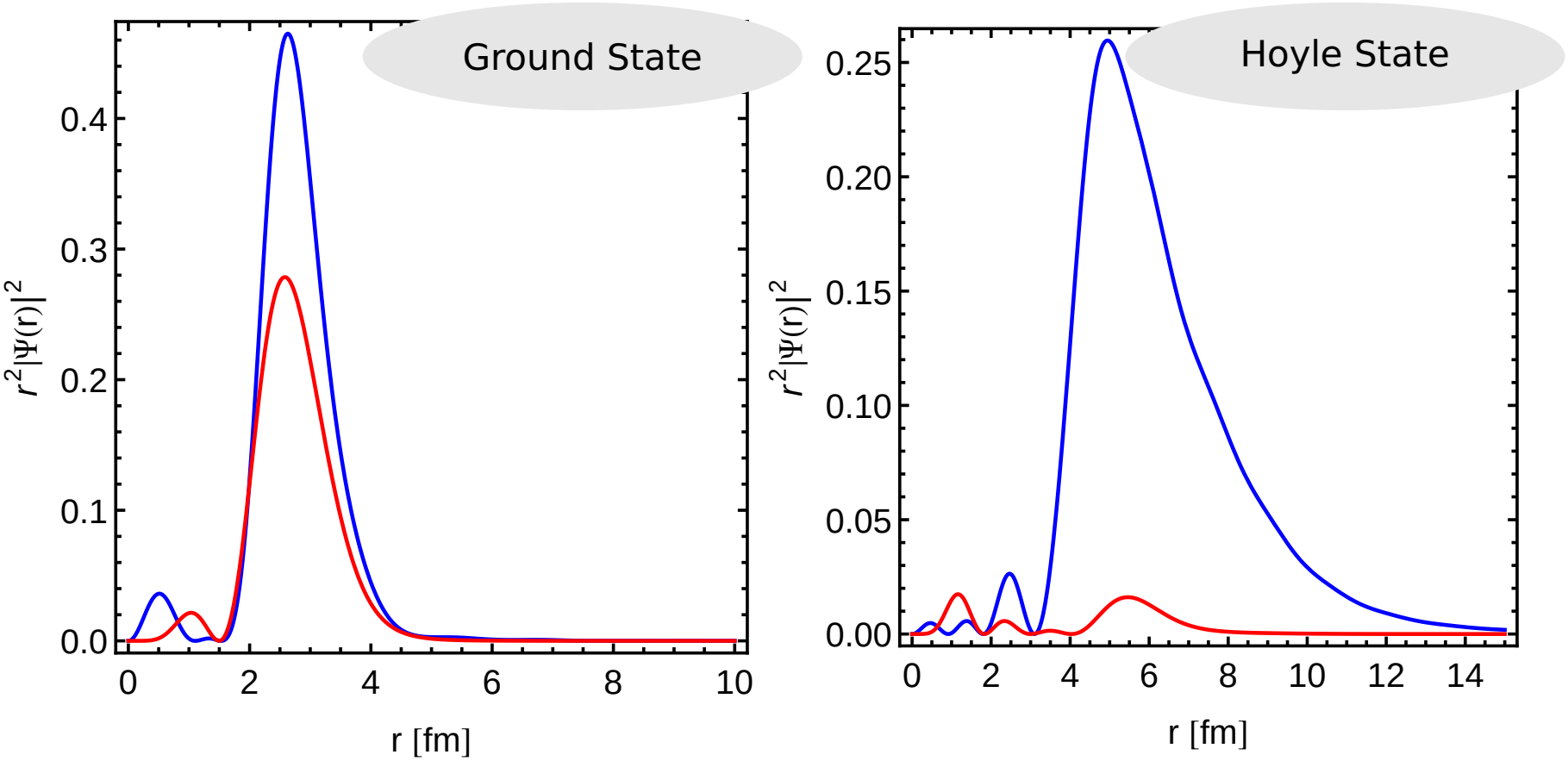

- Ground state overlap with ^{8}Be(0^+)+α and ^{8}Be(2^+)+α configurations of similar magnitude
- Hoyle state overlap dominated by ^{8}Be(0^+)+α configurations, large spatial extension

FMD calculations with ^{8}Be-α continuum

UCOM interaction

- **AV18 UCOM(SRG) (α=0.20 fm^4, λ=1.5 fm^{-}1)**
- **Increase strength of spin-orbit force by a factor of two to partially account for omitted three-body forces**

^{8}Be-α Continuum

- **To get a good description of ^{8}Be it is essential to include polarized configurations**

➳ **Calculate strength distributions**

➳ **Investigate non-cluster states: non-natural parity states, $T = 1$ states, M1 transitions, ^{12}B and ^{12}N β-decay into ^{12}C, . . .**

Model space in internal region

Model Space

- no assumption of α-clustering
- complete basis not feasible, find the "most important" basis states
- determine wave packet parameters by variation

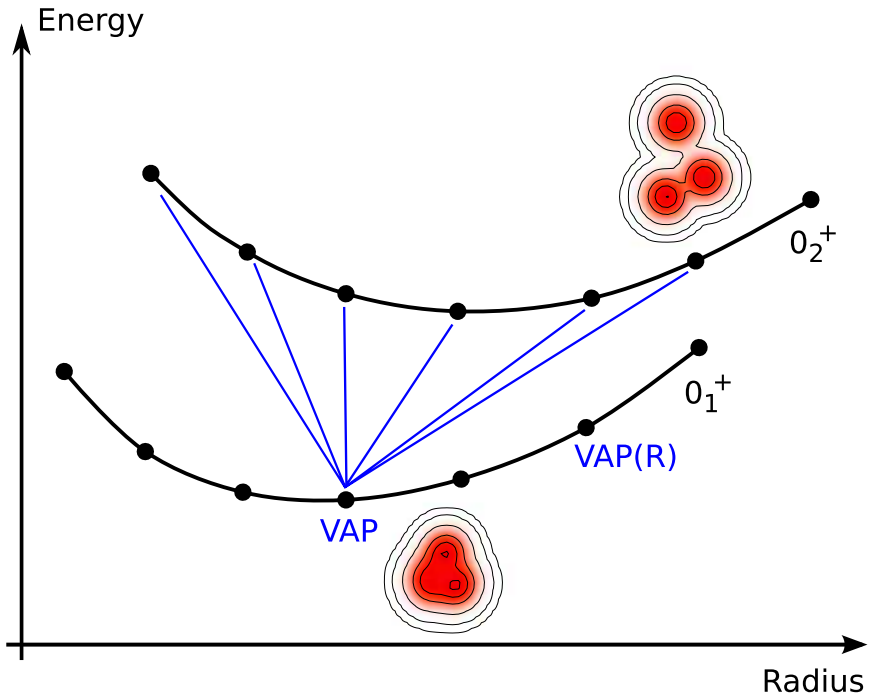

VAP, VAP with constraints, Multiconfiguration-VAP

For each angular momentum (0^+, 1^+, 2^+, ...)

- **VAP**: vary energy of projected Slater determinant $\underset{\sim}{P}^{\pi}\underset{\sim}{P}^{J}_{MK}\left|\, Q(q_i)\,\right\rangle$ with respect to all parameters q_i
- **VAP(R)**: create additional basis states by variation with a constraint on the radius of the intrinsic state
- **MC-VAP**: keep VAP state fix and vary the parameters of a second Slater determinant to minimize the energy of the second eigenstate in a multiconfiguration mixing calculation
- **MC-VAP(R)**: create additional basis states by adding a constraint on the radius of the second intrinsic state

Important Configurations

- Calculate the overlap with FMD basis states to find the most important contributions to the eigenstates (in bound state approximation)

$\left|\left\langle \cdot \mid 0_1^+ \right\rangle\right| = 0.94$

$\left|\left\langle \cdot \mid 2_1^+ \right\rangle\right| = 0.93$

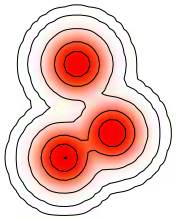

$\left|\left\langle \cdot \mid 0_2^+ \right\rangle\right| = 0.64$

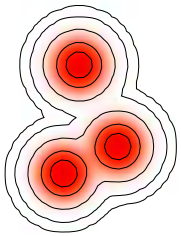

$\left|\left\langle \cdot \mid 0_2^+ \right\rangle\right| = 0.58$

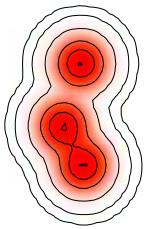

$\left|\left\langle \cdot \mid 0_2^+ \right\rangle\right| = 0.57$

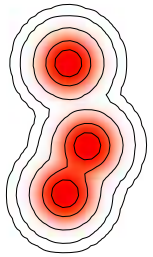

$\left|\left\langle \cdot \mid 0_2^+ \right\rangle\right| = 0.45$

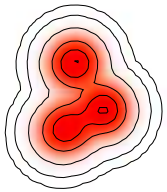

$\left|\left\langle \cdot \mid 3_1^- \right\rangle\right| = 0.91$

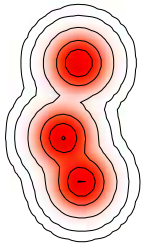

$\left|\left\langle \cdot \mid 2_2^+ \right\rangle\right| = 0.50$

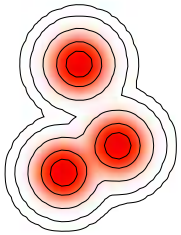

$\left|\left\langle \cdot \mid 2_2^+ \right\rangle\right| = 0.49$

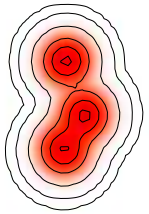

$\left|\left\langle \cdot \mid 2_2^+ \right\rangle\right| = 0.44$

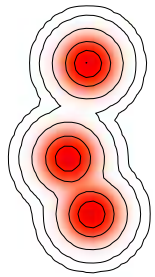

$\left|\left\langle \cdot \mid 2_2^+ \right\rangle\right| = 0.41$

FMD basis states are not orthogonal!

0_2^+ and 2_2^+ states have no rigid intrinsic structure

FMD/Cluster Model: ^{8}Be-α Continuum
Spectrum

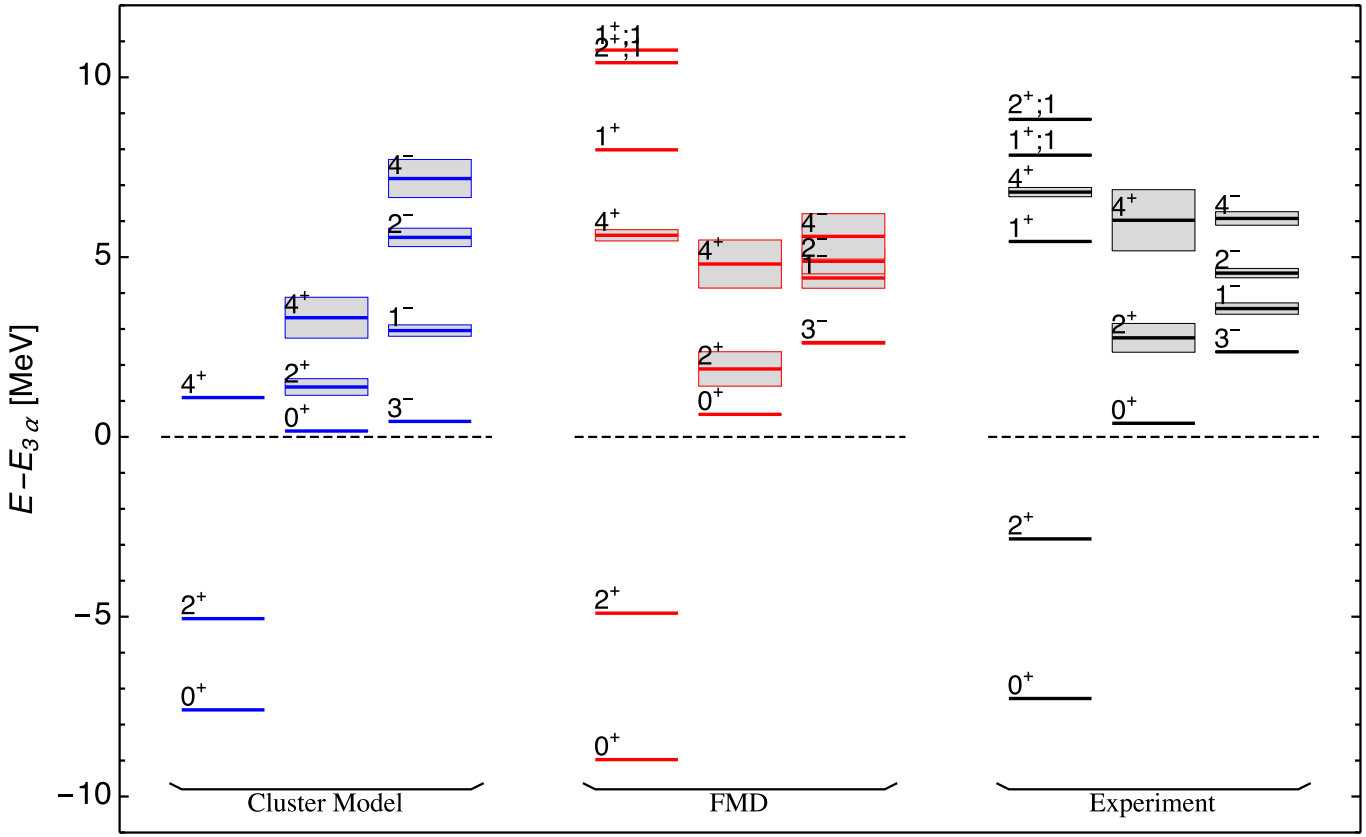

- FMD describes the ground state band, the cluster states related to the Hoyle state and the negative parity states reasonably well
- Spin-flip states (1^+ $T=0,1$ and 2^+ $T=1$) are somewhat too high in energy

FMD: ^{8}Be-α Continuum

Strength distributions

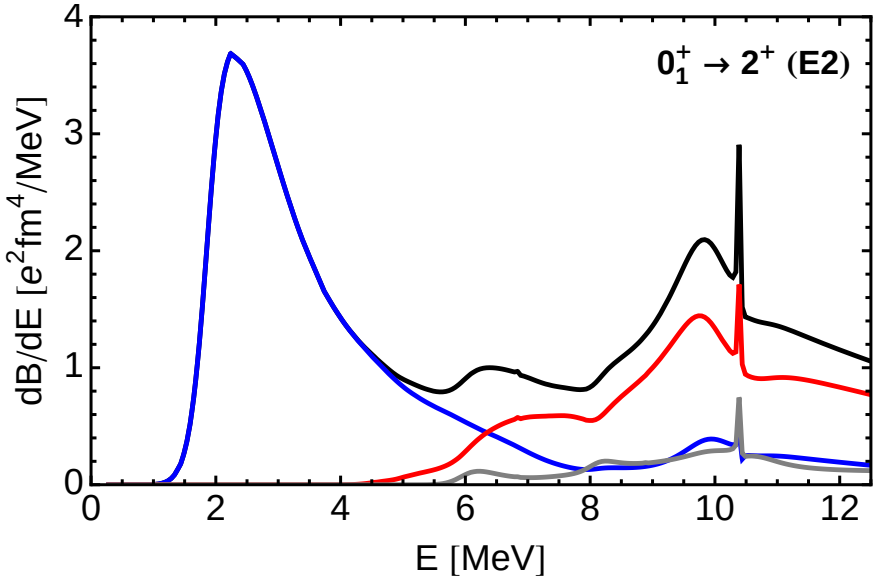

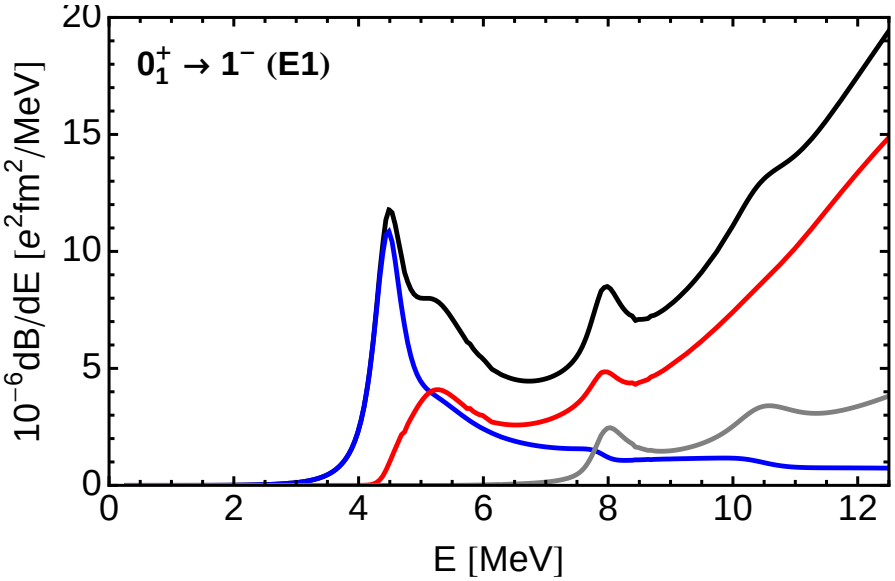

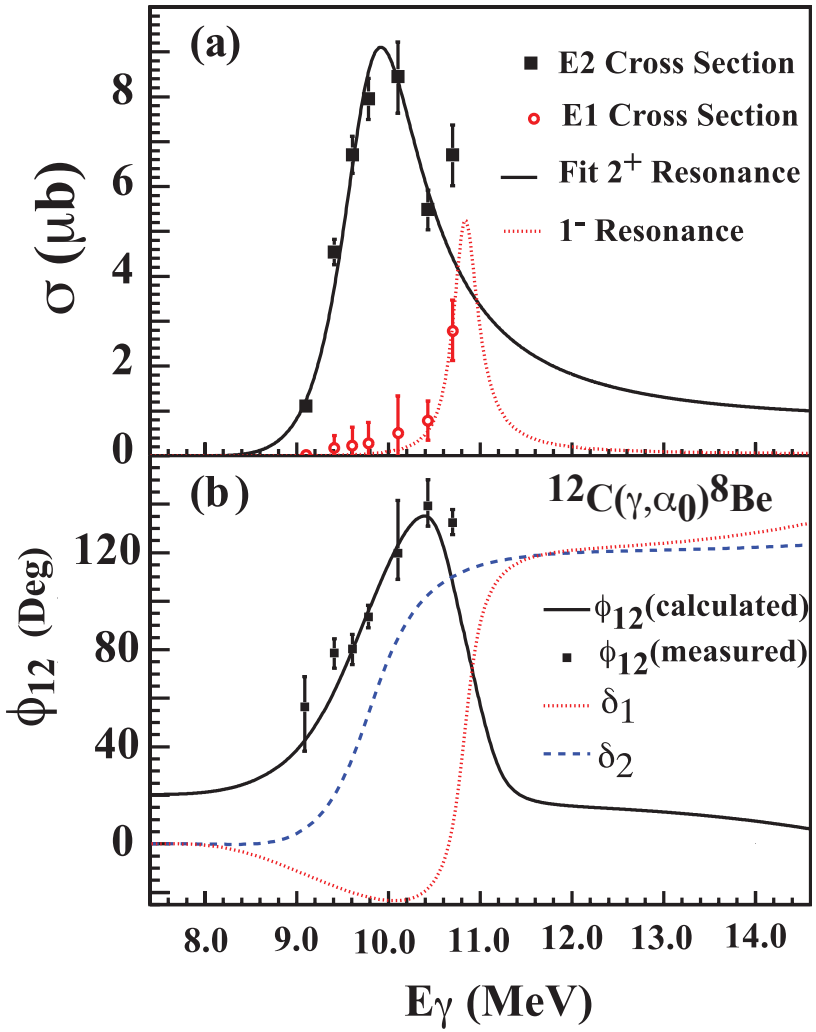

Zimmermann et al.,
Phys. Rev. Lett. **110**, 152502 (2013)

✘ *E*1 transition isospin-forbidden in cluster model !

Population of 0^+ continuum with different reactions

Monopole response

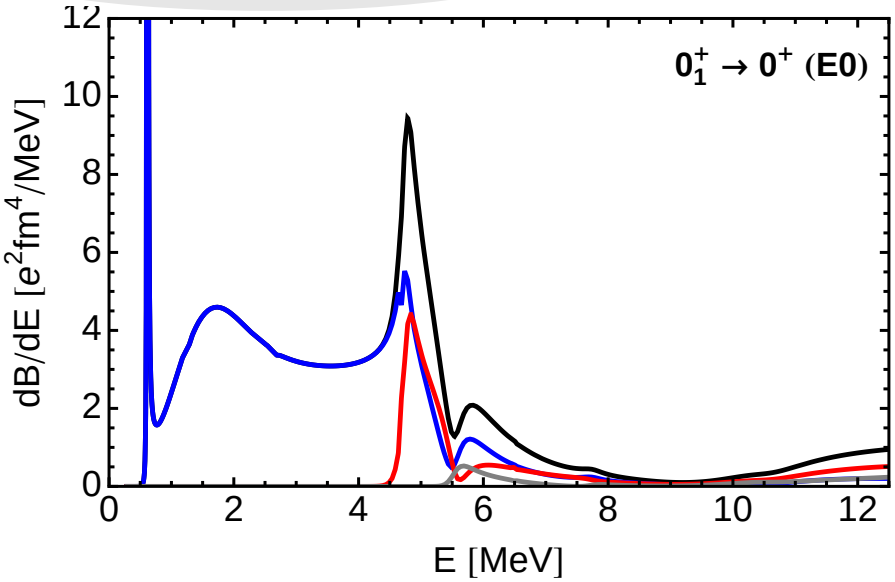

β-decay

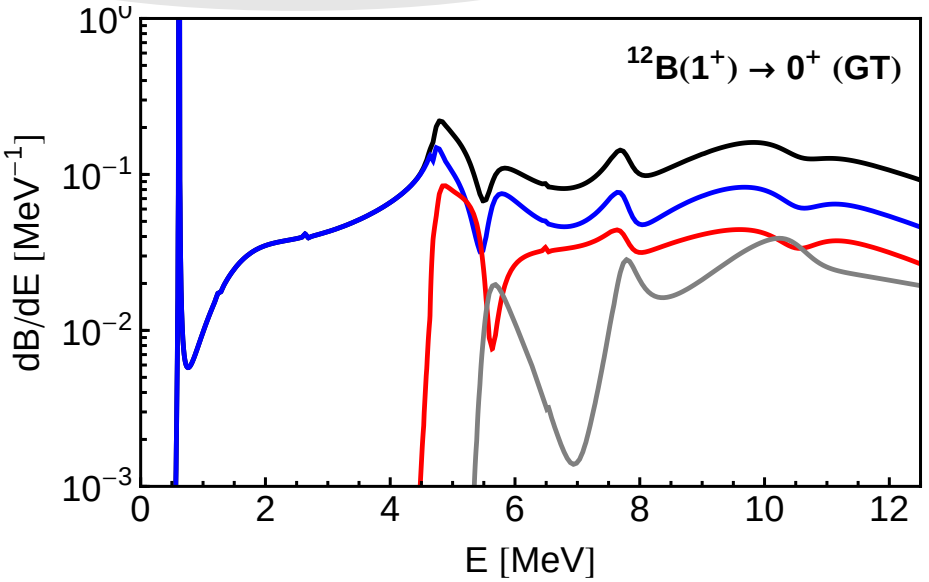

- GT transitions probe admixtures of “shell model” components
- Hoyle state populated in β-decay
- third 0^+ state decays through both ^{8}Be(0^+)-α and ^{8}Be(2^+)-α channels – does this reflect a three-body resonance ?

^{12}C Cluster States in *ab initio* approaches ?

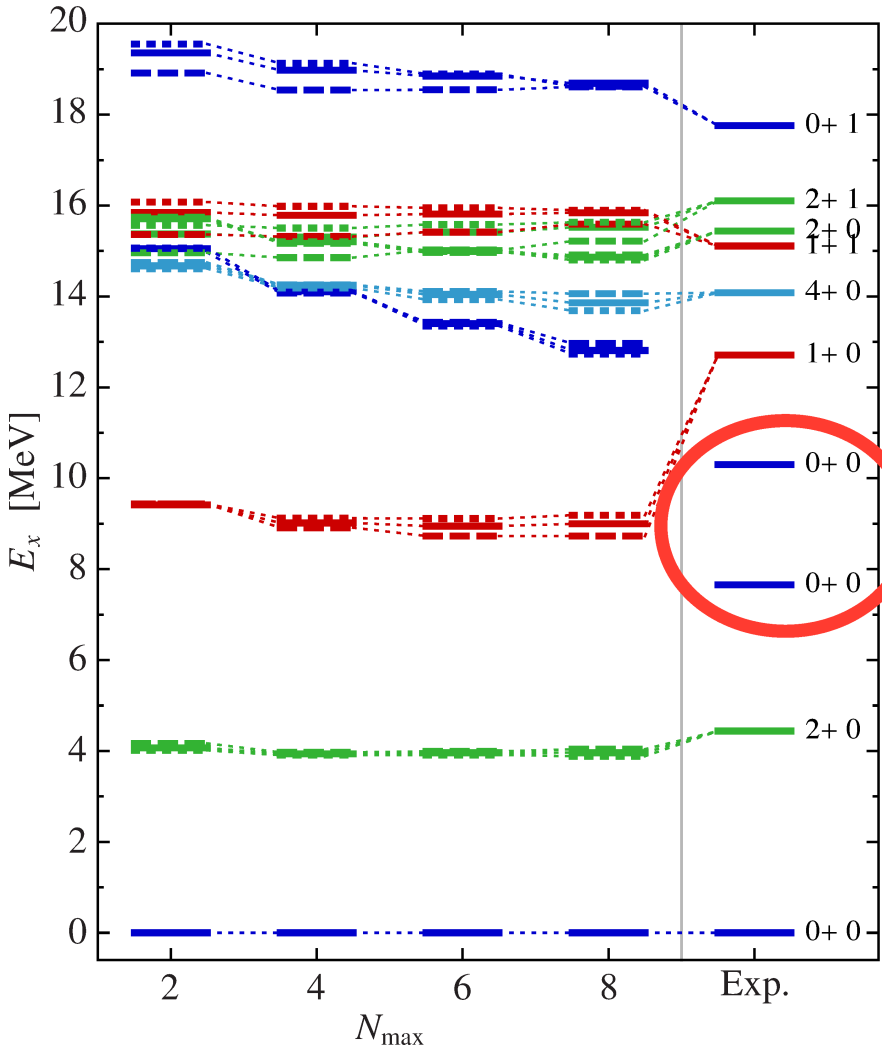

State of the art NCSM calculation with chiral NN+NNN forces

Hoyle state and other cluster states missing !

Lattice EFT

Green's Function Monte Carlo

Maris, Vary, Calci, Langhammer, Binder, Roth, Phys. Rev. C **90**, 014314 (2014)

Overlap with Cluster Model Space

Calculate the overlap of FMD wave functions with pure α-cluster model space

$$N_\alpha = \langle \Psi \left| \underset{\sim}{P}_{3\alpha} \right| \Psi \rangle$$

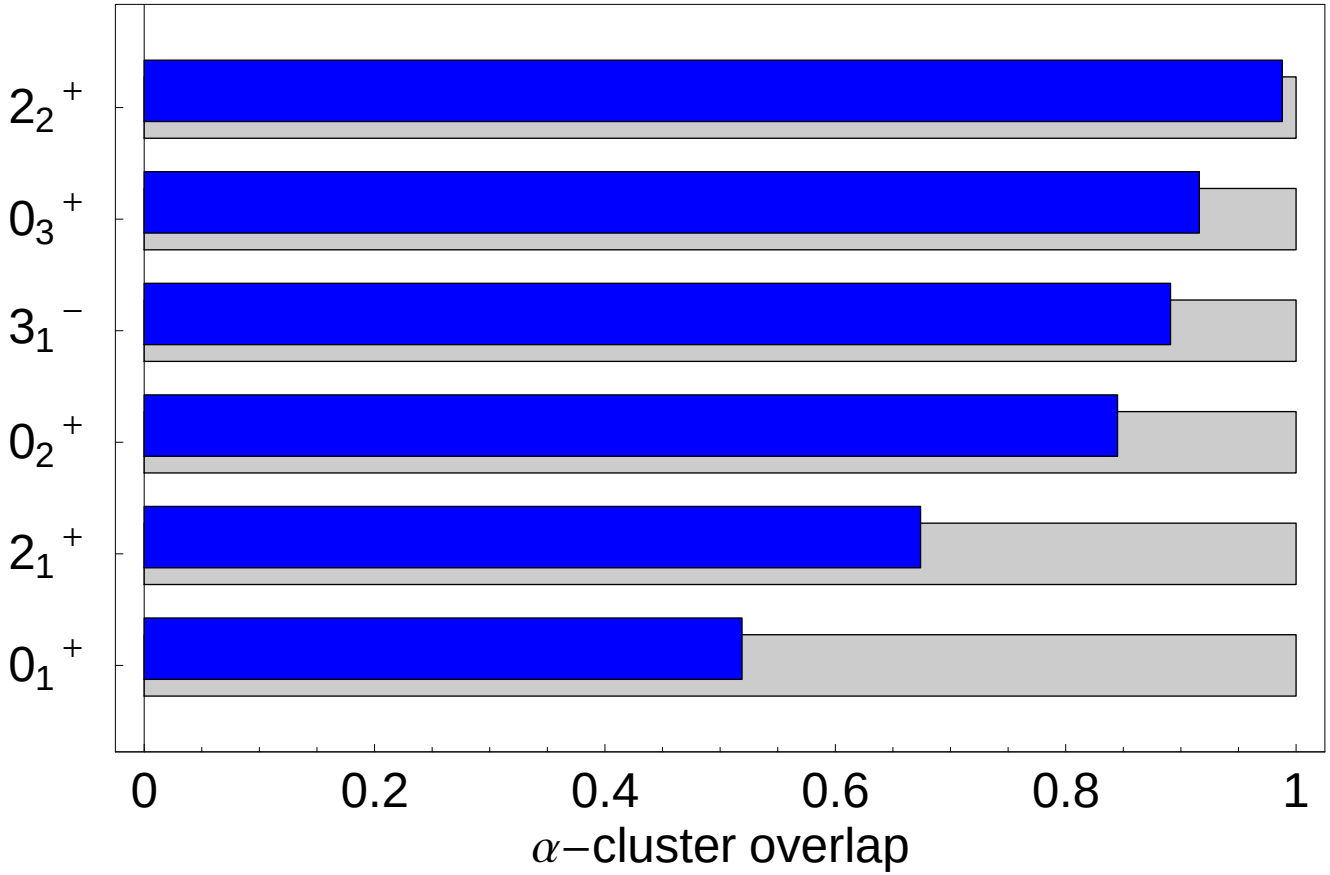

Hoyle state has 15% non-alpha admixtures

Cluster States in ^{12}C
Harmonic Oscillator $N\hbar\Omega$ Excitations

Y. Suzuki *et al*, Phys. Rev. C **54**, 2073 (1996).

$$\mathrm{Occ}(N) = \langle \Psi \left| \delta \left(\sum_i (\underset{\sim}{H}_i^{HO}/\hbar\Omega - 3/2) - N \right) \right| \Psi \rangle$$

Cluster Model